Local structures in metallic and chalcogenide glasses

E. Ma, Y.Q. Cheng and M. Xu

Department of Materials Science and Engineering,

The Johns Hopkins University, Baltimore, MD 21218, USA

Supported by US DoE-BES-MSE

Bulk Metallic Glasses: At the Cutting Edge of Metals Research

A.L. Greer and E. Ma, Guest Editors

Abstract

Glassy alloys (metallic glasses) are currently the focus of intense research in the international metals community. Setting aside elevated-temperature applications, these amorphous metals have exciting potential for structural applications. When metallic glasses were first widely studied in the 1960s, the alloy compositions then known to be quenchable into the glassy state from the liquid required high cooling rates on the order of 10^6 K s^{-1} and were consequently restricted to thin sections. The current interest in metallic glasses has its origin mainly in the increasing range of compositions that can now be cast into glasses at much lower cooling rates, permitting minimum sections of 1 mm to 1 cm or even larger. These bulk metallic glasses (BMGs) are the focus of the articles in this issue of *MRS Bulletin*. Our goal is to illustrate the major materials issues for BMGs, from processing to structures to properties and from the fundamental science of glasses to viable industrial applications. We hope that the articles, in providing a snapshot of a rapidly moving field, show why BMGs are attracting such intense interest and serve to highlight some challenging issues awaiting resolution.

cal, chemical, and tribological properties. In what follows, we highlight the state of the art of research on bulk metallic glasses (BMGs) and introduce the individual articles in this issue, where in-depth discussions can be found on several key issues.

Processing and Glass-Forming Ability

No pure metals and few metallic alloys

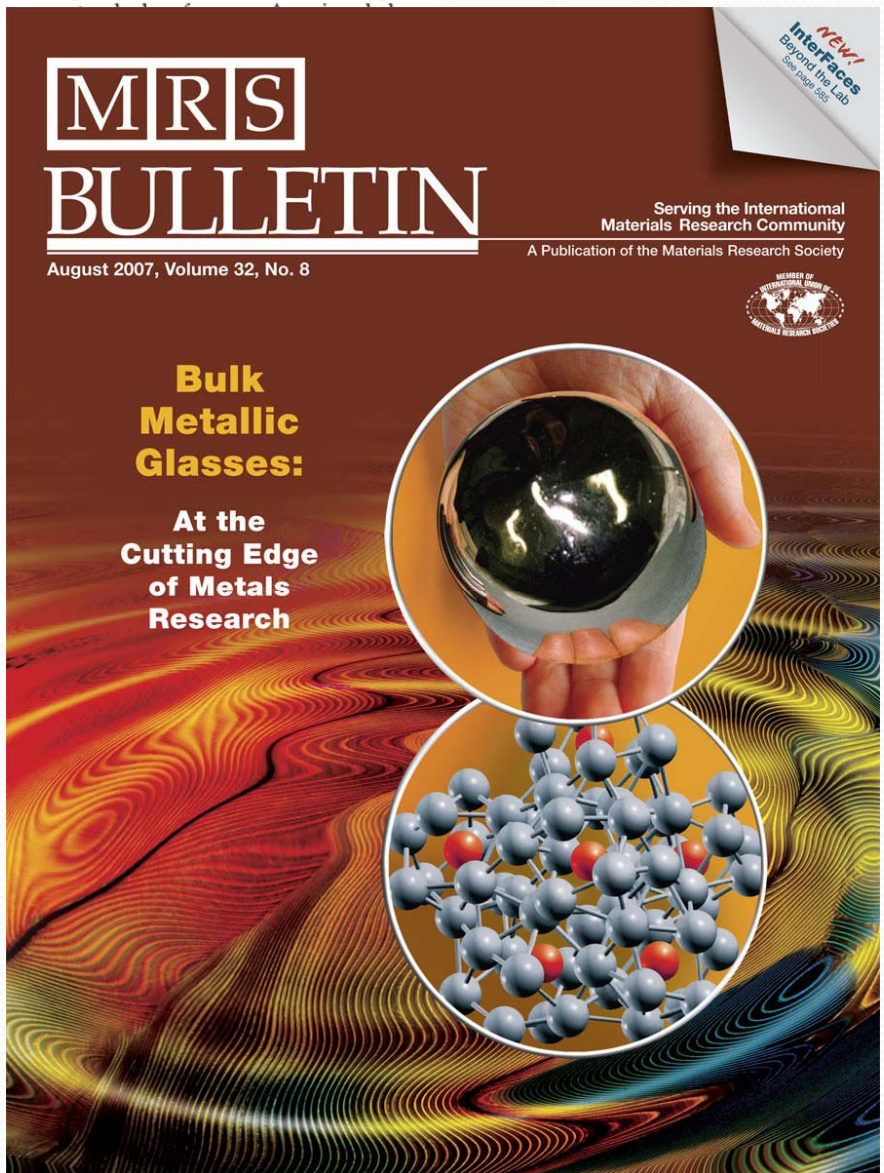

Zr-Cu and Zr-Cu-Al systems are prototypes of BMGs

Optical discs

Amorphous
chalcogenide
films in CD-RW discs

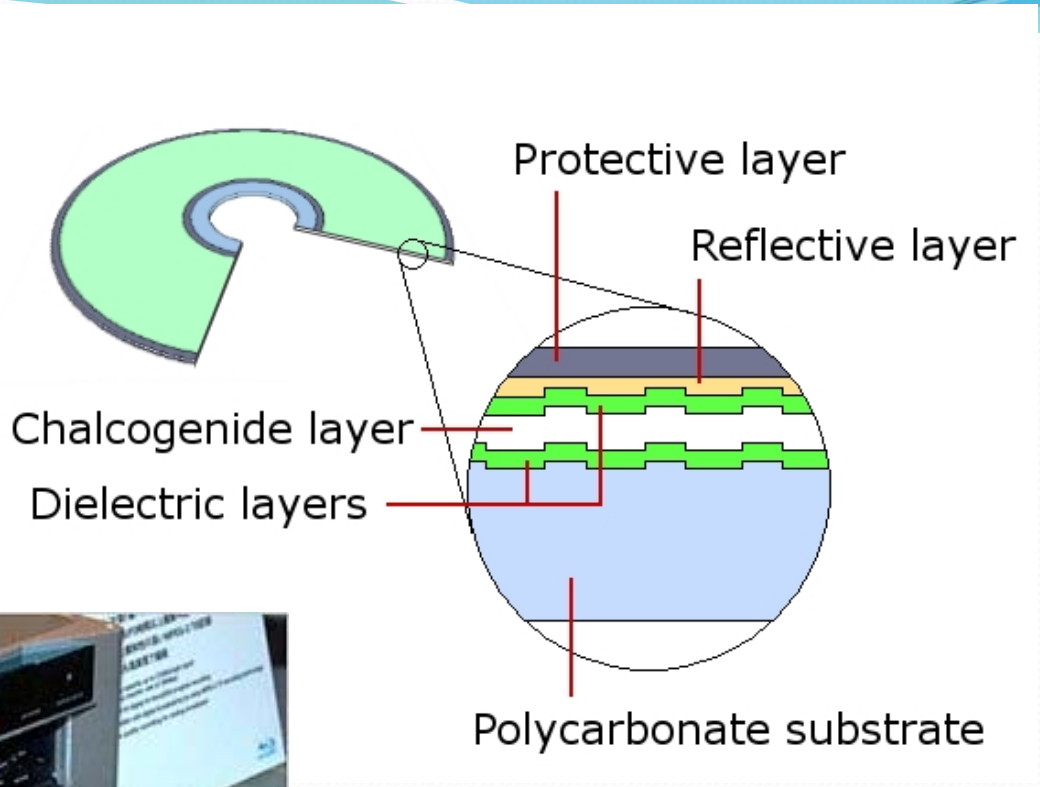

Ge2Sb2Te5 (GST)

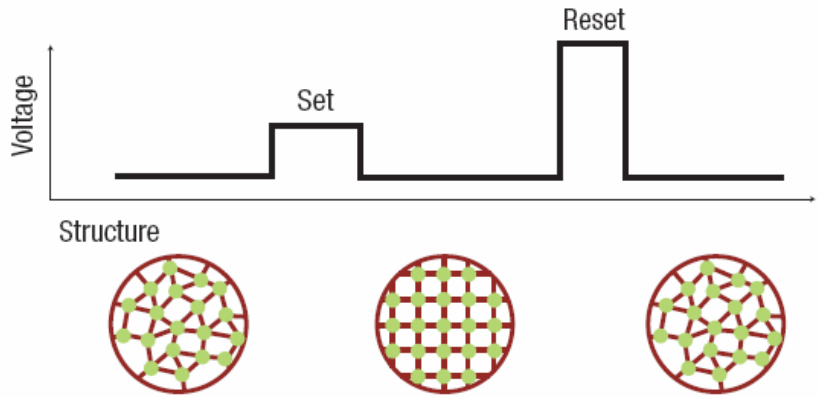

From AL Greer

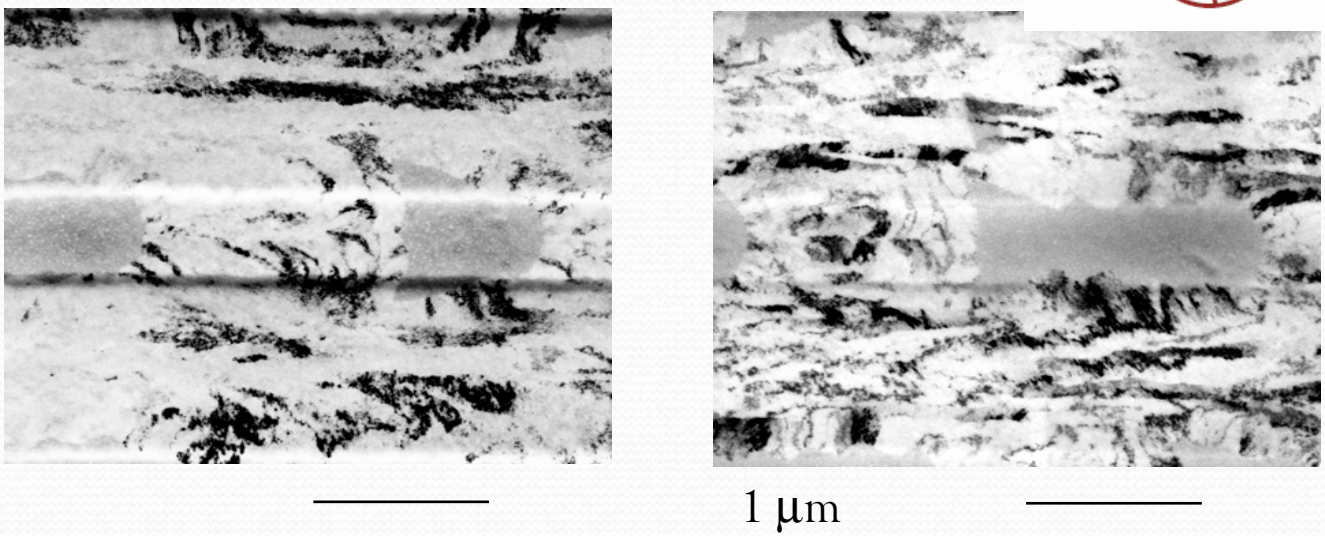

- "Initialization" by laser scanning gives a crystalline thin film
- Data marks written by laser-melting/quenching to give a glass
- Reading is by laser, exploiting contrast in reflectivity

Q#1: Amorphous alloys have structures?

- They seem “structure-less” under HRTEM,

  but have structure in the “short-to-medium range”…

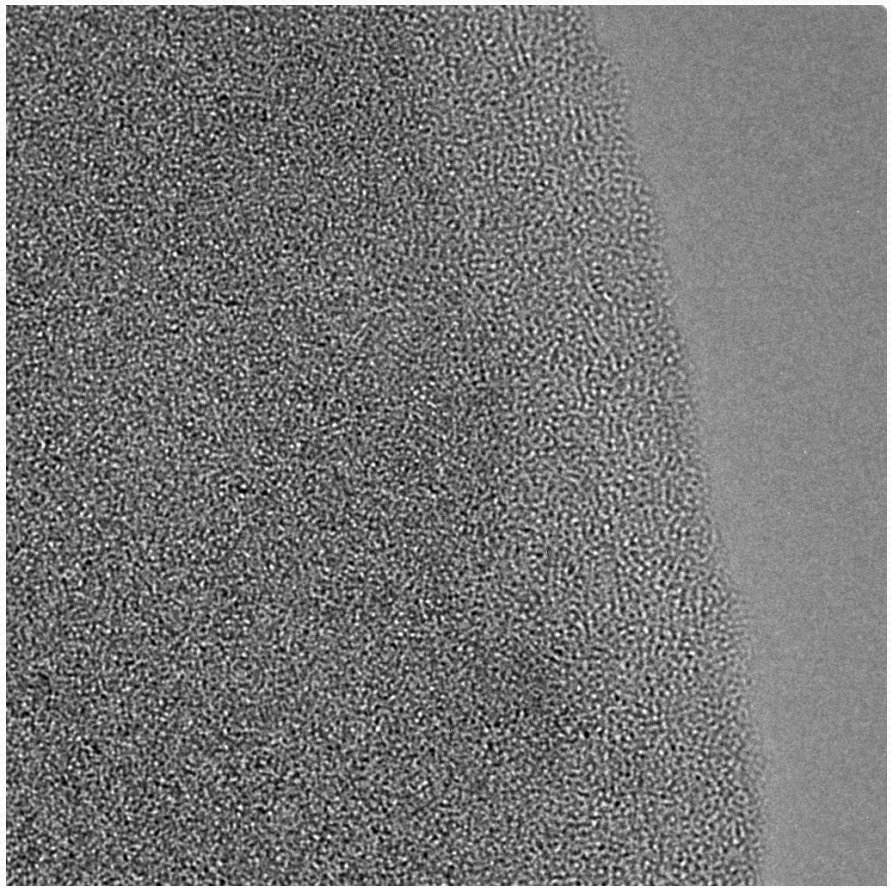

Short-to-medium-range order in metallic glass: early models

❖ **Dense random packing of hard spheres**
J. D Bernal, Nature 165, 68 (1960)

Dense and random: compatible?

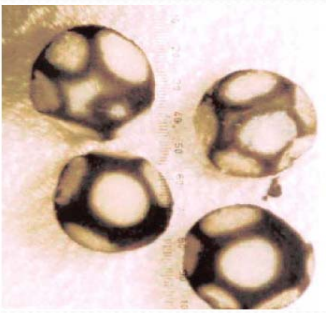

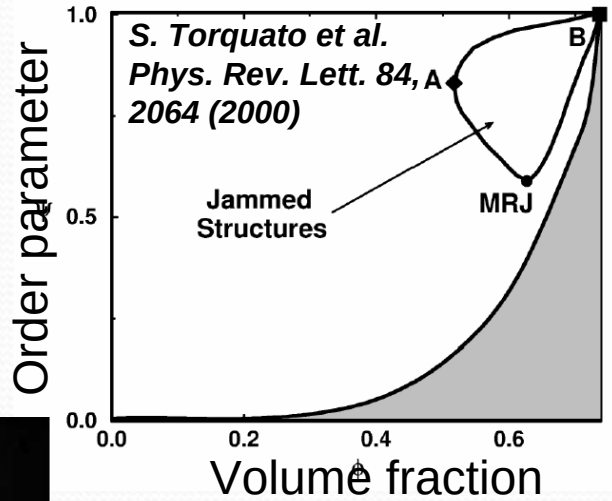

❖ **Stereochemical model**
P. H. Gaskell, Nature 276, 484 (1978)

Covalent and metallic: comparable?

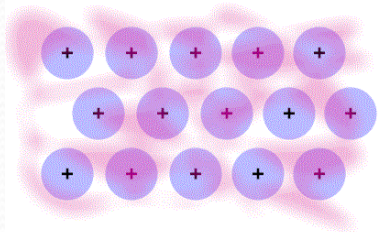

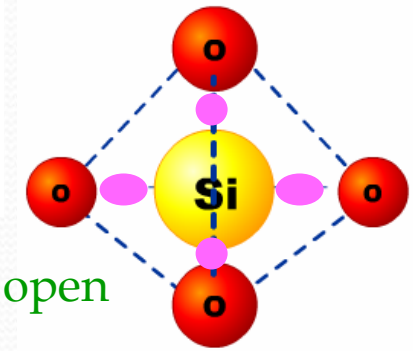

Wikipedia

➢ Covalent bond: rigid, directional, open
➢ Metallic bond: flexible, diffusive, dense

Dense for sure, but not Really random

Motifs may differ from compounds

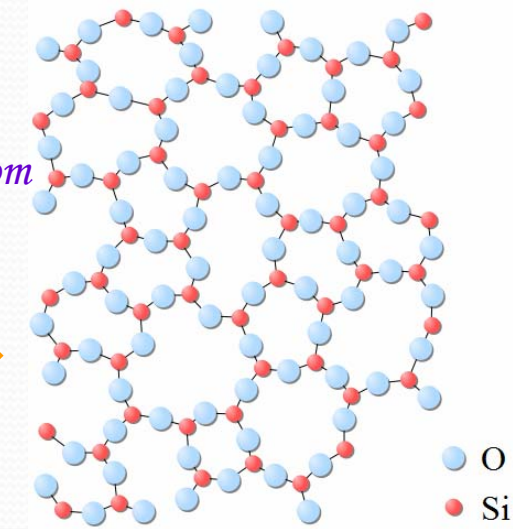

Short-to-medium range order in MG

Structure models for metallic glass: recent progress

❖ Efficient packing of quasi-equivalent clusters

❑ Short-range order (SRO): solute-centered quasi-equivalent clusters (solute-lean)

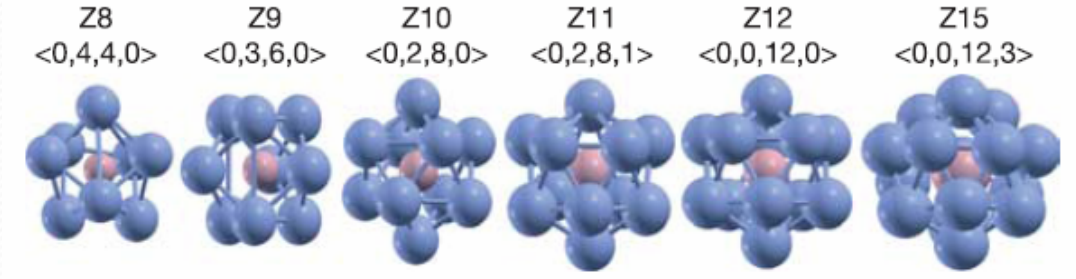

❑ Medium-range order (MRO): efficient packing of the clusters (e.g., icosahedral)

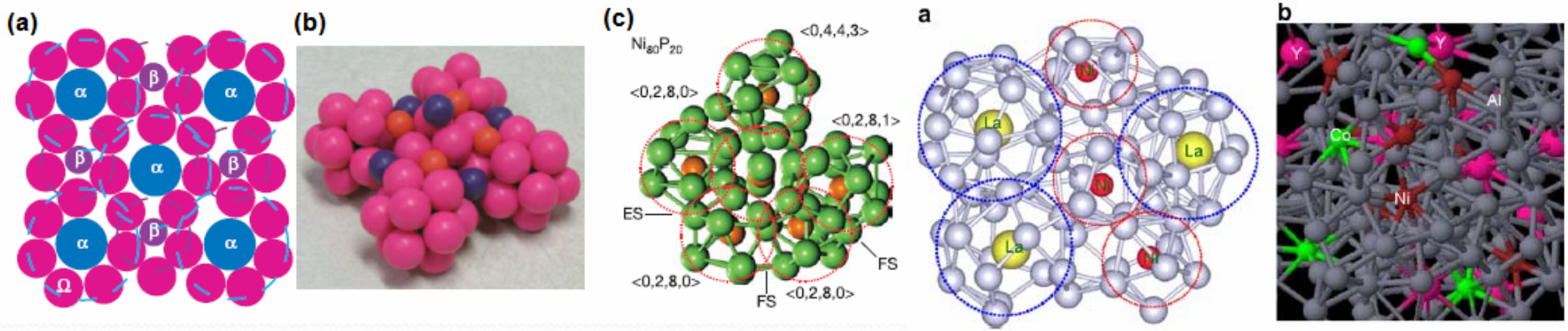

D. B. Miracle, Nature Mater. 3, 697 (2004)

H. W. Sheng et al., Nature 493, 419 (2006)
(Ni-P, Ni-B, Fe-B, Zr-Pt, Ni-Nb,….)

H. W. Sheng et al., Acta Mater. 56, 6264 (2008)
$Al_{89}La_6Ni_5$

Q#2: Why do we care about such amorphous structure in glasses (and liquids) ?

For metallic-glass-forming liquids:

P. G. Debenedetti and F. H. Stillinger, Nature 410, 259 (2001)

❖ **Evolution of viscosity with temperature**

$$\eta(T) = \eta_\infty \exp\left[\frac{B(T)}{TS_c(T)}\right]$$

$$\eta(T) = \eta_\infty \exp\left[\frac{B}{TS_c(T)}\right] \qquad \eta(T) = \eta_\infty \exp\left[\frac{W(T)}{kT}\right]$$

Adam-Gibbs

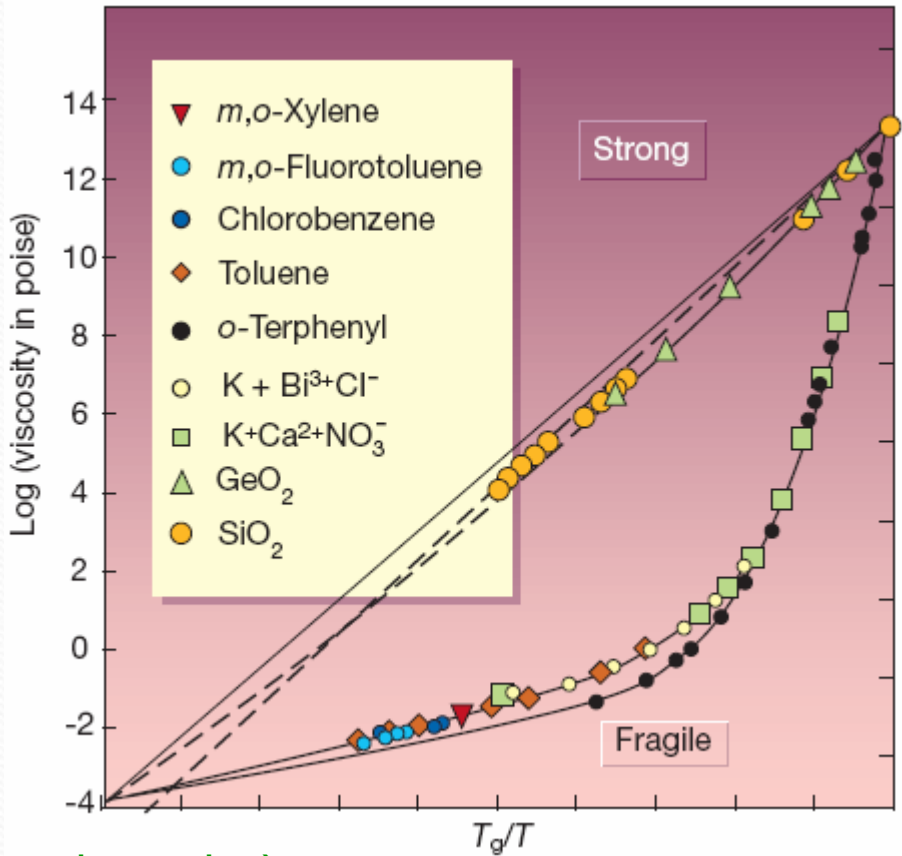

With cooling, viscosity increases due to …

- Lower T (kinetic effect)
- Higher barrier (enthalpy effect)
- Fewer configurations (entropy effect)

Arrhenius vs Non-Arrhenius

Changes in kinetics and internal state (thermodynamics)

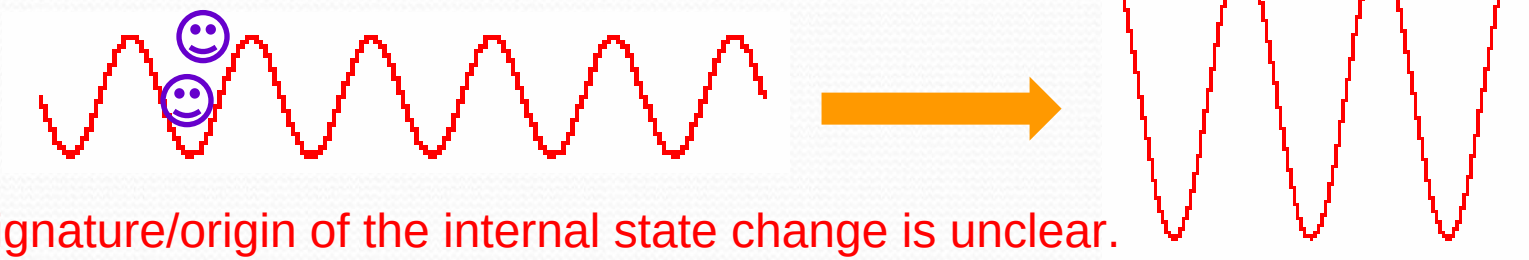

The structure signature/origin of the internal state change is unclear.

Elastic and plastic properties of MGs

Dependent on cooling rate used to make the MG

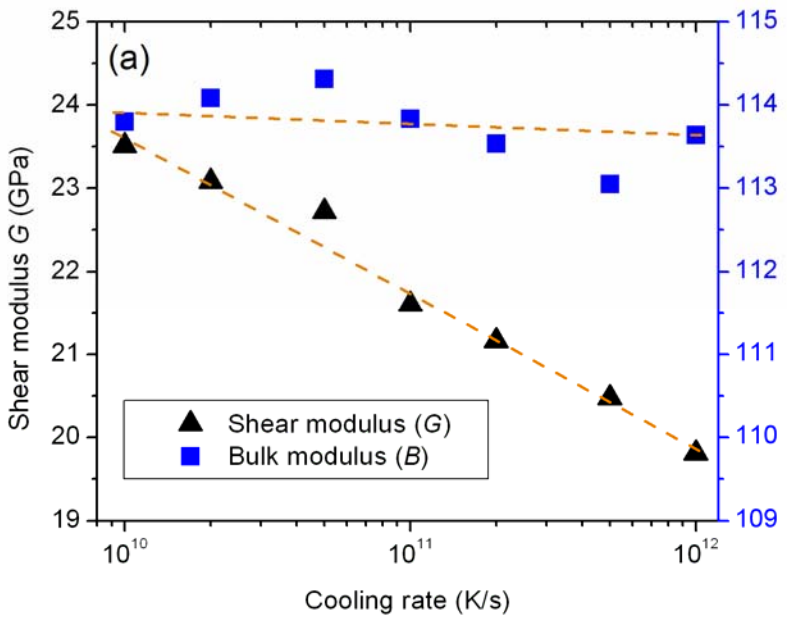

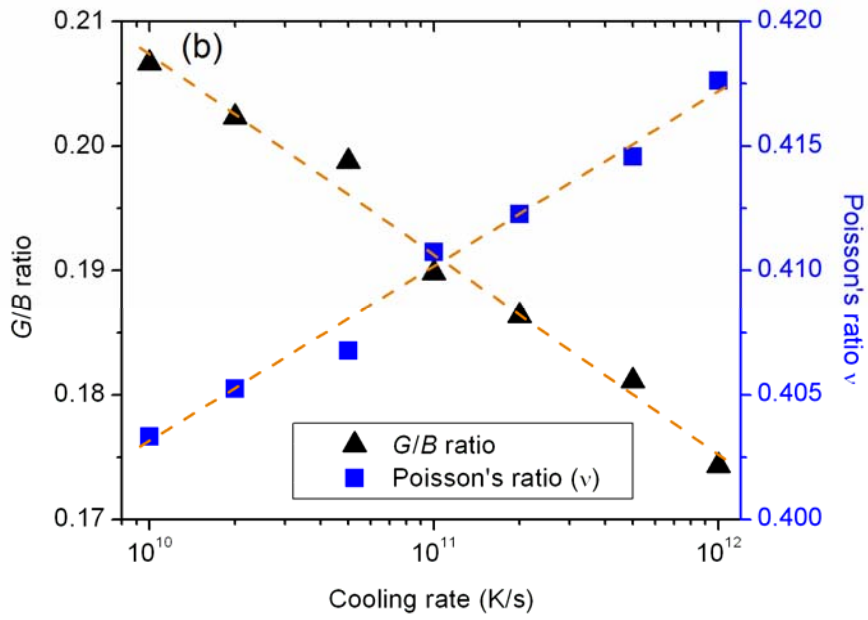

A. J. Cao et al., Acta Mater. 2009

Shear localization in MGs

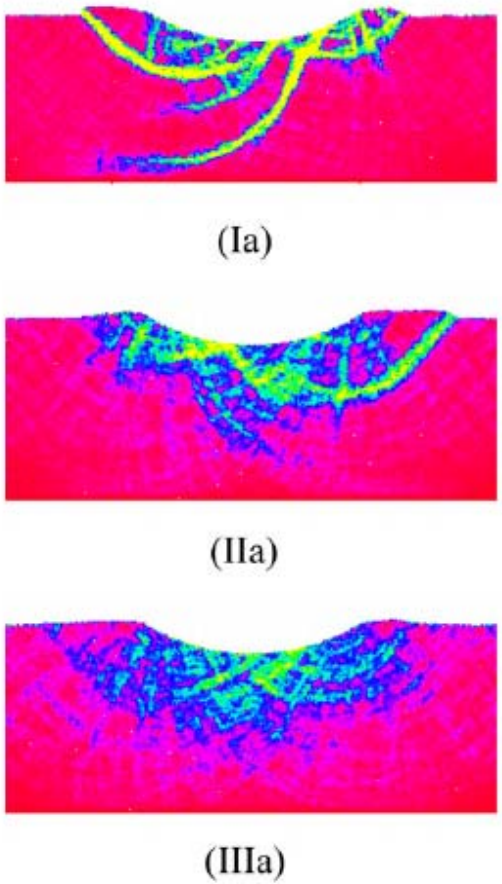

Y. Shi and M.L. Falk,
Acta Mater. 55 (2007) 4317

Indentation of binary L-J glass models,
different degrees of SRO and free volume

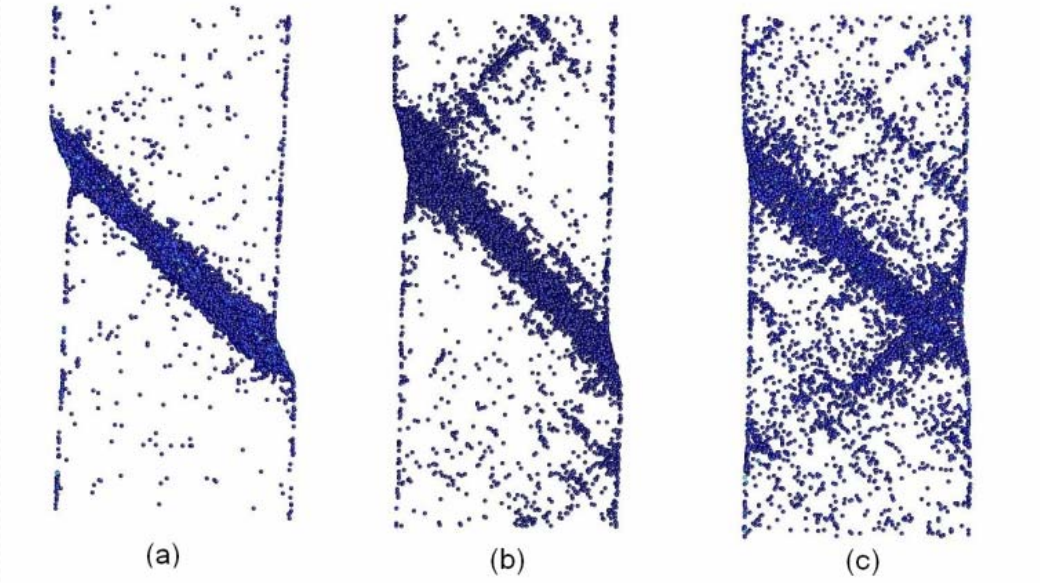

1×10^{10} K/s 1×10^{11} K/s 1×10^{12} K/s

A.J. Cao et al.,
Acta Mater. 2009

Tensile and compressive loading of
Cu-Zr MGs, quenched at different rates
(different ISRO)

For GST DVD glass in phase-change storage media:

Extreme conditions associated with amorphization or crystallization pulses

	Cooling rate ($K\ s^{-1}$)	Temp. gradient ($K\ m^{-1}$)	**Crystal front velocity** ($m\ s^{-1}$)	Melt volume (m^3)
metallurgical solidification	1 to 10	$\sim 10^{4}$	$\sim 10^{-3}$	10^{-5} to 30
phase-change crystallization	$\sim 10^{10}$	10^{9} to 10^{12}	1 to 100	10^{-21} to 10^{-20}

From AL Greer

How could the crystallization finish within a few nanoseconds?

(any role of the structure of the glass ?)

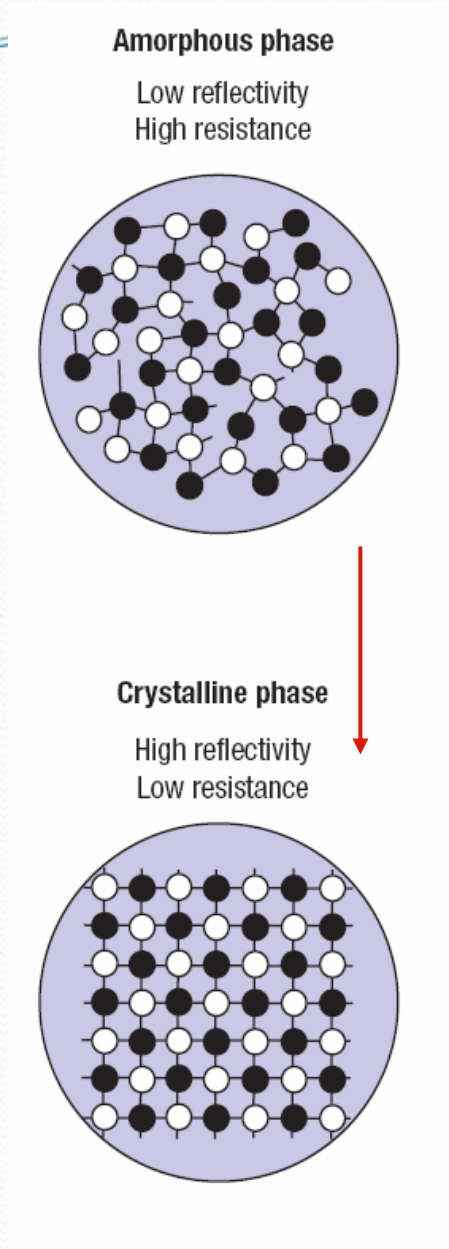

M. Wuttig *et al*., Nature Mater. (2007)

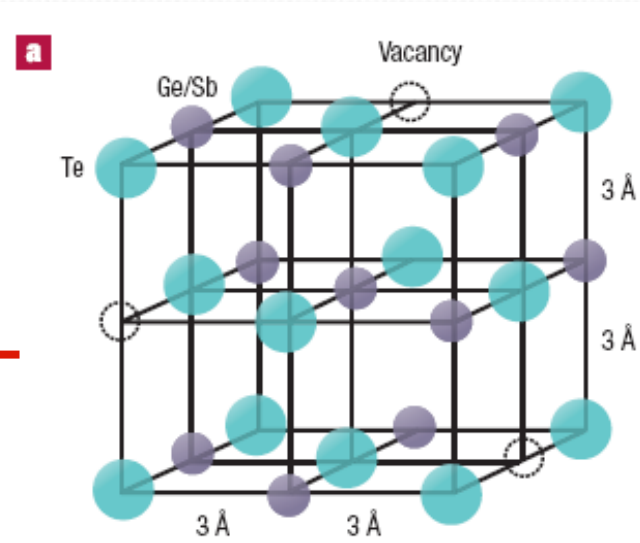

Rocksalt-like metastable crystal

Q#3: How to probe atomic-level structure in glasses?

Experimental structural information acquired via:

Synchrotron X-ray Diffraction (XRD)

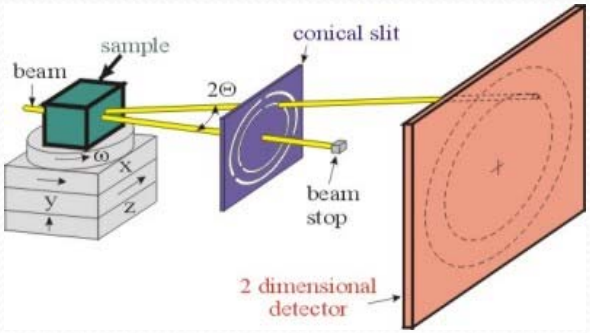

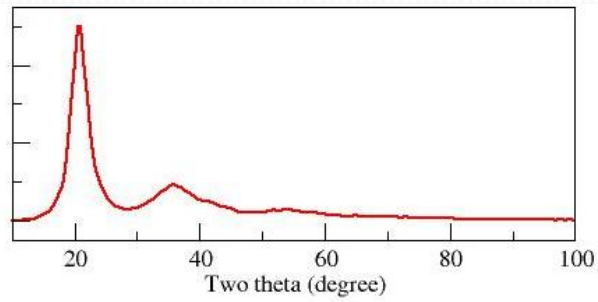

Extended X-ray Absorption Fine Structure (EXAFS)

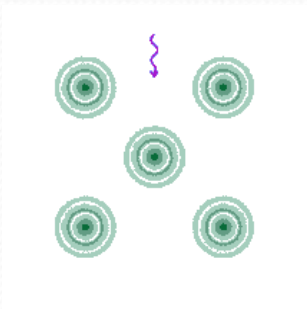

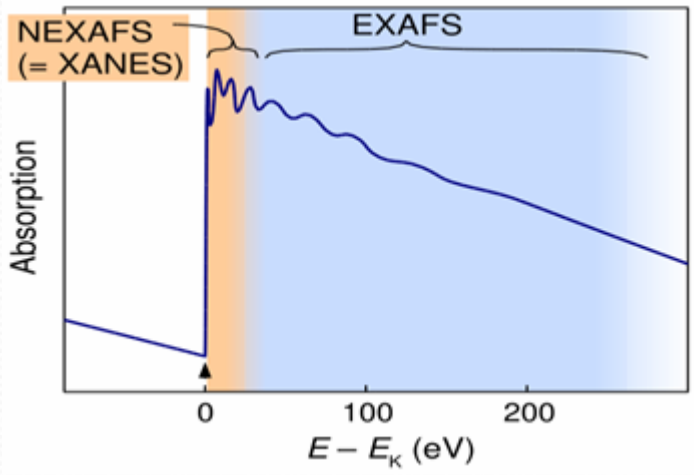

To obtain the 3D atomic structures of MGs:

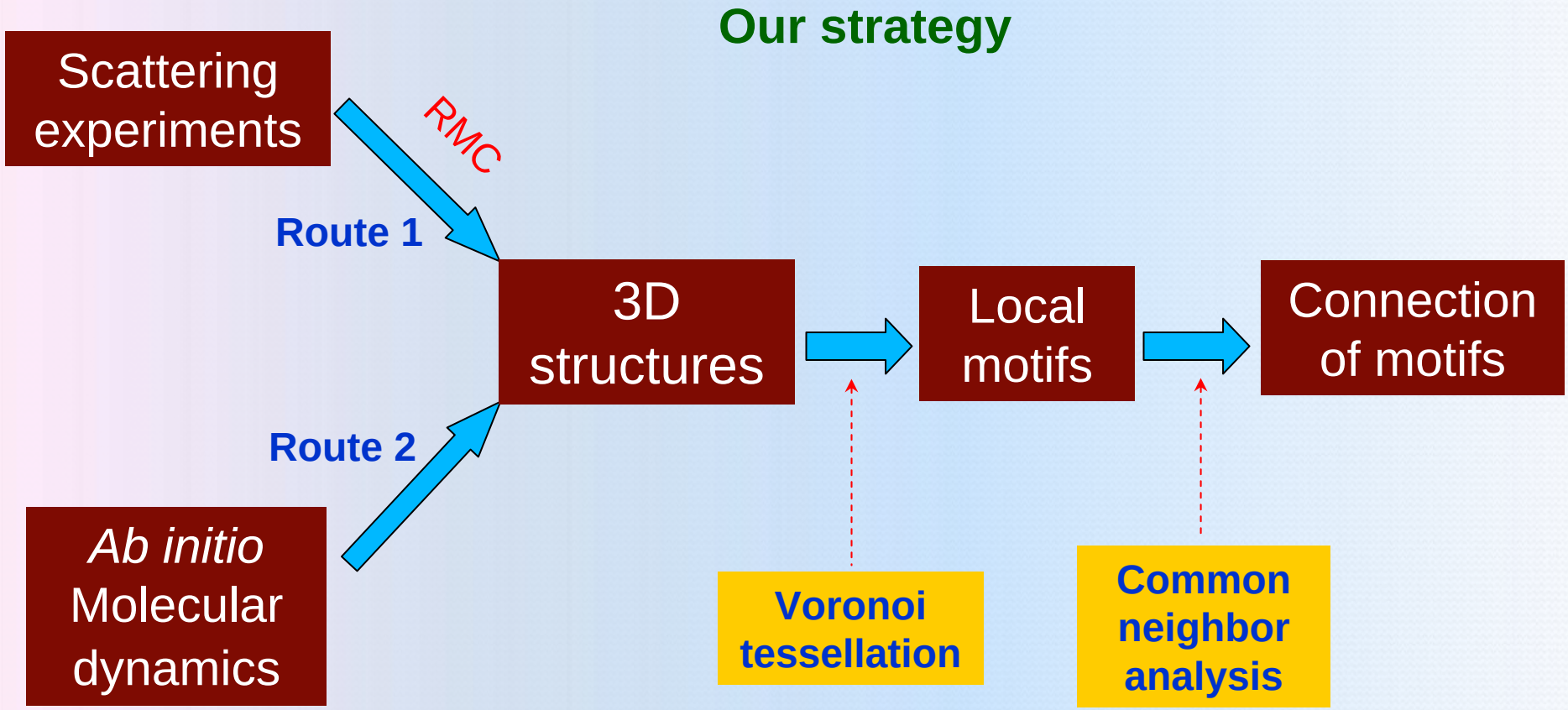

For details, see
H.W. Sheng et al., *Nature* 439 (2006) 419-425

Quench from high temperature liquid

ab initio MD

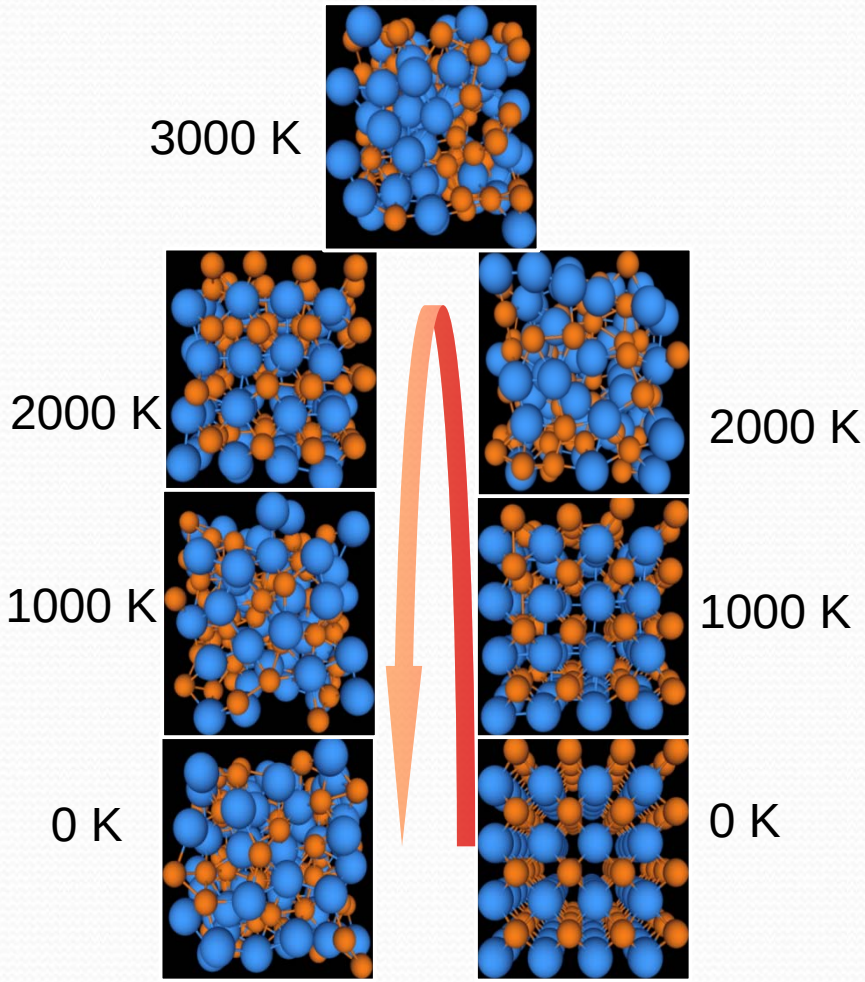

Voronoi tessellation and Voronoi cell

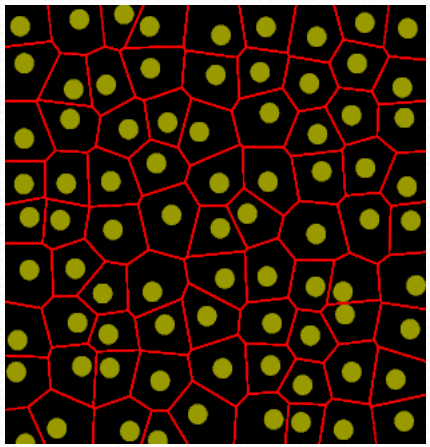

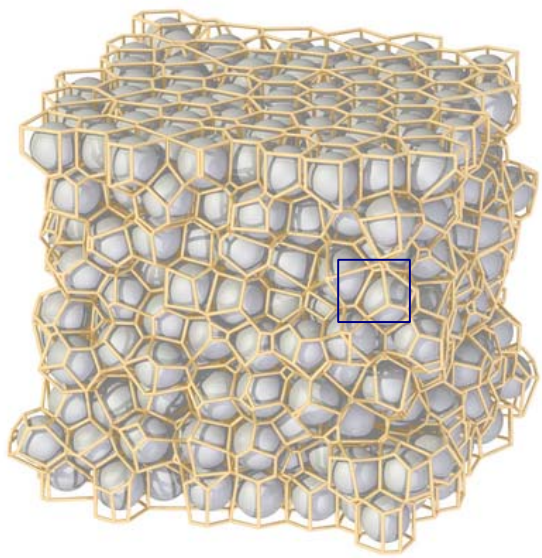

Voronoi cell

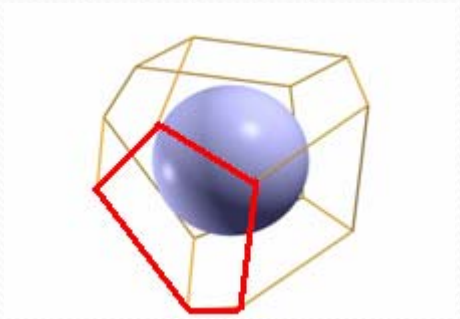

e.g. five-fold symmetry
and five-fold bond

What packing details to look for ?

Atomic domain volume
Cell symmetric property
Coordination number
Voronoi index <n3,n4,n5,n6>

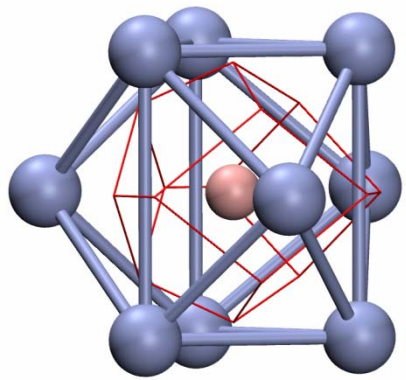

<0,3,6,0>
trigonal prism

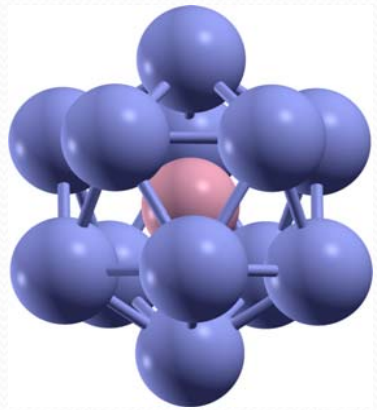

<0,0,12,0>
full icosahedron

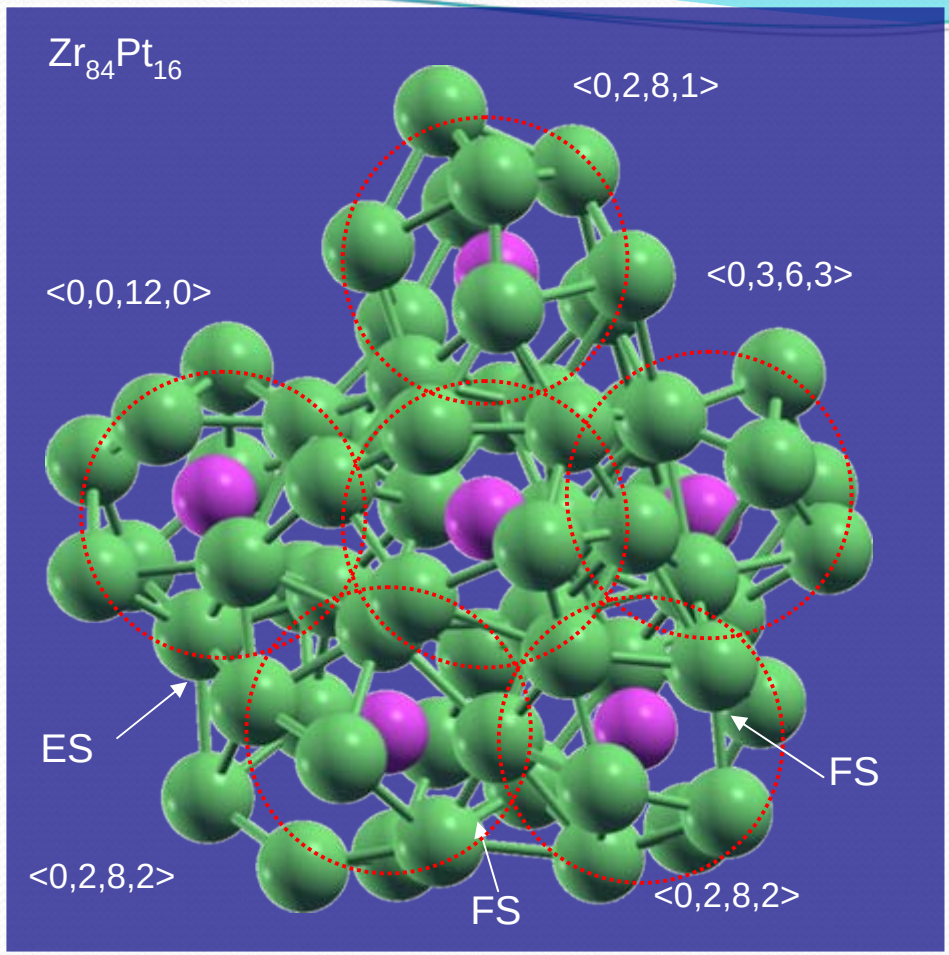

Dense packing of "quasi-equivalent clusters"

Atomic packing and short-to-medium range order in metallic glass

H.W. Sheng, W. Luo, F. Alamgir, J. Bai and E. Ma, ***Nature*** 439 (2006) 419-425.

Can we simply keep doing these to construct

the structure of (multi-component) BMGs ?

Answer: RMC and ab initio MD are often inadequate

- BMG-forming systems are concentrated alloys and usually not simple (such as solute-lean) binaries

- RMC solution is not unique, and structural details cannot be adequately revealed by fitting just the total structure factor

- *ab initio* MD is limited to

  ~200 atoms (few solutes), ~10^{13} K/s quench rate, and NVT

  (quench rate not as much of a problem, for GST glass)

MD w/ empirical but realistic potentials (not just hard sphere, pair potential)

- EAM potentials for ternary Zr-Cu-Al (developed by Dr. H. W. Sheng)
- LAMMPS code (http://lammps.sandia.gov/)
- >10,000 atom cubic box (>~6 nm) with periodic boundary condition

liquid
- Construct 2000K liquid structure
- Equilibrate for 2ns

quench
- Quench under NPT at various rates
- 300 K glass configurations

minimize
- Energy minimization
- Solve inherent structures

analyze
- Pair distribution functions
- Voronoi tessellation

$Cu_{46}Zr_{47}Al_7$

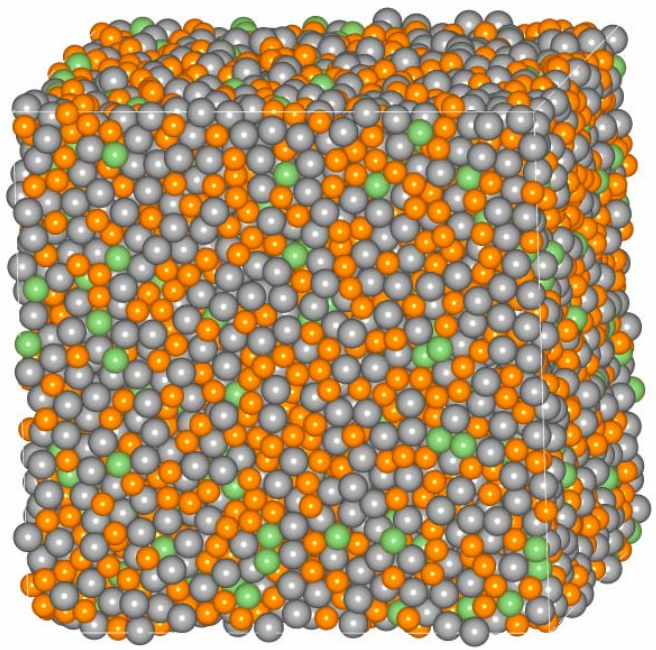

The potentials (in format compatible with LAMMPS) can be downloaded from:
http://sites.google.com/a/gmu.edu/eam-potential-database/

The potentials and the website are developed and maintained by Prof. H.W. Sheng.
Dr. Sheng can be reached at hsheng@gmu.edu

See Supplementary Materials in this paper:

PRL, **102** (2009) 245501 PHYSICAL REVIEW LETTERS

Atomic Level Structure In Multicomponent Bulk Metallic Glass

Y. Q. Cheng,[1] E. Ma,[1] and H. W. Sheng[2,*]

[1]*Department of Materials Science and Engineering, Johns Hopkins University, Baltimore, Maryland 21218, USA*
[2]*Department of Computational and Data Sciences, George Mason University, Fairfax, Virginia 22030, USA*
(Received 17 April 2008)

The atomic-level structure of a representative ternary Cu-Zr-Al bulk metallic glass (BMG) has been resolved. Cu- (and Al-) centered icosahedral clusters are identified as the basic local structural motifs. Compared with the Cu-Zr base binary, a small percentage of Al in the ternary BMG leads to dramatically increased population of full icosahedra and their spatial connectivity. The stabilizing effect of Al is not merely topological, but also has its origin in the electronic interactions and bond shortening.

DOI: PACS numbers: 61.43.Dq

Are the new Zr-Cu-Al potentials realistic and reliable ?

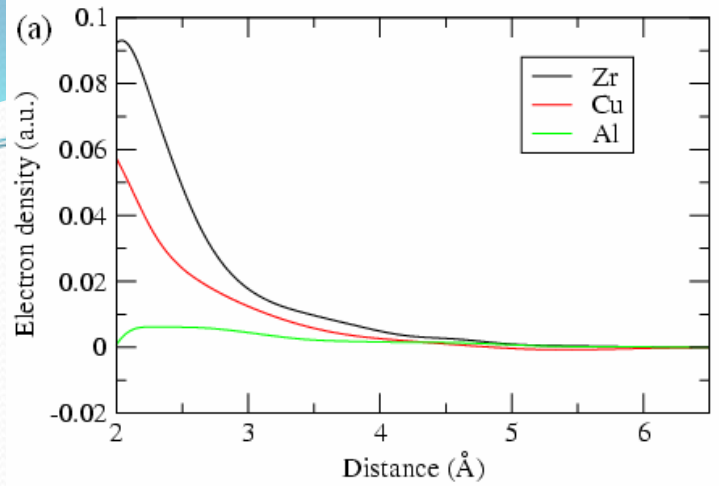

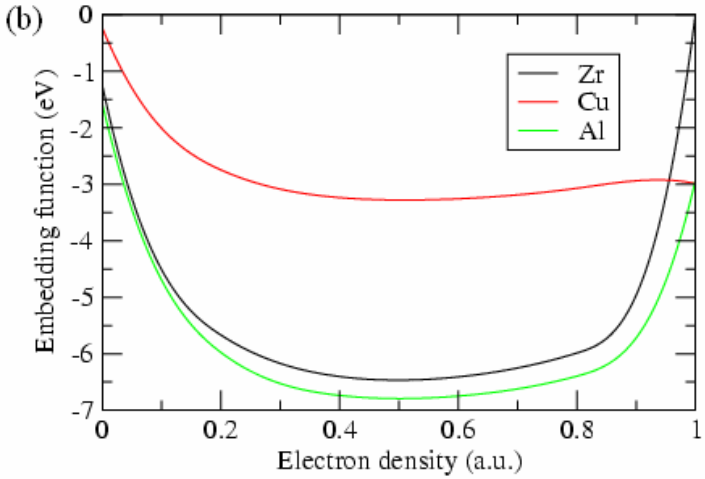

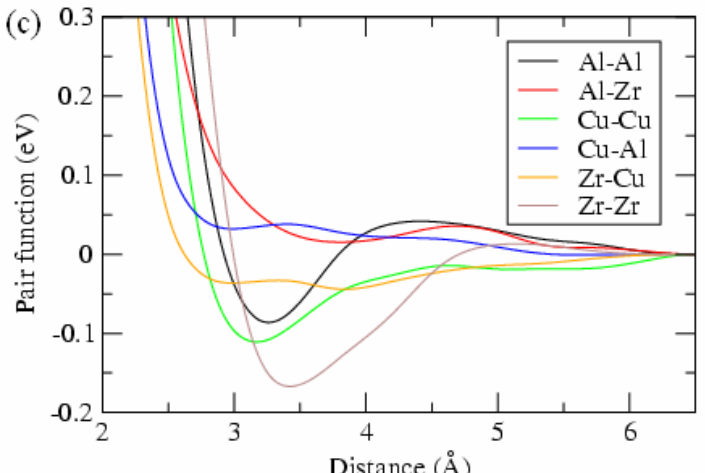

Figure S1. As-developed EAM functions.

(a) Charge density functions.
(b) Embedding functions.
(c) Pair potential functions.

YQ Cheng, HW Sheng and E Ma

Phys. Rev. Lett. 102 (2009) 245501

Table S2. Comparison of cohesive energies for other Zr phases.

Zr	Crystalline					Cluster		
	ω	bcc	fcc	diamond	sc	Zr_9	Zr_{15}	Zr_{21}
ab initio	-6.33	-6.25	-6.28	-6.12	-6.12	-4.31	-4.86	-4.95
EAM	-6.32	-6.26	-6.31	-6.18	-6.18	-4.28	-4.91	-4.99

Table S3. Comparison of cohesive energies for other Cu phases.

Cu	Crystalline				Cluster		
	hcp	bcc	diamond	sc	Cu_9	Cu_{15}	Cu_{21}
ab initio	-3.53	-3.50	-2.69	-3.09	-2.18	-2.42	-2.55
EAM	-3.53	-3.50	-2.71	-3.11	-2.19	-2.44	-2.54

Table S4. Comparison of cohesive energies for other Al phases.

Al	Crystalline				Cluster		
	hcp	bcc	diamond	sc	Al_9	Al_{15}	Al_{21}
ab initio	-3.34	-3.28	-2.69	-3.03	-2.23	-2.57	-2.66
EAM	-3.35	-3.28	-2.71	-3.09	-2.23	-2.57	-2.65

Table S5. Comparison of compound properties.

	Space group	Proto-type	Lattice parameter (a, b, c: Å, β: degree)		Cohesive energy (eV/atom)		Bulk modulus (10^{11} Pa)	
			Exp.* or *ab initio*	EAM	*ab initio*	EAM	*ab initio*	EAM
$CuZr_3$**	$Pm\bar{3}m$	$AuCu_3$	a=4.30	a=4.30	-5.60	-5.60	0.97	0.96
$CuZr_2$	I4/mmm	$MoSi_2$	a=3.220 c=3.728	a=3.23 c=3.75	-5.54	-5.54	1.06	1.07
$CuZr_2$**	$Fd\bar{3}m$	$NiTi_2$	a=12.31	a=12.26	-5.47	-5.48	1.07	1.07
$CuZr_2$**	I4/mcm	Al_2Cu	a=6.751 c=5.057	a=6.741 c=5.049	-5.51	-5.52	1.10	1.11
CuZr	$Pm\bar{3}m$	CsCl	a=3.252	a=3.242	-5.06	-5.07	1.22	1.22
$Cu_{10}Zr_7$	C2ca	$Ni_{10}Zr_7$	a=9.347 b=9.322 c=12.68	a=9.440 b=9.410 c=12.80	-4.81	-4.82	1.20	1.41

Cu_8Zr_3	Pnma	Cu_8Hf_3	*a*=7.869 *b*=8.147 *c*=9.977	*a*=7.940 *b*=8.229 *c*=10.07	-4.43	-4.46	1.25	1.25
Al_3Zr	I4/mmm	Al_3Zr	*a*=3.999 *c*=17.28	*a*=4.02 *c*=17.38	-4.59	-4.60	0.96	1.13
Al_2Zr	$P6_3/mmc$	$MgZn_2$	*a*=5.281 *c*=8.742	*a*=5.32 *c*=8.82	-4.89	-4.89	1.21	1.29
AlZr	Cmcm	CrB	*a*=3.353 *b*=10.87 *c*=4.266	*a*=3.372 *b*=10.93 *c*=4.290	-5.29	-5.29	1.23	1.39
Al_3Zr_4	$P\bar{6}$	Al_3Zr_4	*a*=5.433 *c*=5.390	*a*=5.419 *c*=5.376	-5.52	-5.52	1.09	1.13
Al_3Zr_5	I4/mcm	W_5Si_3	*a*=8.184 *c*=5.702	*a*=8.211 *c*=5.728	-5.54	-5.60	1.12	1.24
$AlZr_2$	$P6_3/mcm$	$InNi_2$	*a*=6.854 *c*=5.501	*a*=6.771 *c*=5.434	-5.64	-5.69	1.12	1.15
$AlZr_3$	$Pm\bar{3}m$	$AuCu_3$	*a*=4.391	*a*=4.390	-5.89	-5.90	0.93	0.92

Al_2Cu	$Fm\bar{3}m$	CaF_2	a=5.765	a=5.783	-3.63	-3.62	1.07	1.12
Al_2Cu	I4/mcm	Al_2Cu	a=6.063 c=4.872	a=6.068 c=4.876	-3.60	-3.61	0.97	1.01
Al_3Cu_2	$P\bar{3}m1$	Al_3Ni_2	a=4.127 c=5.029	a=4.139 c=5.043	-3.61	-3.69	1.16	1.19
AlCu	I2/m	AlCu	a=9.889 b=4.105 c=6.913 β=89.7	a=9.888 b=4.105 c=6.913 β=89.7	-3.68	-3.69	1.25	1.24
Al_2Cu_3	$P6_3/mmc$	NiAs	a=4.118 c=10.00	a=4.183 c=10.16	-3.66	-3.66	1.18	1.26
Al_4Cu_9	$P\bar{4}3m$	Al_4Cu_9	a=8.707	a=8.750	-3.71	-3.69	1.28	1.41
$AlCu_3$**	$Fm\bar{3}m$	$AlFe_3$	a=5.820	a=5.850	-3.66	-3.67	1.28	1.47
$AlCu_4$	$P4_132$	βMn	a=6.30	a=6.32	-3.60	-3.61	1.19	1.16
$ZrCu_2Al$	$Fm\bar{3}m$	$MnCu_2Al$	a=6.215	a=6.215	-4.52	-4.54	1.28	1.34
ZrCuAl	$Fd\bar{3}m$	$MgCu_2$	a=7.308	a=7.308	-4.80	-4.79	1.23	1.26

* Lattice parameters of intermetallic compounds are found from Inorganic Crystal Structure Database (ICSD, e.g., http://icsdweb.fiz-karlsruhe.de/)

** Note that these phases are hypothetical and may not exist in experiments (phase diagrams). These hypotehtical structures are constructed mainly for potential fitting purposes. Lattice parameters of these structures are obtained through *ab inito* calculations.

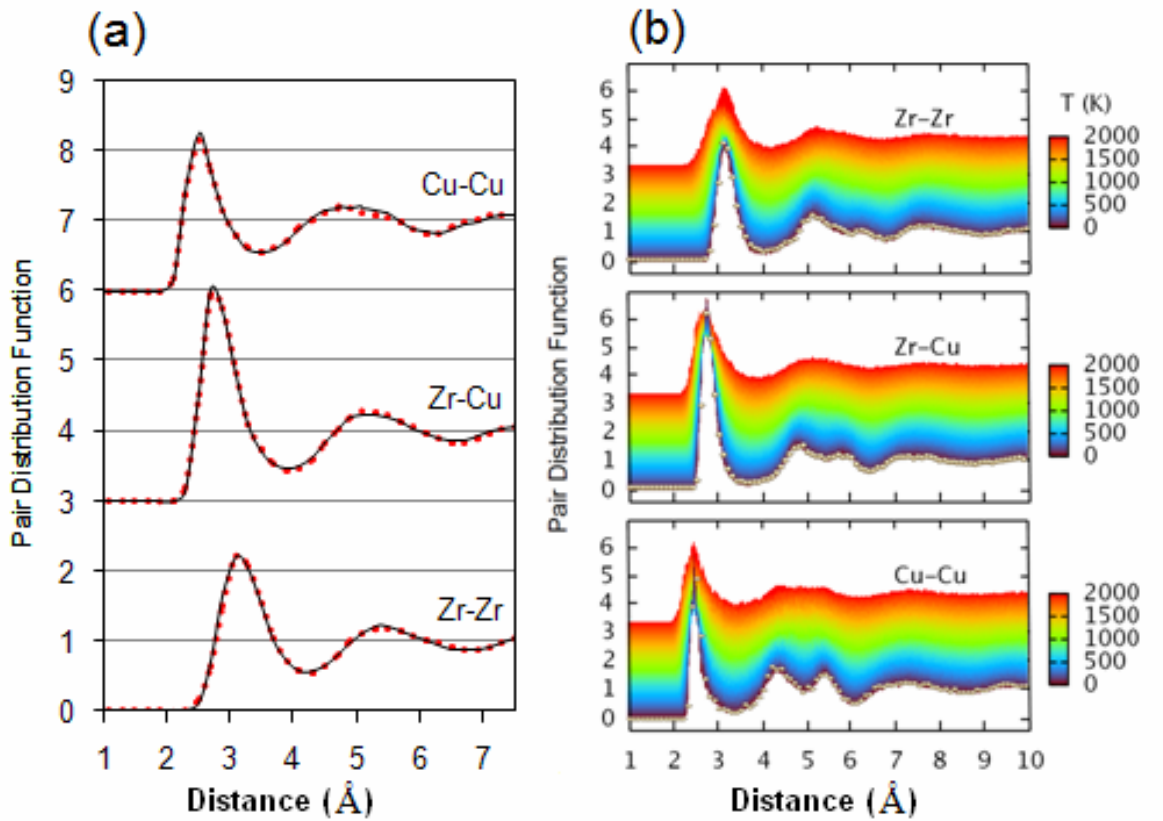

Figure S9. Validation of EAM potentials by comparing Cu46Zr54 partial PDFs at different temperatures. (a) Partial PDFs of liquid Cu46Zr54 (200 atoms) at 1500 K obtained using EAM (black solid lines) and *ab initio* MD (red dotted lines). The density is fixed at 6.76 g/cc, at which the average pressure is below 1 GPa for both EAM and *ab initio* simulations. (b) Evolution of the partial PDFs (colored lines) as a function of temperature during *NPT* quenching (EAM MD, 500 atoms) of Cu46Zr54. The final configuration at 0 K was further relaxed using the conjugated gradient method with *ab initio* many-body descriptions, and the partial PDFs of this optimized structure are also shown (circles).

Cu46Zr47Al7

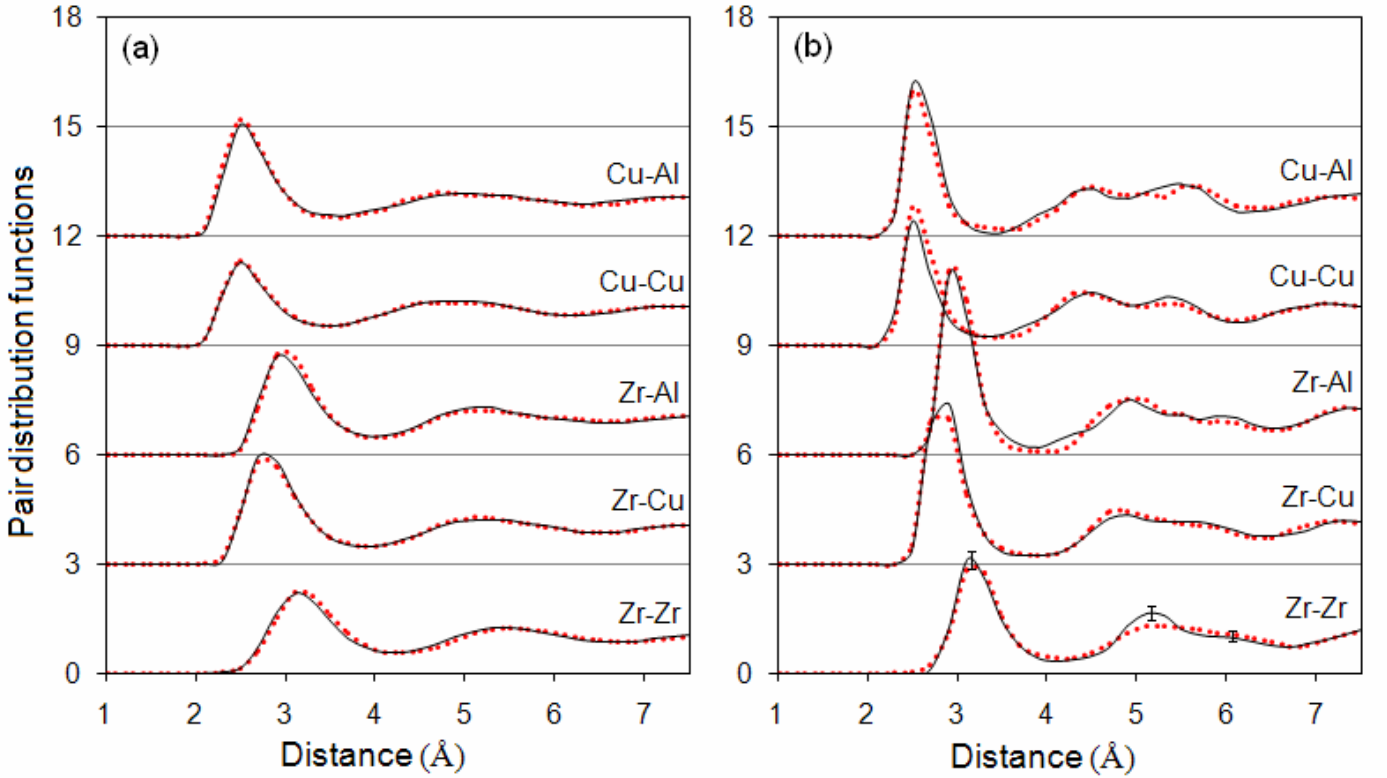

Figure S10. (a) Partial PDFs of equilibrium liquid Cu46Zr47Al7 (200 atoms) at 1500 K obtained using EAM (black solid lines) and *ab initio* MD (red dotted lines). The density is fixed at 6.49 g/cc, at which the average pressure is below 1 GPa for both EAM and *ab initio* simulations. (b) Comparison of partial PDFs of the *ab initio* MD-quenched (red dashed lines) and EAM MD-quenched (black solid lines) Cu46Zr47Al7 MGs (200 atoms, quenching rate 10^{13} K/s). Representative error bars (large statistical fluctuations due to the small sample size and fast quenching rate) for the EAM MD quenching are labeled for Zr-Zr pair, estimated by 10 quenching runs from independent high-temperature liquid structures.

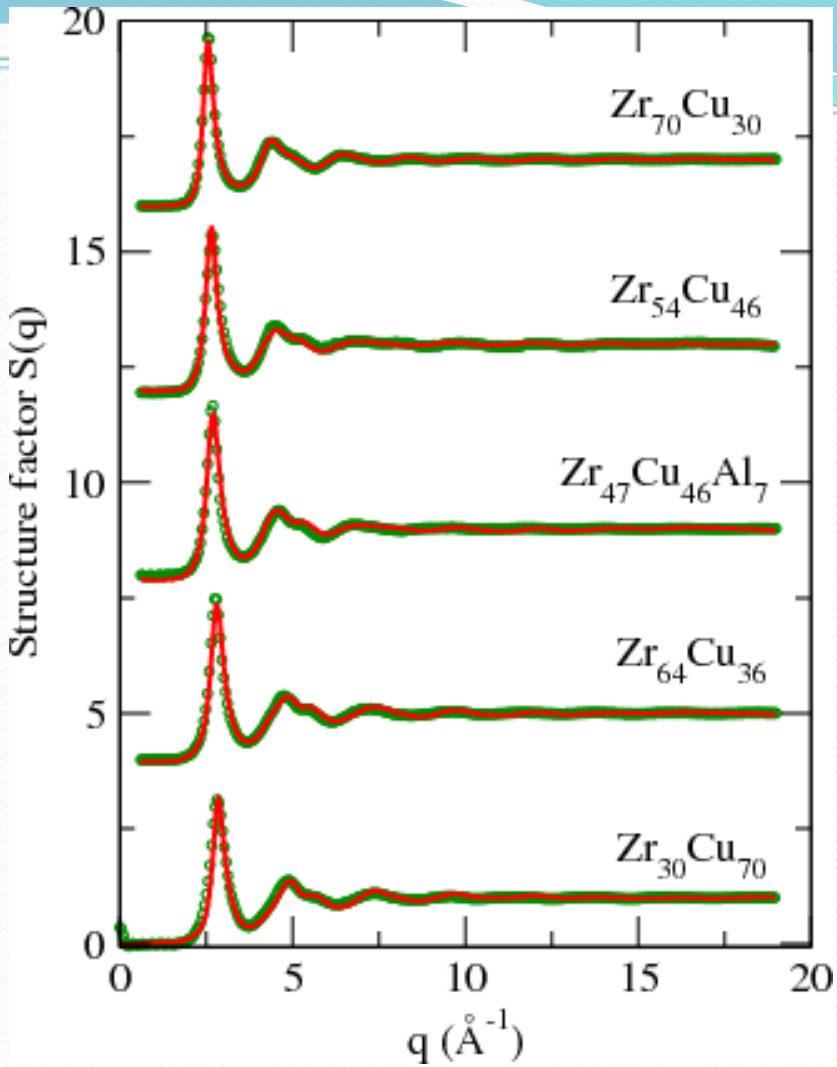

Structure factors of various Cu-Zr binary MGs, as well as $Cu_{46}Zr_{47}Al_7$. Green circles are measured data from experiments. Red lines are simulated data based on the configurations obtained with our EAM potentials.

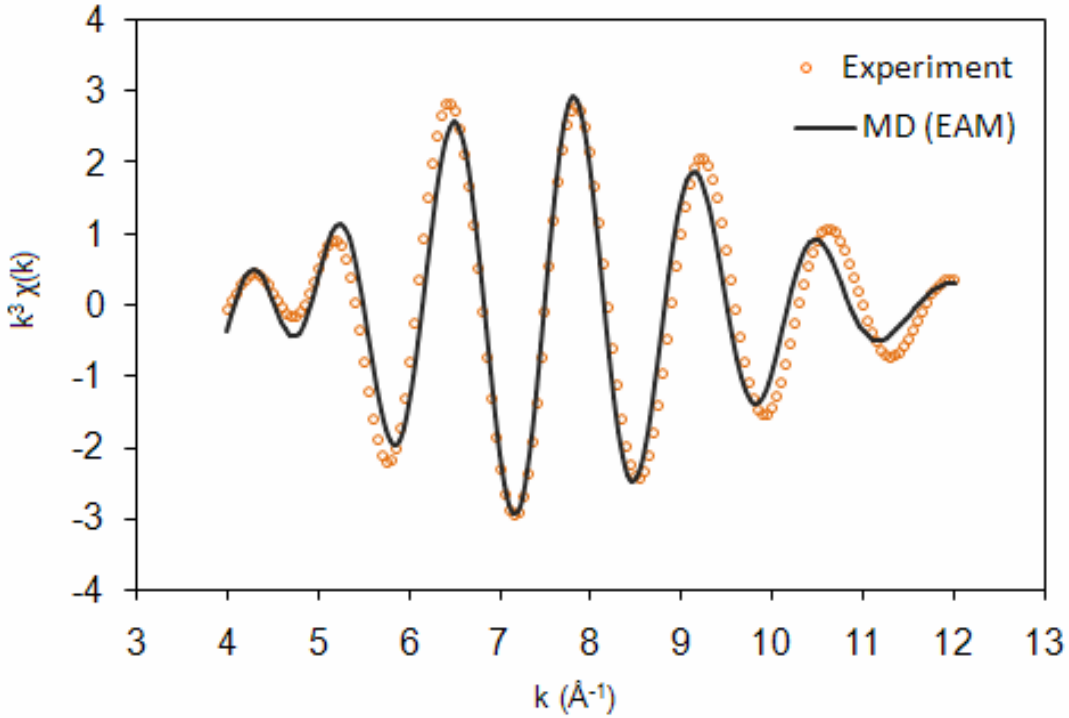

Cu K-edge EXAFS of Cu46Zr54.

Orange circles are measured data in experiment. Black line is simulated result based on the configuration obtained with our EAM potentials.

The potentials (in format compatible with LAMMPS) can be downloaded from:
http://sites.google.com/a/gmu.edu/eam-potential-database/

The potentials and the website are developed and maintained by Prof. H.W. Sheng.
Dr. Sheng can be reached at hsheng@gmu.edu

See Supplementary Materials in this paper:

PRL, **102** (2009) 245501 PHYSICAL REVIEW LETTERS

Atomic Level Structure In Multicomponent Bulk Metallic Glass

Y. Q. Cheng,[1] E. Ma,[1] and H. W. Sheng[2,*]

[1]*Department of Materials Science and Engineering, Johns Hopkins University, Baltimore, Maryland 21218, USA*
[2]*Department of Computational and Data Sciences, George Mason University, Fairfax, Virginia 22030, USA*
(Received 17 April 2008)

The atomic-level structure of a representative ternary Cu-Zr-Al bulk metallic glass (BMG) has been resolved. Cu- (and Al-) centered icosahedral clusters are identified as the basic local structural motifs. Compared with the Cu-Zr base binary, a small percentage of Al in the ternary BMG leads to dramatically increased population of full icosahedra and their spatial connectivity. The stabilizing effect of Al is not merely topological, but also has its origin in the electronic interactions and bond shortening.

DOI: PACS numbers: 61.43.Dq

Q#4: What are the dominant structural features (i.e., motifs) in these BMGs?

Atomic structures

YQ Cheng *et al.*,

Phys. Rev. Lett. 102 (2009) 245501

$Cu_{46}Zr_{54}$

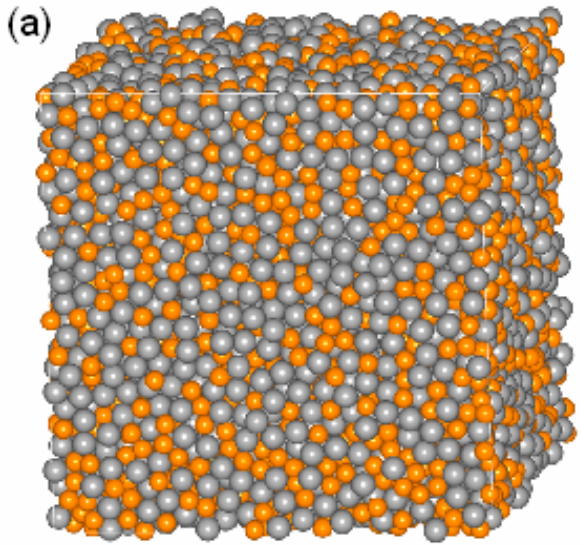

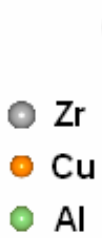

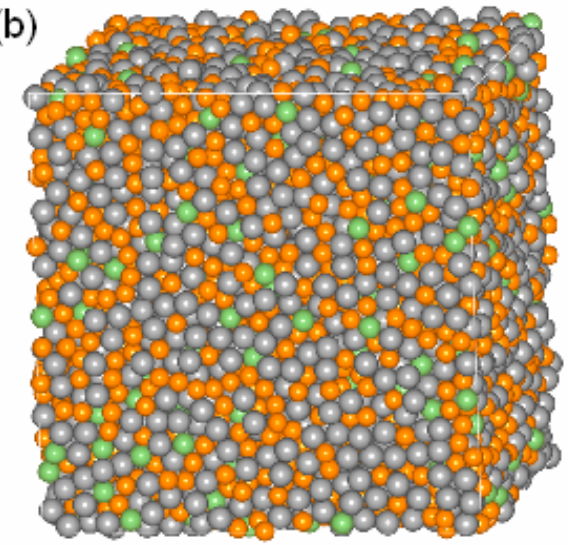

$Cu_{46}Zr_{47}Al_7$

Cu-<0,0,12,0>

Full icosahedra

Cu-<0,0,12,0>

Al-<0,0,12,0>

Cu-<0,2,8,0>

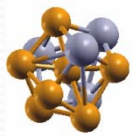

Cu-<0,2,8,1>

Cu-<0,2,8,2>

Atomic-level structure of $Cu_{46}Zr_{54}$ binary BMG

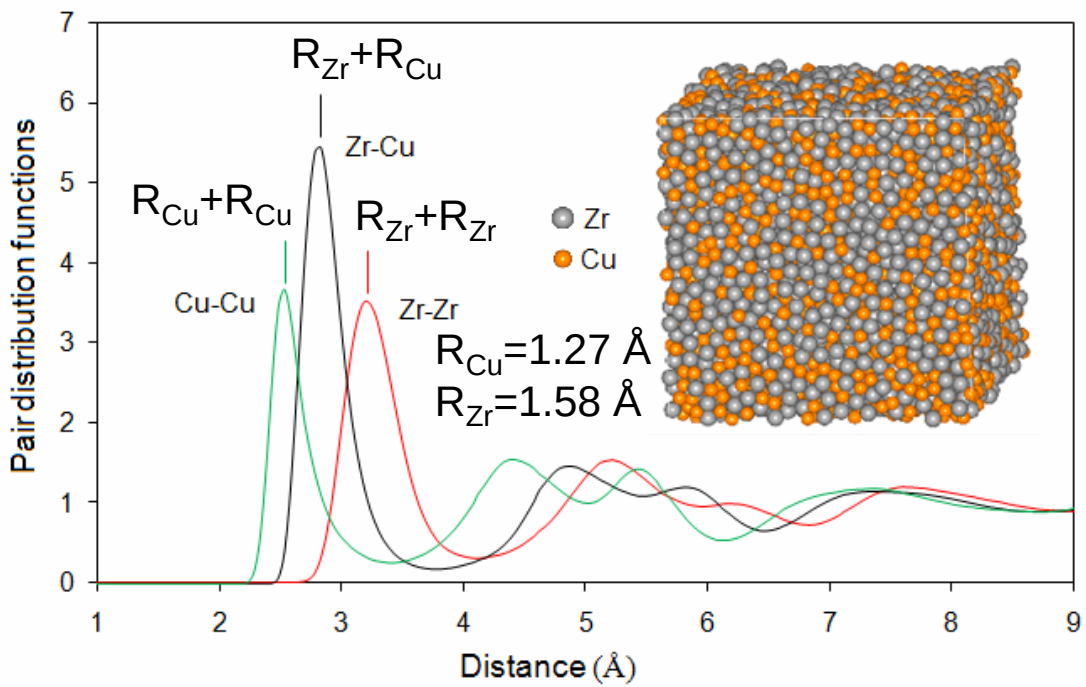

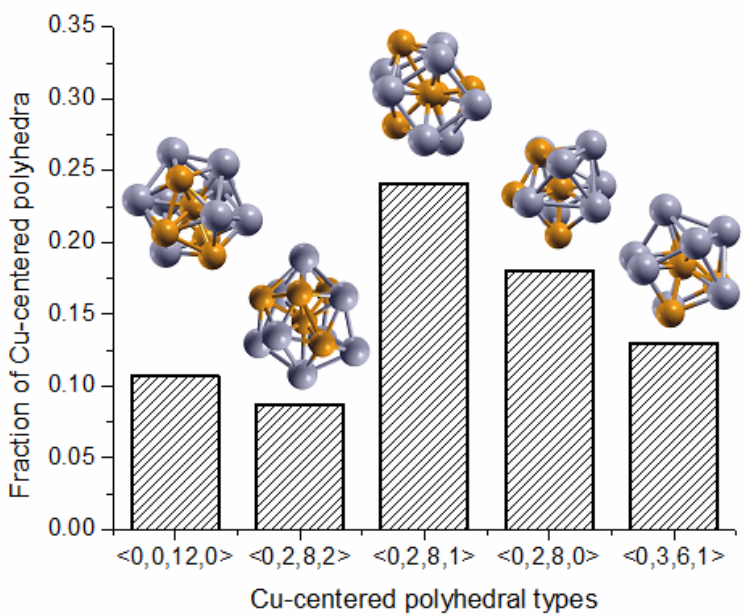

SRO in Cu-Zr: Cu-centered icosahedral dense-packing with five-fold bonds

Composition-dependent structure of $Cu_xZr_{(100-x)}$ binary BMGs

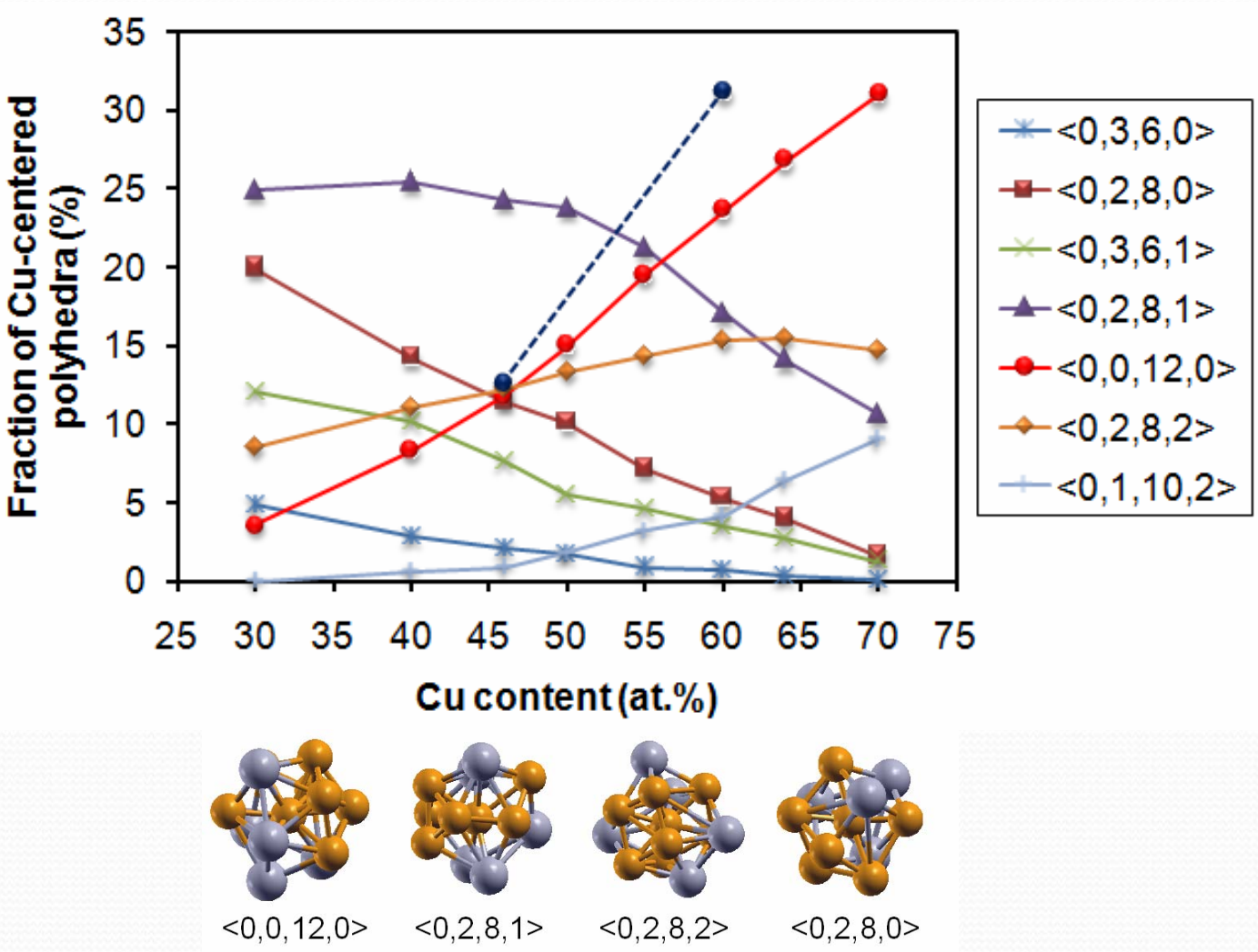

Dashed blue line is for cooling rate 1 order of magnitude slower

❖ How to understand the structure features of $Cu_xZr_{(100-x)}$

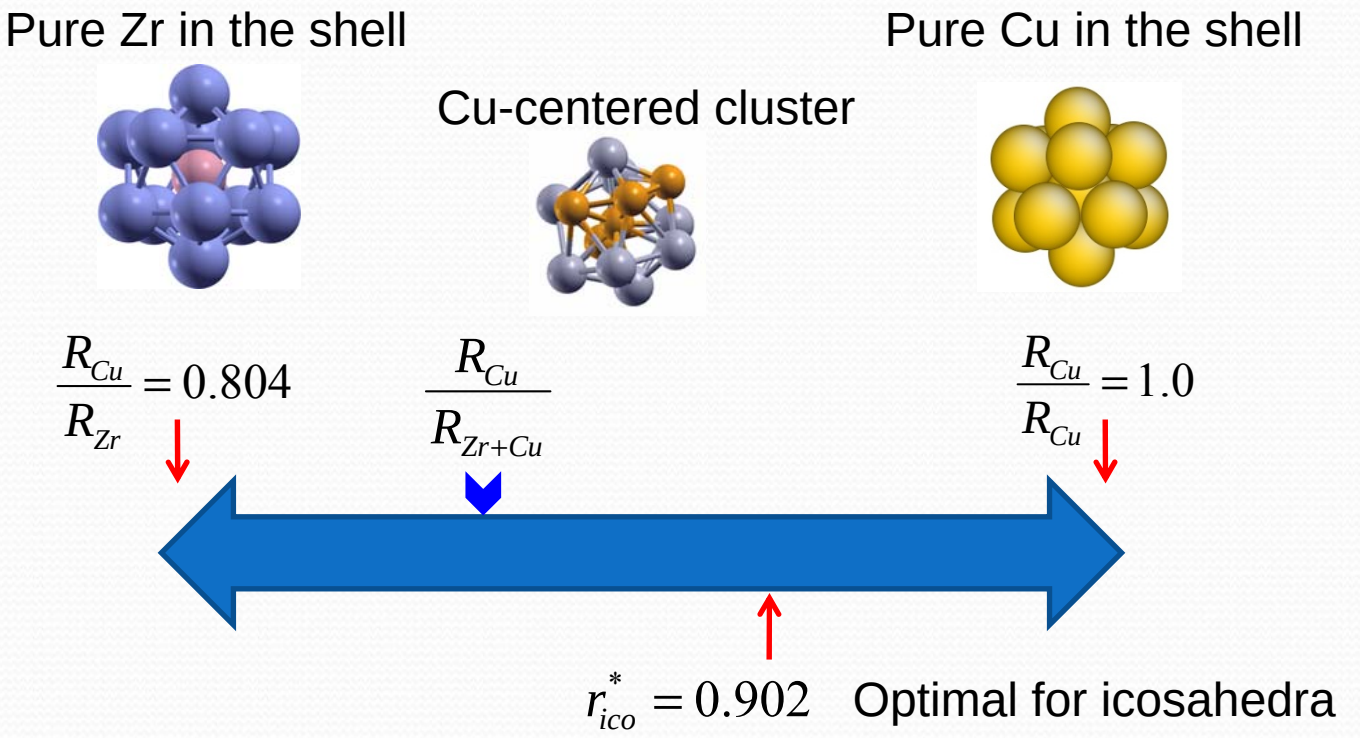

- Mixed Cu and Zr in the Cu-centered nearest-neighbor shell yields effective size ratio close to 0.9, favoring icosahedral packing.
- The changing SRO with composition in Cu-Zr is mainly a size effect.
- In terms of structure, Cu-Zr can be approximated as a homogeneous ideal solution/mixture of Cu and Zr atoms.

YQ Cheng *et al.*,

Phys. Rev. Lett. 102 (2009) 245501

Binary vs ternary:

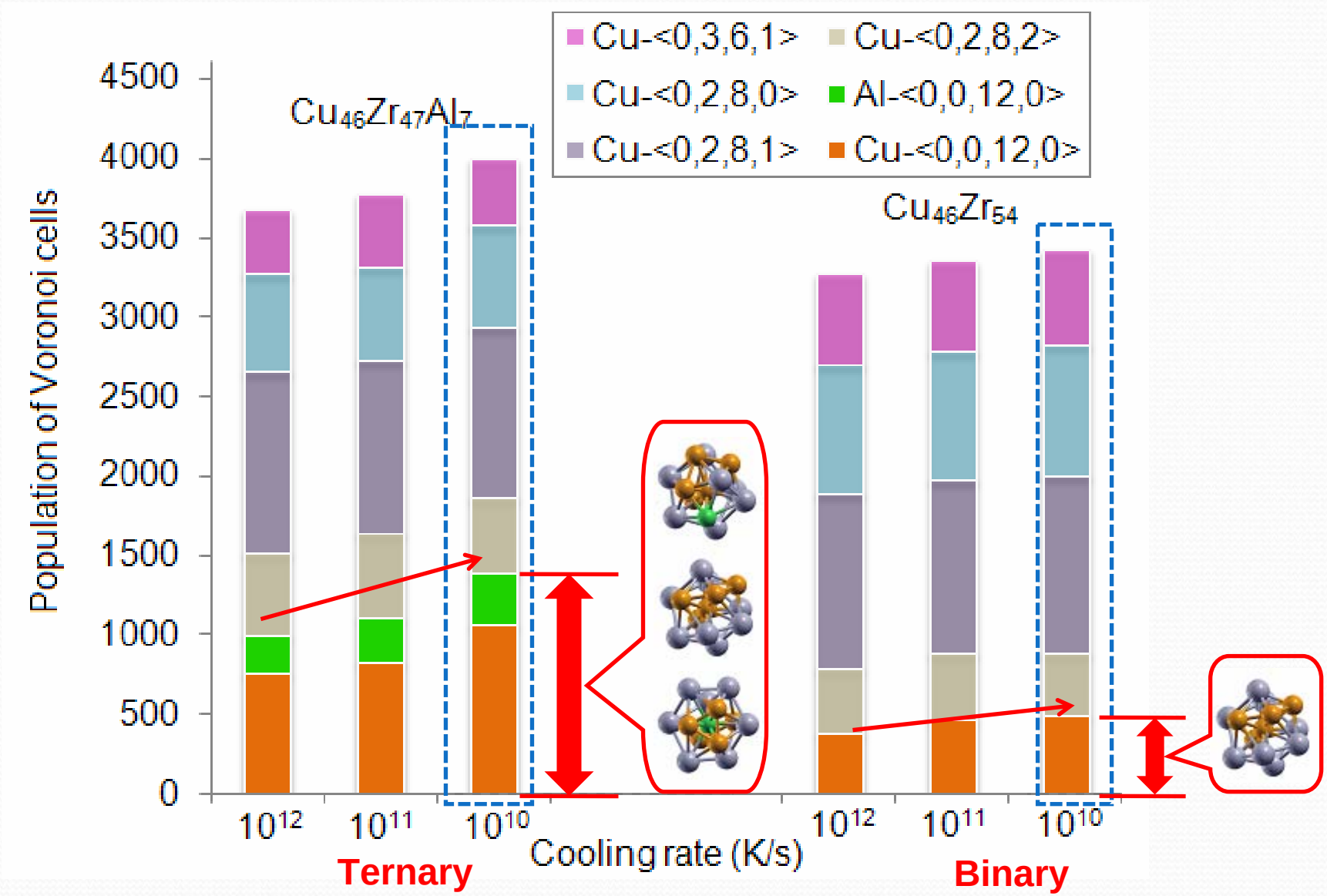

Evolution of full icosahedra during liquid cooling

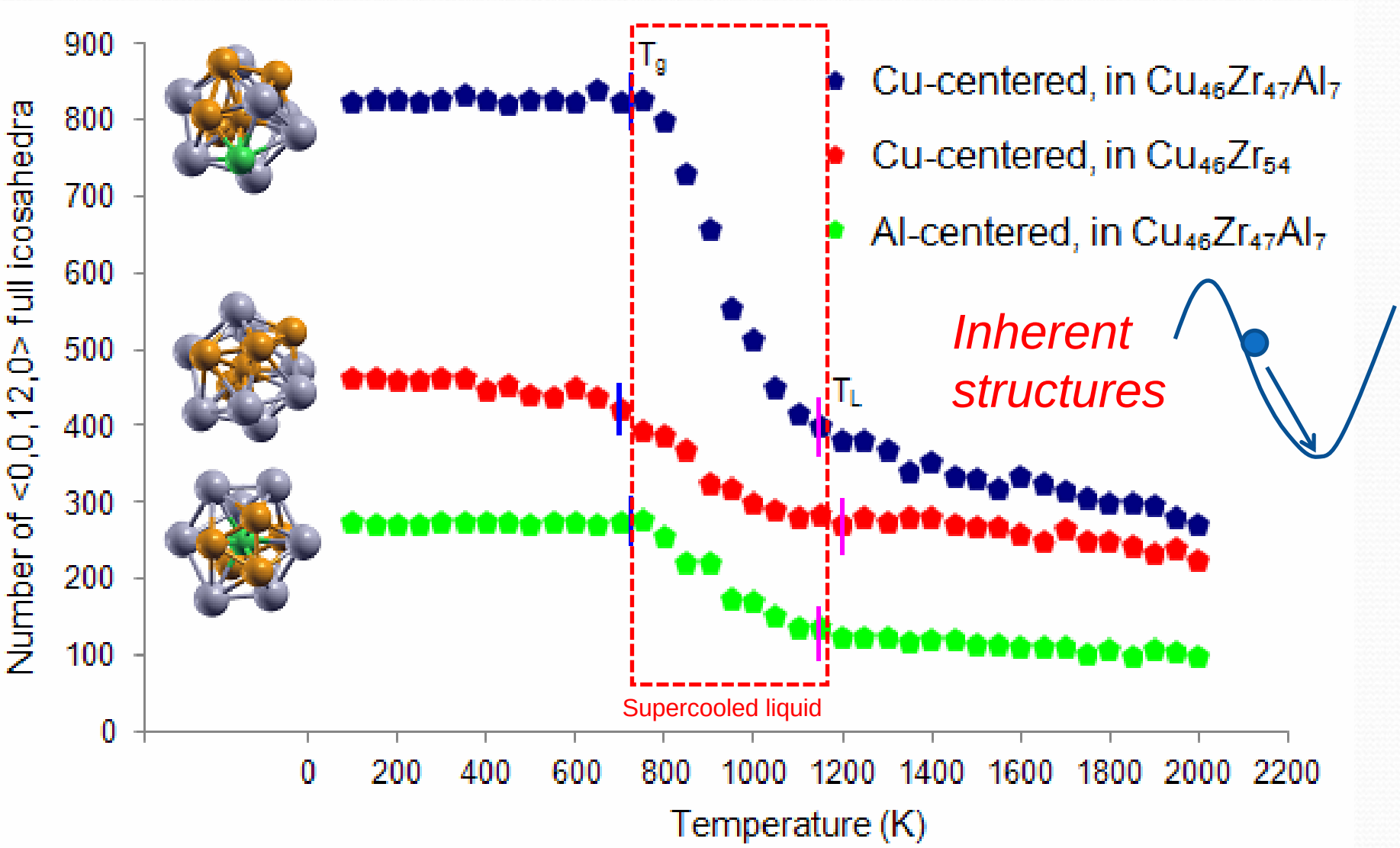

Real “amorphous structure” w/o crystal nuclei?

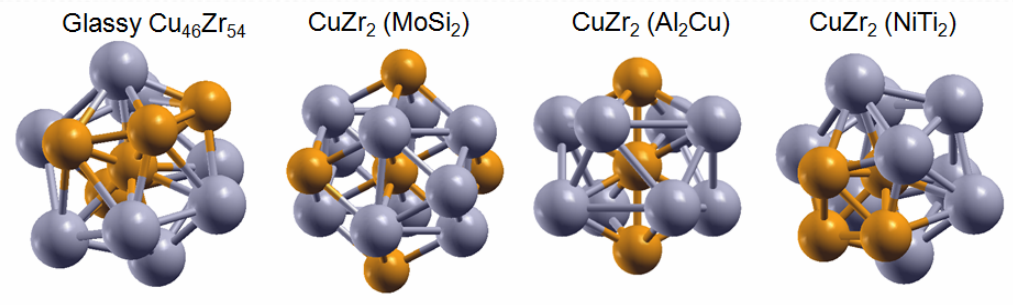

Different from crystal embryos, in terms of five-fold bonds, CN, bond lengths…

Icosahedral order means quasicrystals ?

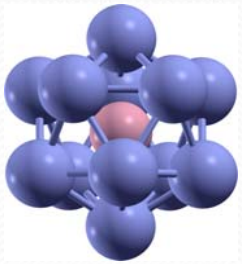

<0,0,12,0>
full icosahedron

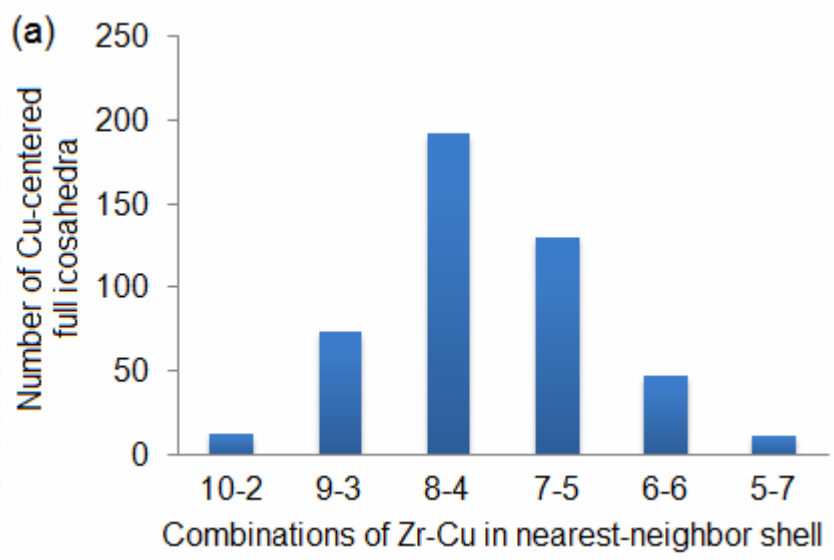

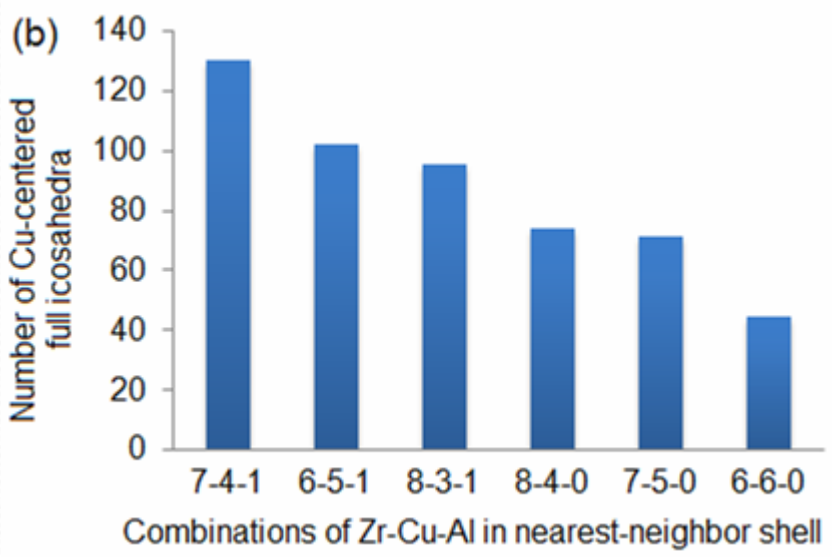

Interpenetrating connections to give medium-range order,

but no quasi-crystals

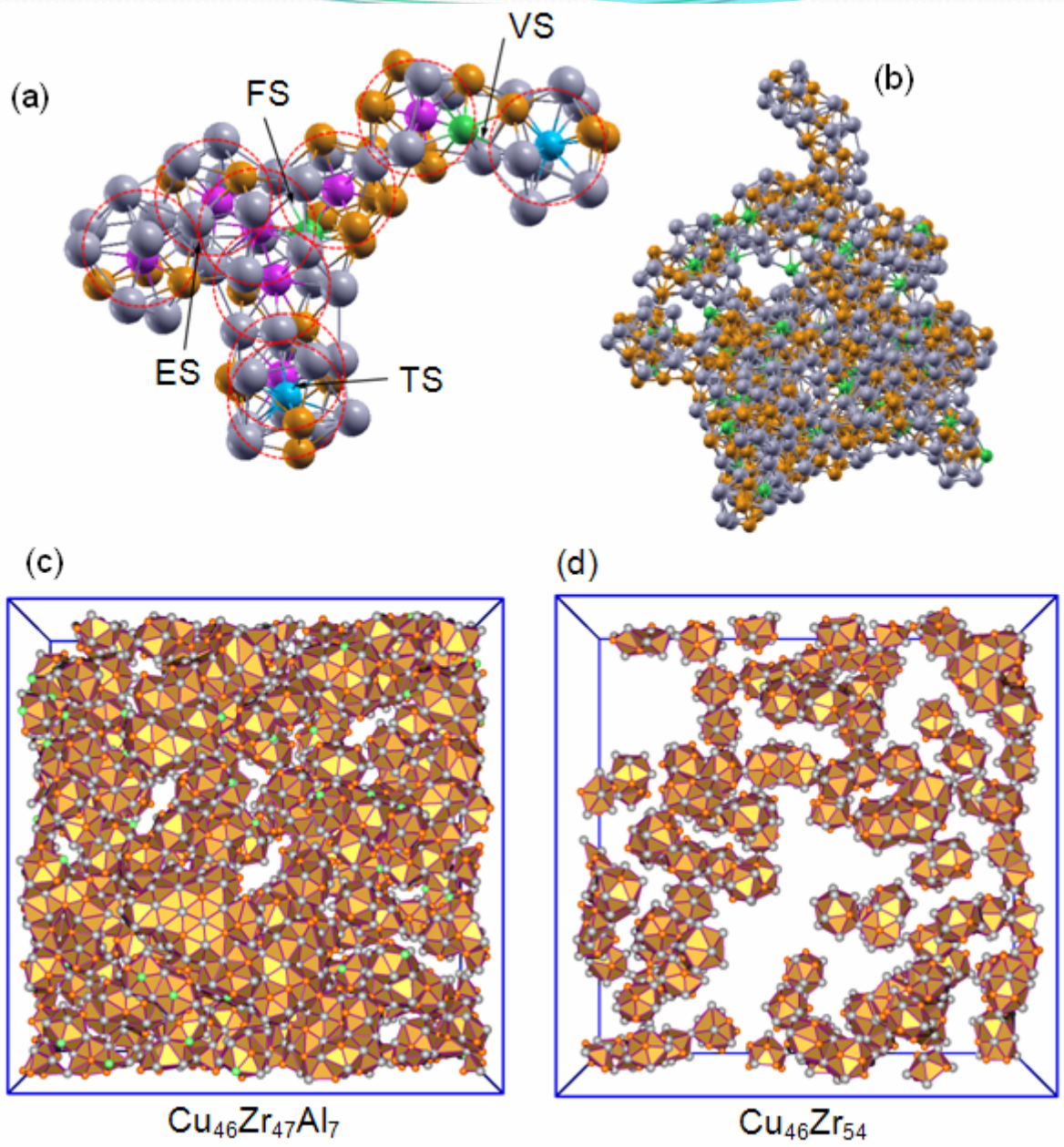

YQ Cheng *et al.*,

Phys. Rev. Lett. 102 (2009) 245501

Icosahedra formation means

hard-sphere packing and "topological order" only?

Full icosahedral order is a useful indicator of not only the local topology, but also the local chemistry (see Q#5 next) and energetic state, and can be conveniently used for differentiating different structural states

Q#5: Why would Al make a pronounced difference in structural ordering?

Effect of Al-addition on the structure

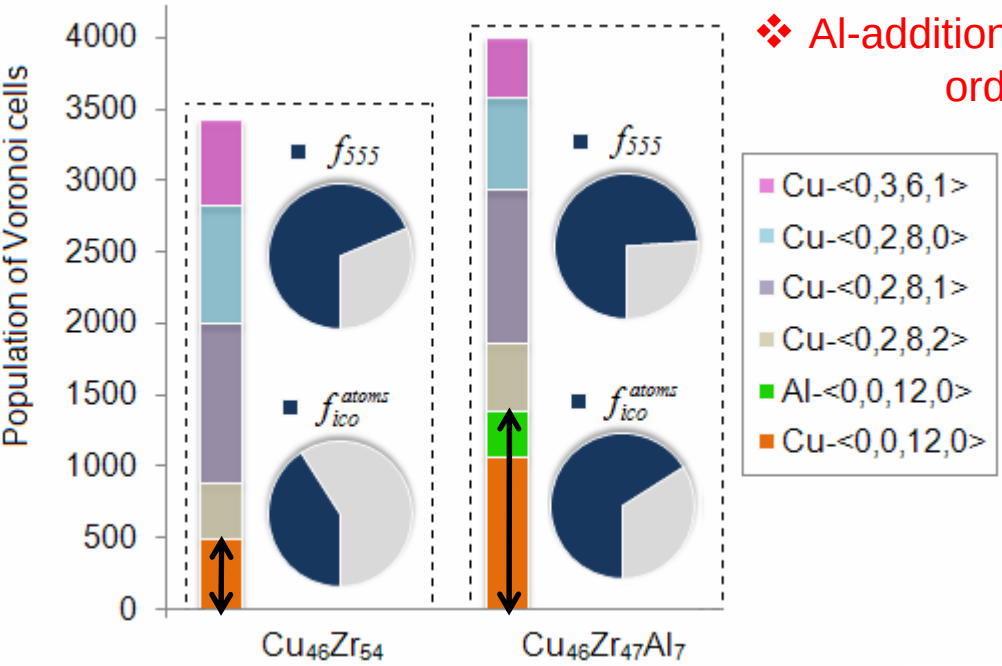

❖ Al-addition greatly enhances the degree of icosahedral ordering and five-fold bonds.

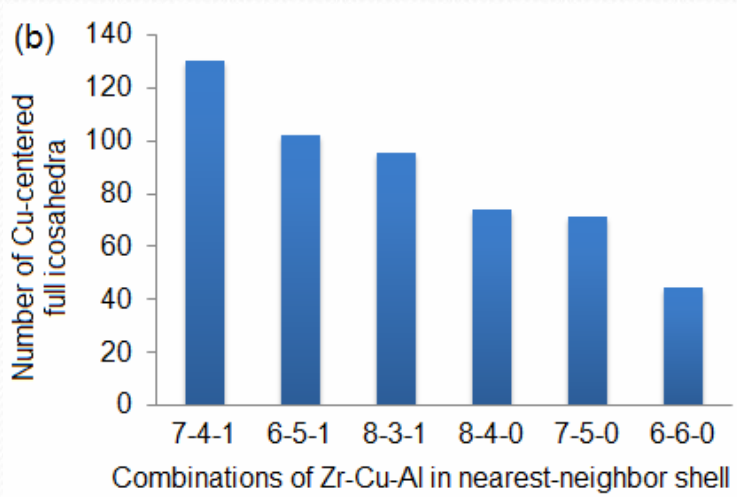

Topologically, more options to make Cu-icosahedra

$\frac{R_{Cu}}{R_{Zr}} = 0.804$ $\quad \frac{R_{Cu}}{R_{(Zr+Al)+Cu}}$ $\quad \frac{R_{Cu}}{R_{Cu}} = 1.0$

More combinations

$r_{ico}^{*} = 0.902$ Optimal for icosahedra

Metallic radii:

R_{Cu}=1.27 Å

R_{Zr}=1.58 Å

R_{Al}=1.43 Å

Atomic “size” can be local environment (chemistry) specific

There is also bond shortening, due to Hybridization b/t Al *sp* and Cu *d* electrons, chemically stabilizing the icosahedra, and producing many Al-centered icosahedra w/ Cu and Zr in the shell even though

$R_{Al}/R_{Zr} = 0.905$

Cu-Al bond ~5% shorter

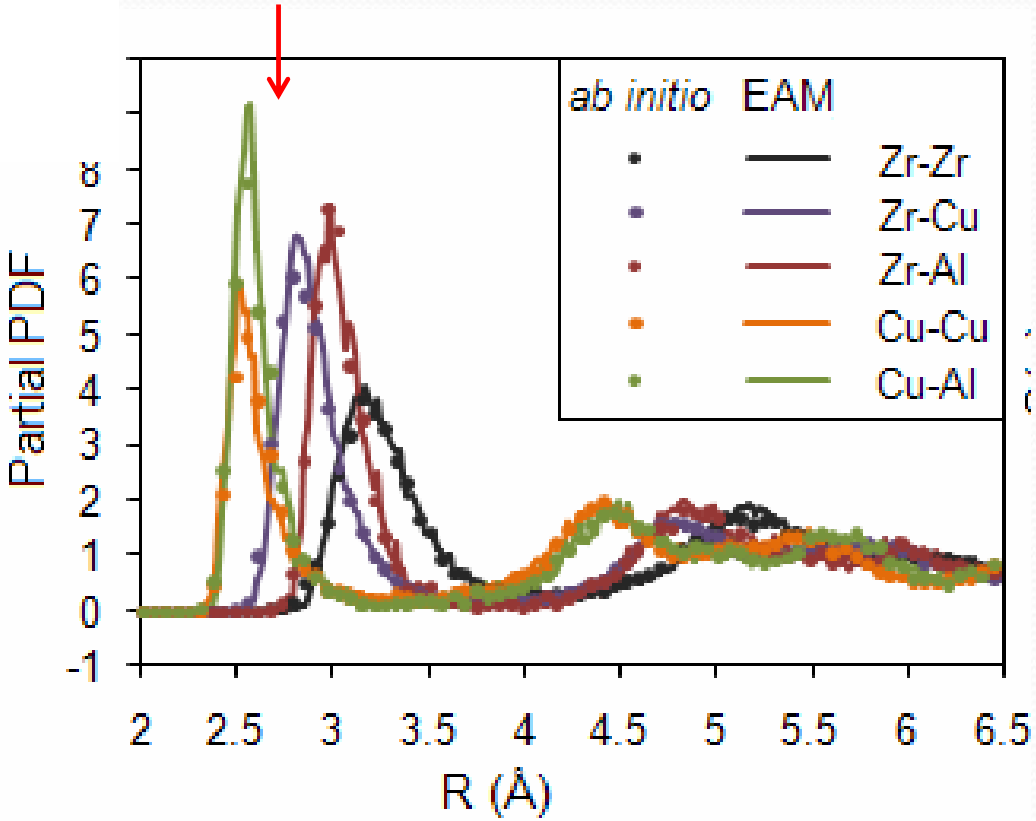

Al-centered icosahedra: the effects of Cu-Al bond shortening

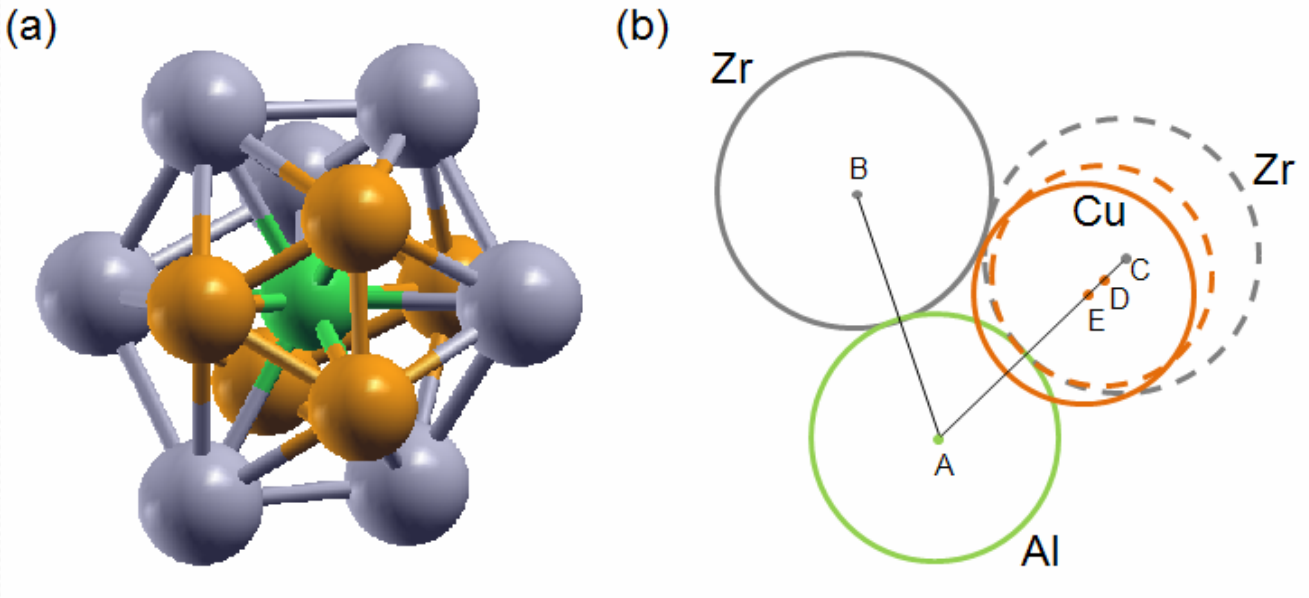

Cu (replacing Zr) appears larger than expected (taking larger solid angle) from the view point of the center Al.

The plot above using real bond lengths shows compact packing eliminating the extra space b/t Cu and Zr

YQ Cheng *et al.*
Phys. Rev. Lett. (2009)

Cu-Al bond shortening:

atomic “size” can be local environment (chemistry) specific

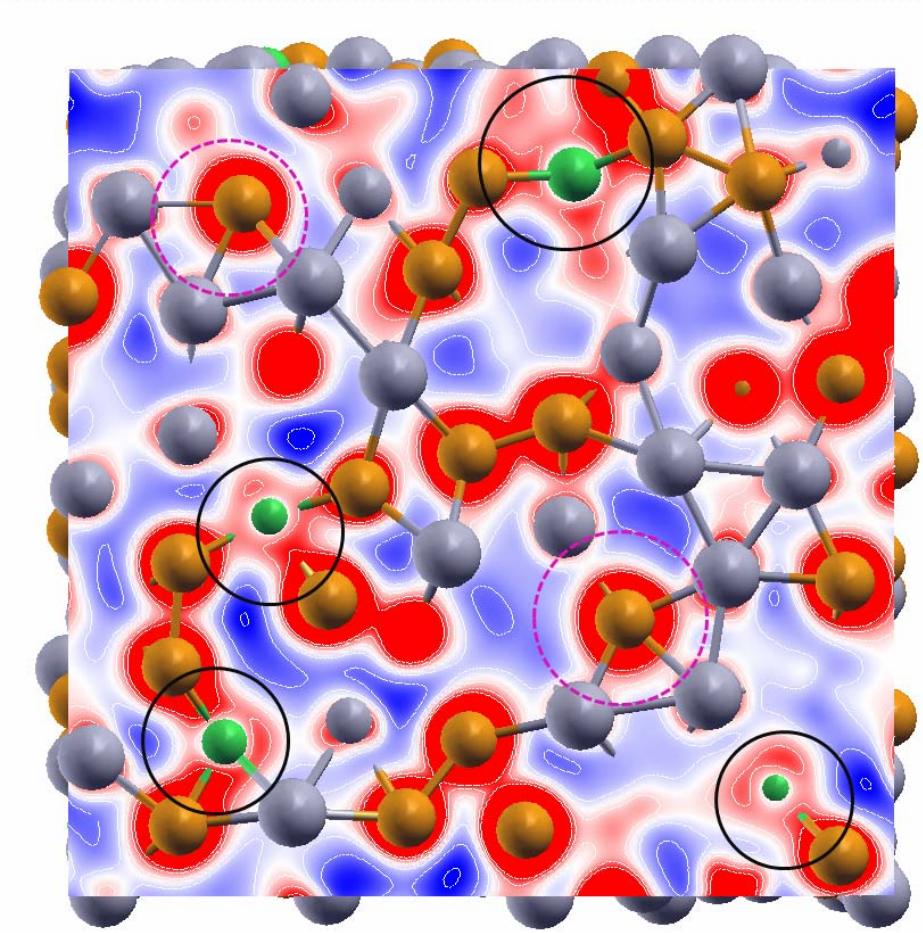

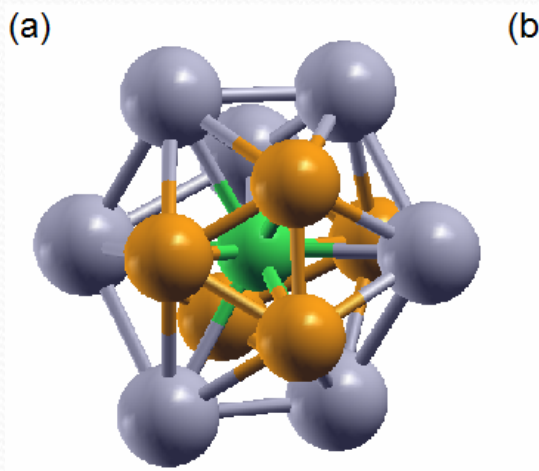

Q#6: These structure features

influence relaxation properties ?

Relaxation dynamics in Cu-Zr supercooled liquid

❖ Measure the relaxation rate in MD-simulated Cu-Zr

$$F_s^a(q,t) = N_a^{-1}\left(\sum_{j=1}^{N_a} \exp\{i\vec{q}\cdot[\vec{r}_j^{\,a}(t) - \vec{r}_j^{\,a}(0)]\}\right)$$

Intermediate scattering function (ISF): decay with structural relaxation

How fast the ISF decays ⇔ α -relaxation time ⇔ Viscosity

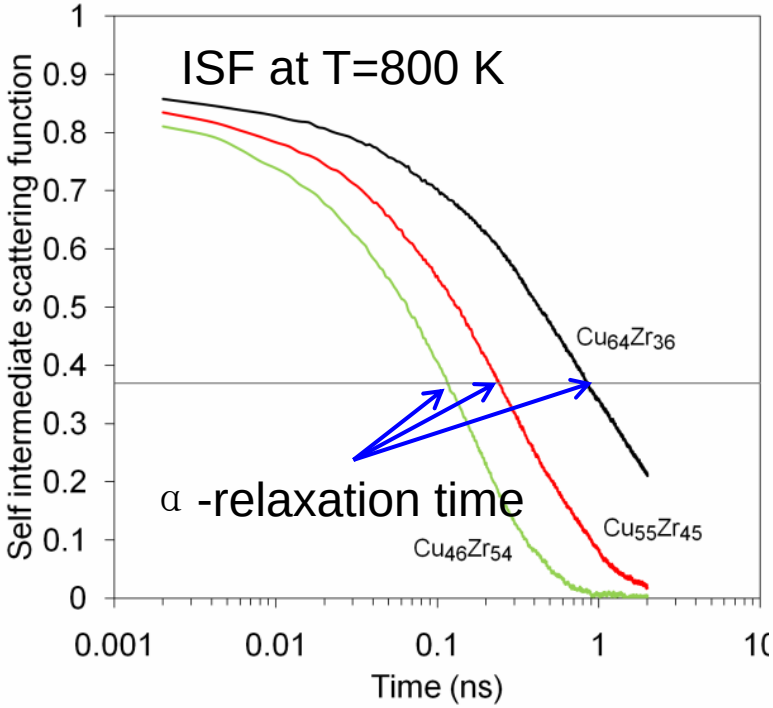

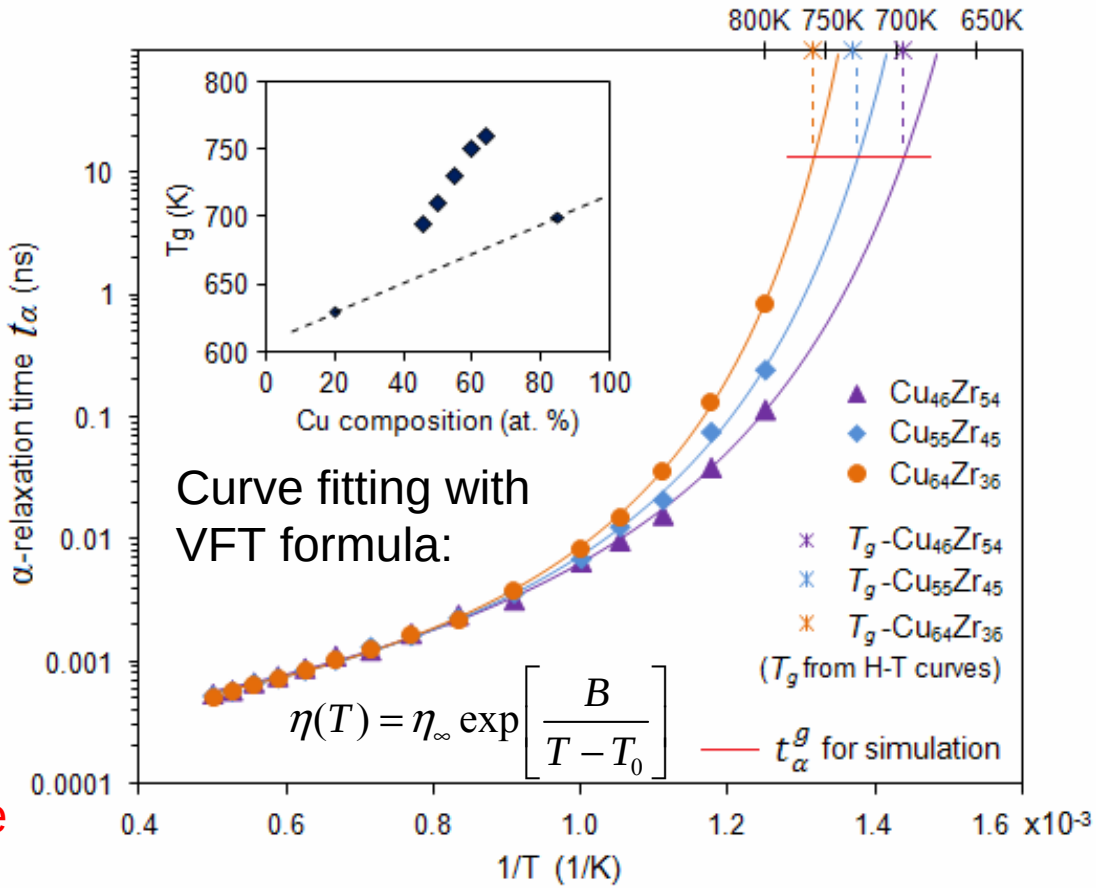

Cu-richer liquid has longer relaxation time and larger viscosity, at the same temperature.

Structure-dynamics correlation in Cu-Zr supercooled liquid

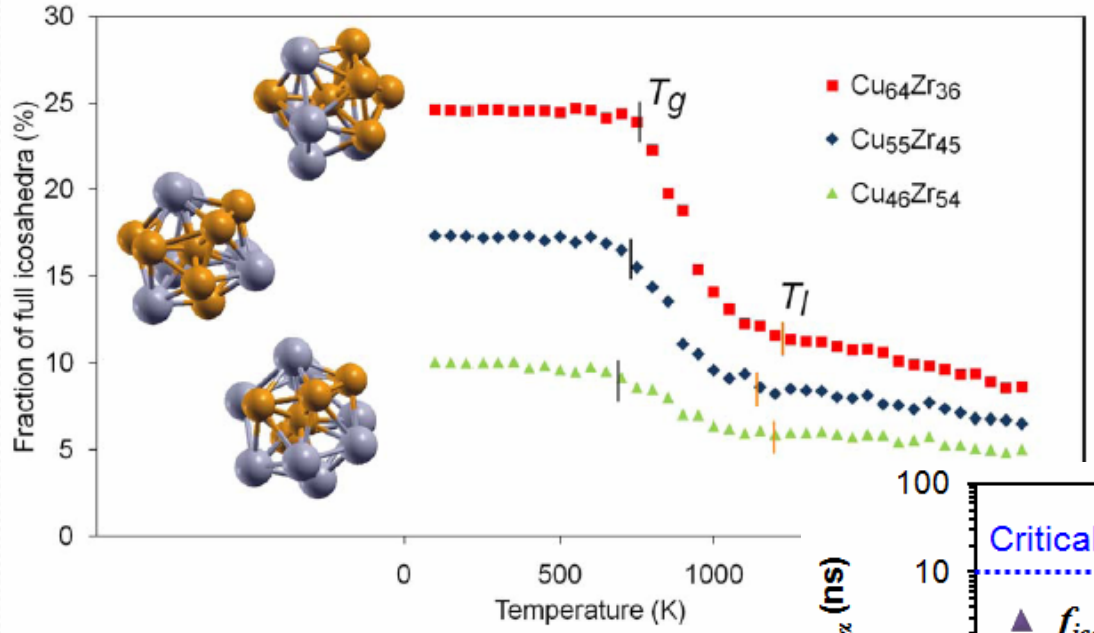

Structural ***signature*** of the dynamical slowdown

Y.Q. Cheng et al., APL 93, 111913 (2008).
Y.Q. Cheng et al., PRB 78, 014207 (2008).

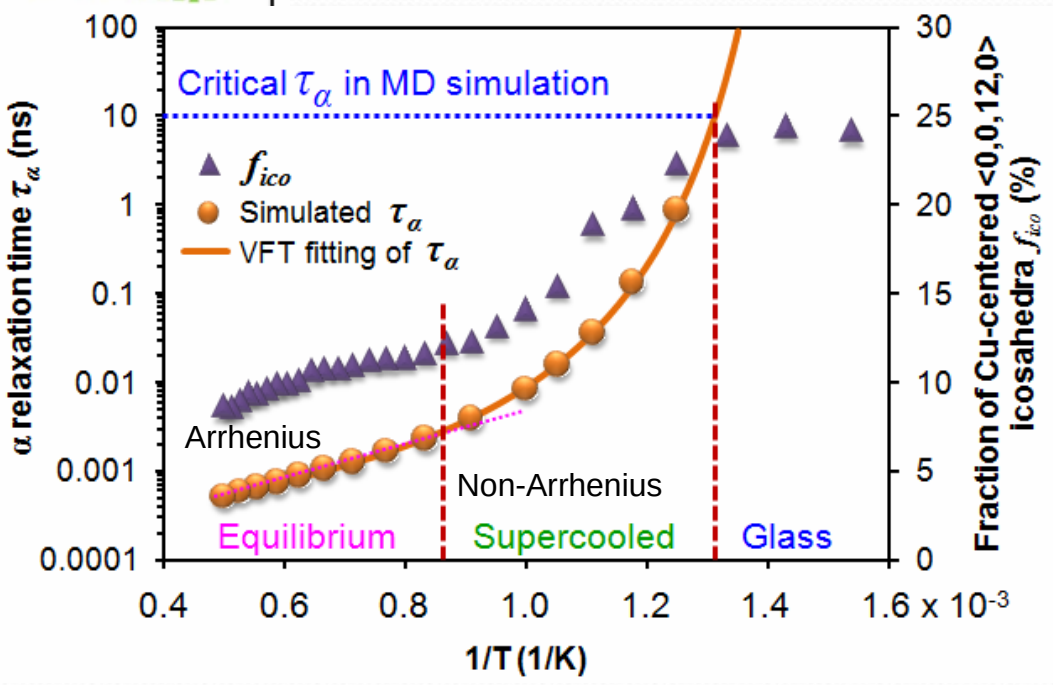

❖ Evolution of Inherent structures, i.e., the change of intrinsic structural state, in the liquid.

❖ The rapid formation of full icosahedra in supercooled liquid may be responsible for the dynamical slowdown and subsequent glass transition.

Structure-dynamics correlation in Cu-Zr supercooled liquid

❖ Structure ***origin*** of the dynamical slowdown

Correlation between atomic mobility and local structure

Measure of atomic mobility: the mean square displacement

✓ Maximize the influence of structure

$$\alpha_2(t) = \frac{3\langle r^4(t)\rangle}{5\langle r^2(t)\rangle^2} - 1$$

✓ Minimize the influence of initial momentum: ensemble average

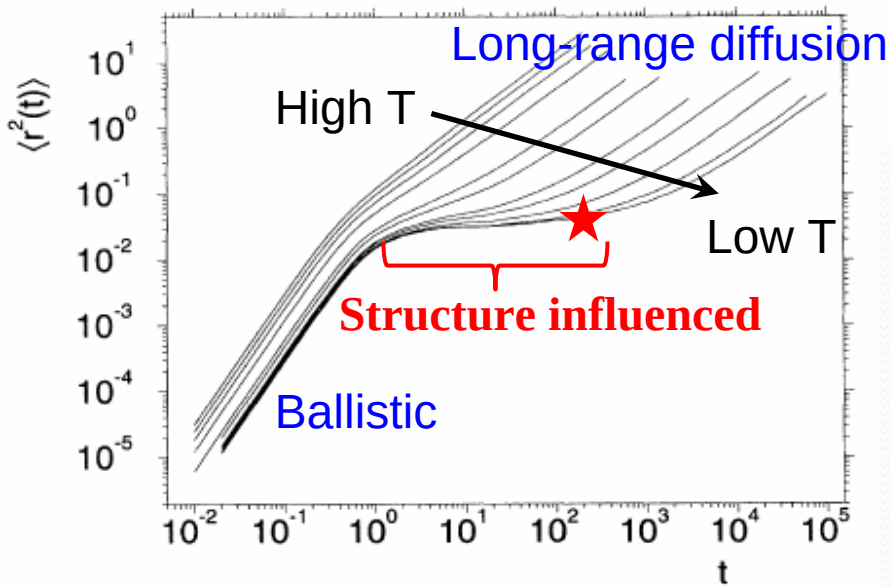

W. Kob, et al. Phys. Rev. E 51, 4626 (1995)

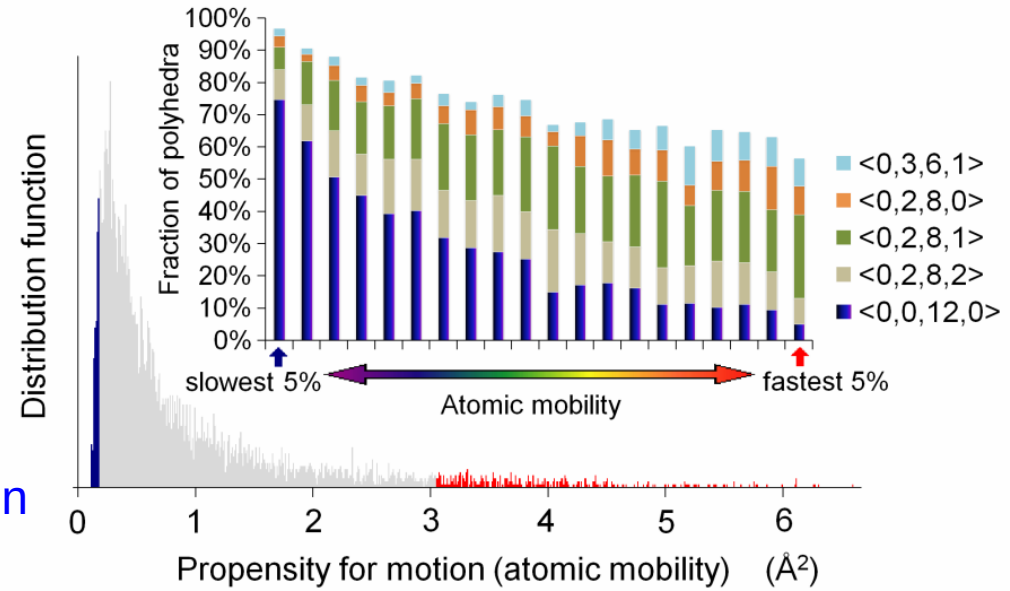

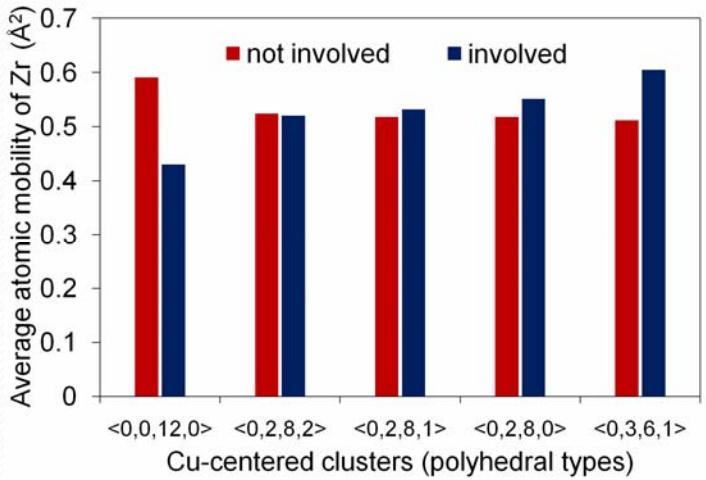

Structural origin of the thermodynamics, kinetics & GFA

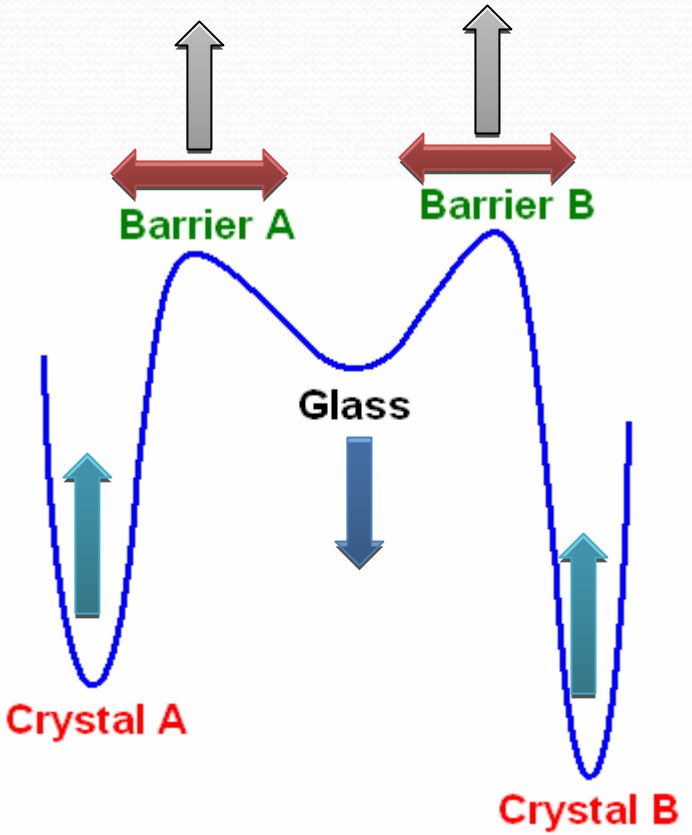

Thermodynamics:

Stabilize glass: more icosahedra,
more (Al) stable icosahedra,
better connection,
higher local symmetry,
less atomic-level stresses

Kinetics:

1. Frustrate and confuse compound formation
2. Increase transition barriers:
   full icosahedra as stabilizer,
   slower α-relaxation,
   stronger liquid

Q#7: Structural origin of the shear transformations ?

Important structural motifs in $Cu_{64}Zr_{36}$ MG

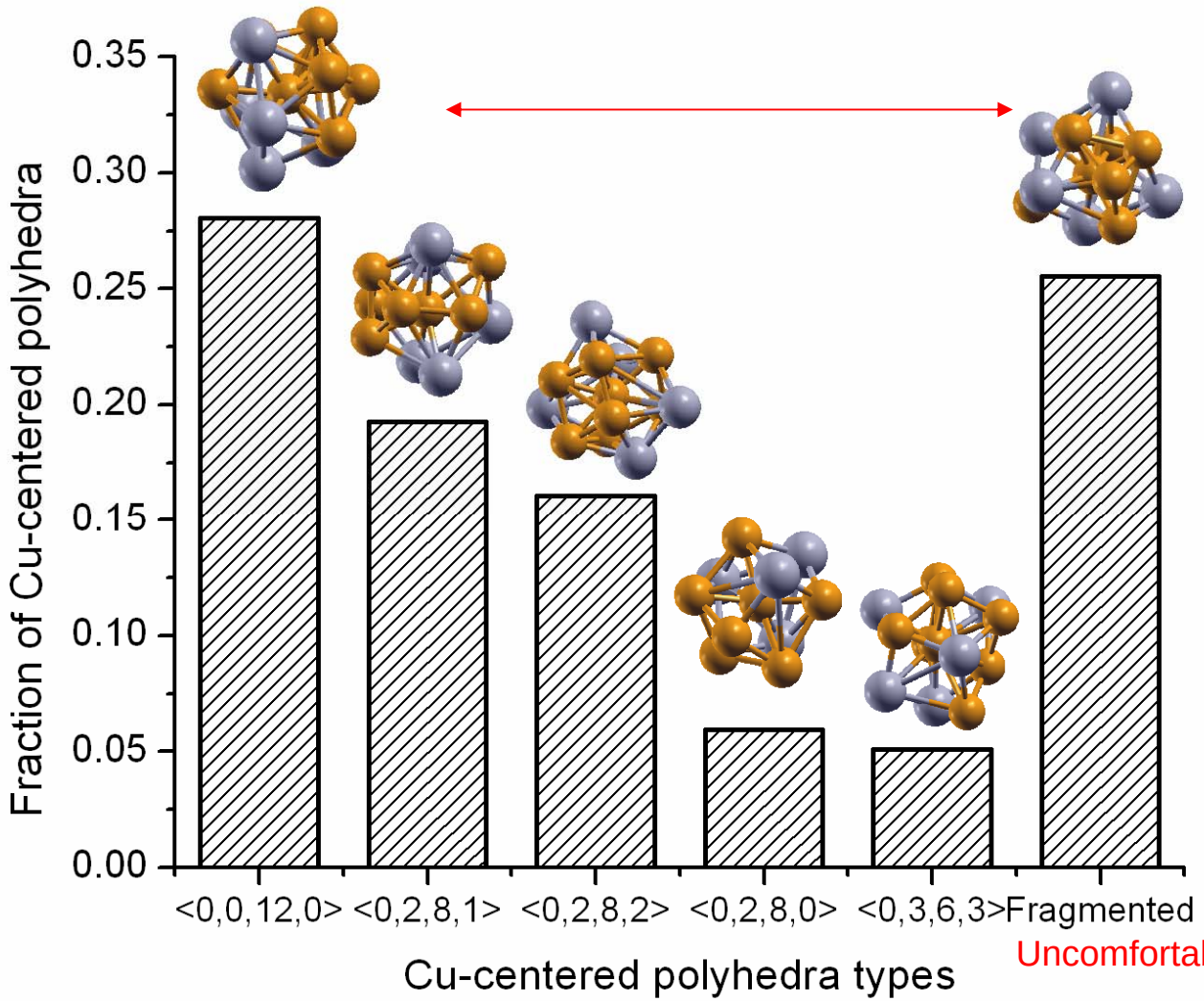

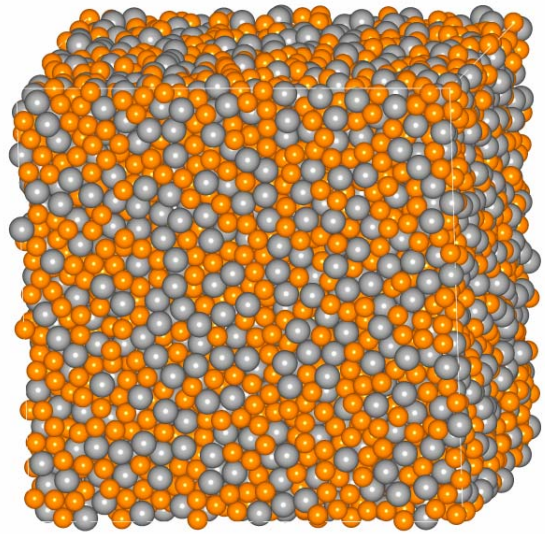

Undesirable and
unusually high/low CN

Low population for each type,
Decreasing w/ increasing FI

Non(or fragmented)-
Kasper clusters

Relatively unstable,
willing to re-configure to lower E,

Fertile sites for
shear transformations ?

Uncomfortable clusters (***liquid-like structure***)

Evolution upon cooling:

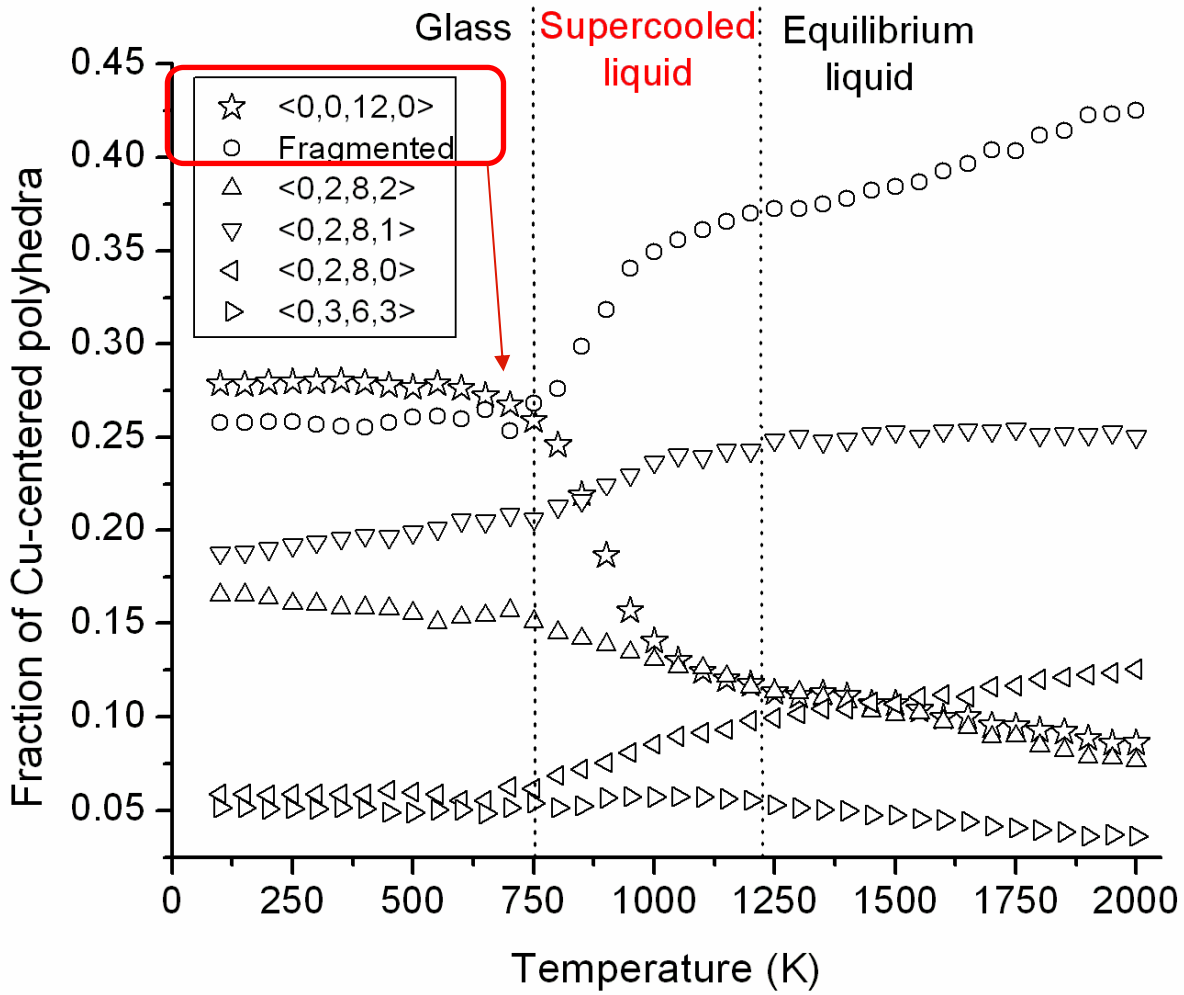

$Cu_{64}Zr_{36}$

Structure is inhomogeneous on nm scale (potential " flow defects")

plasticity carriers

~ 80 atoms

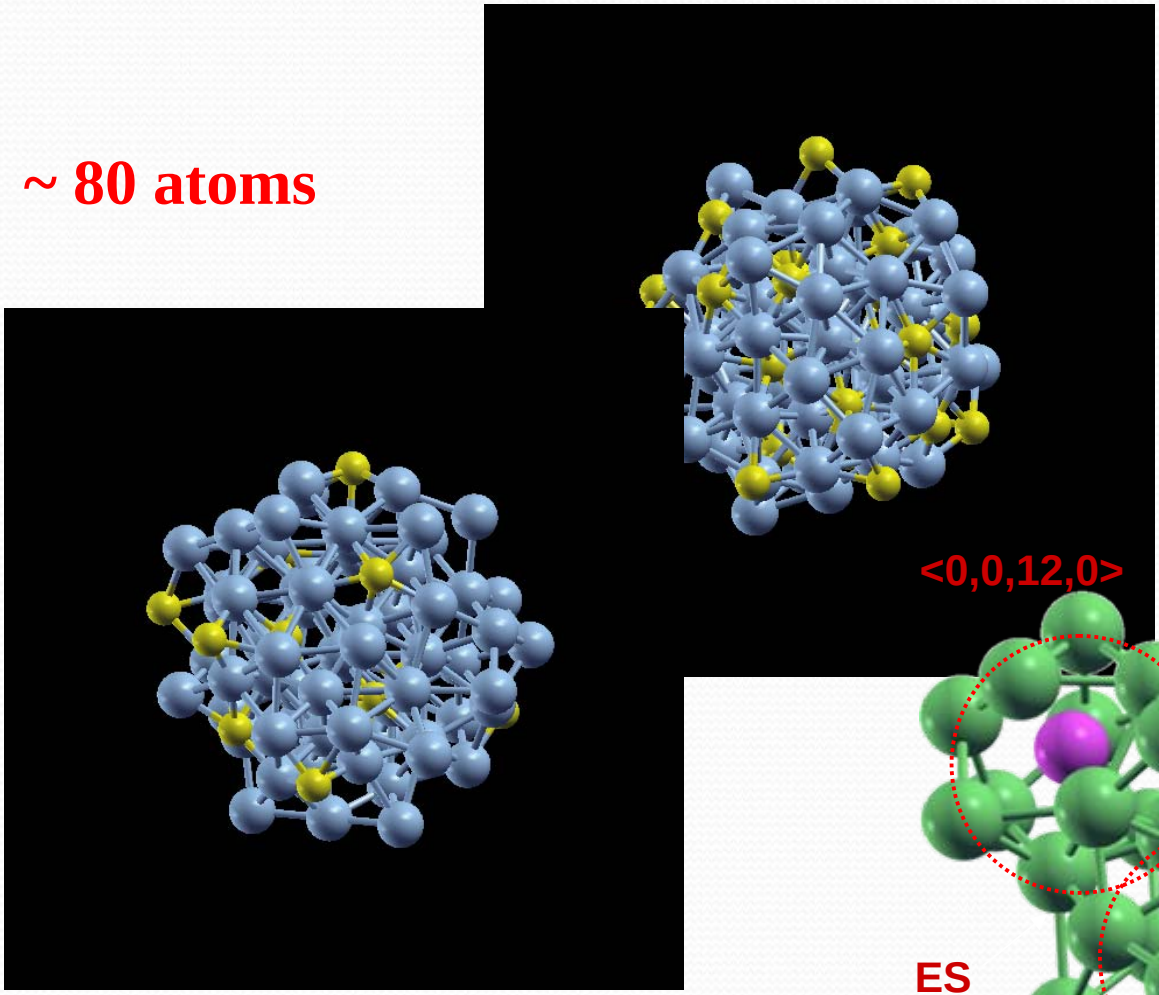

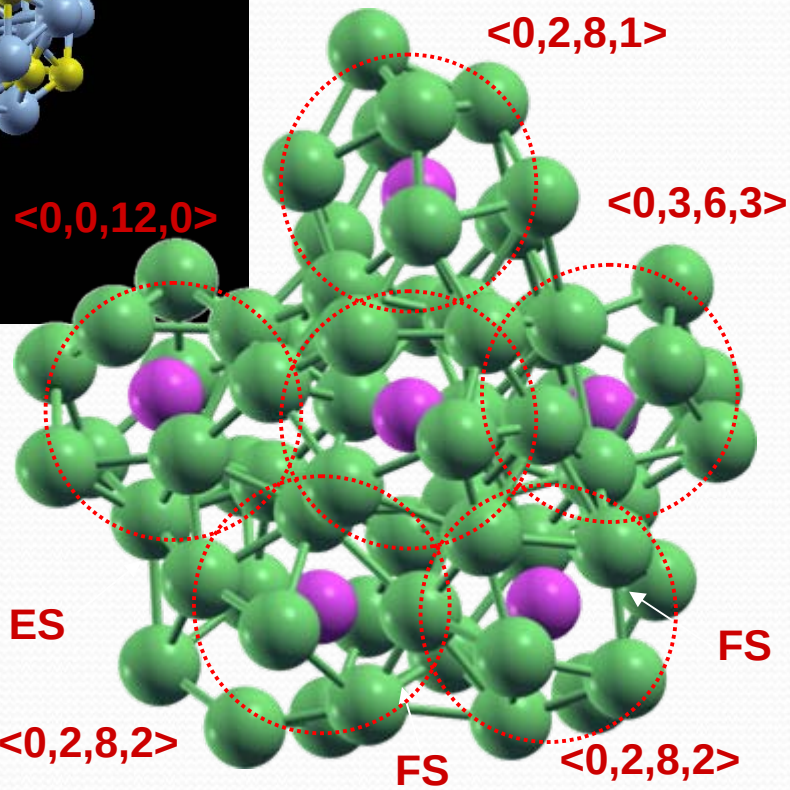

Upon shearing the box……

YQ Cheng, A Cao, HW Sheng and E Ma
Acta Mater. 56 (2008) 5263

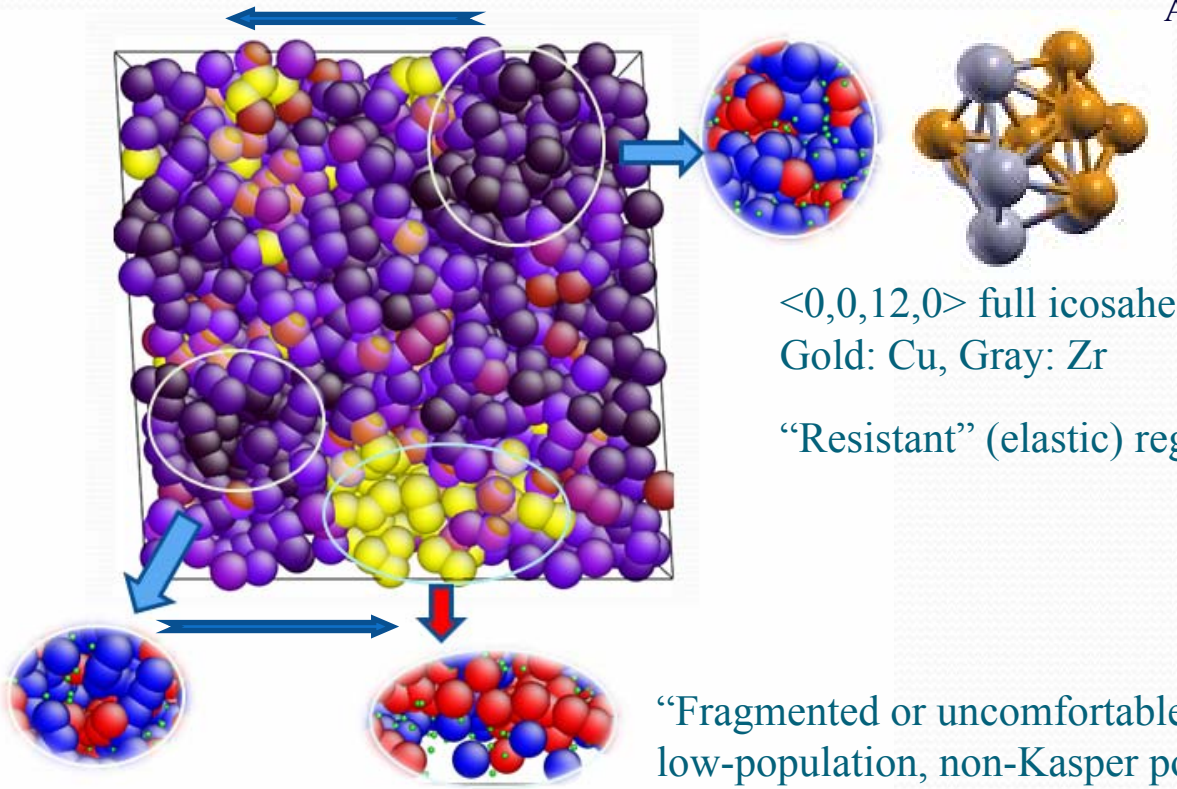

<0,0,12,0> full icosahedron
Gold: Cu, Gray: Zr

"Resistant" (elastic) region

Non-affine strain
as an indicator,
see Falk & Langer

"Fragmented or uncomfortable"
low-population, non-Kasper polydedra

"Fertile" (plastic) sites in these ***liquid-like*** regions

Different local structure is indeed the origin of different ST behavior

Sample overall strain →

Full icosahedron

versus

Uncomfortable clusters

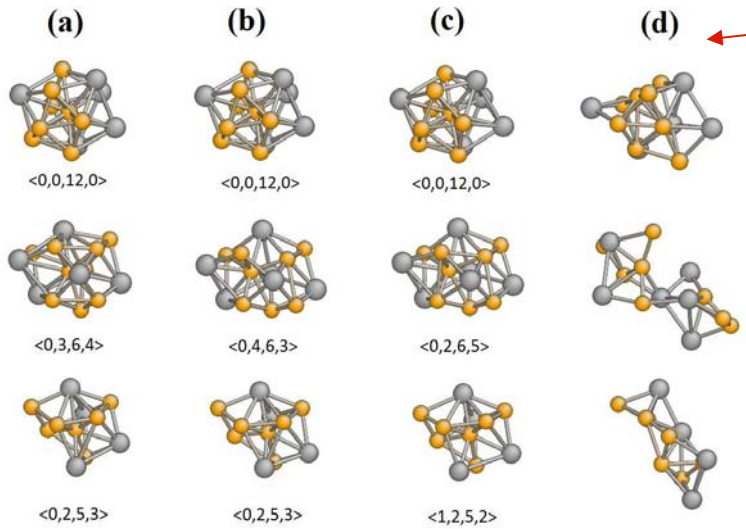

Upon the initiation of shear localization

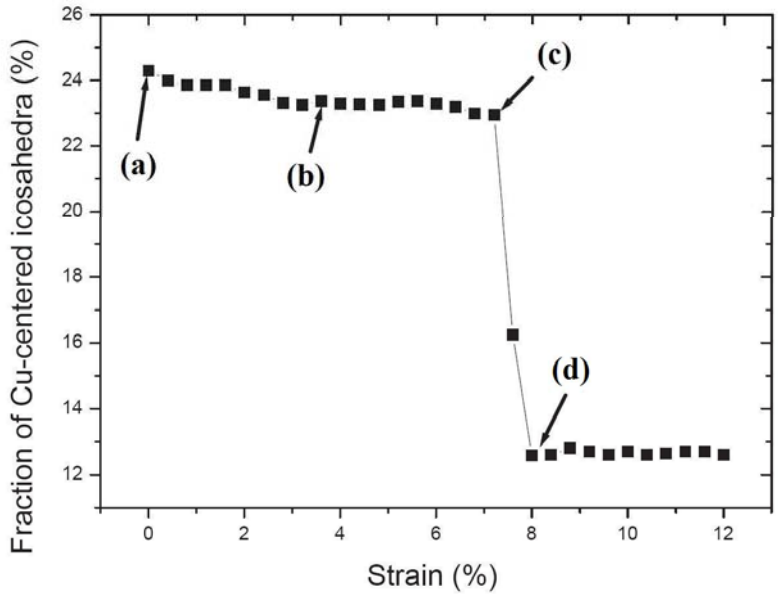

AJ Cao et al.,
Acta Mater. 57 (2009) 5146

Shear band initiation and the structural process

Atomic strain

Fraction of full icosahedra

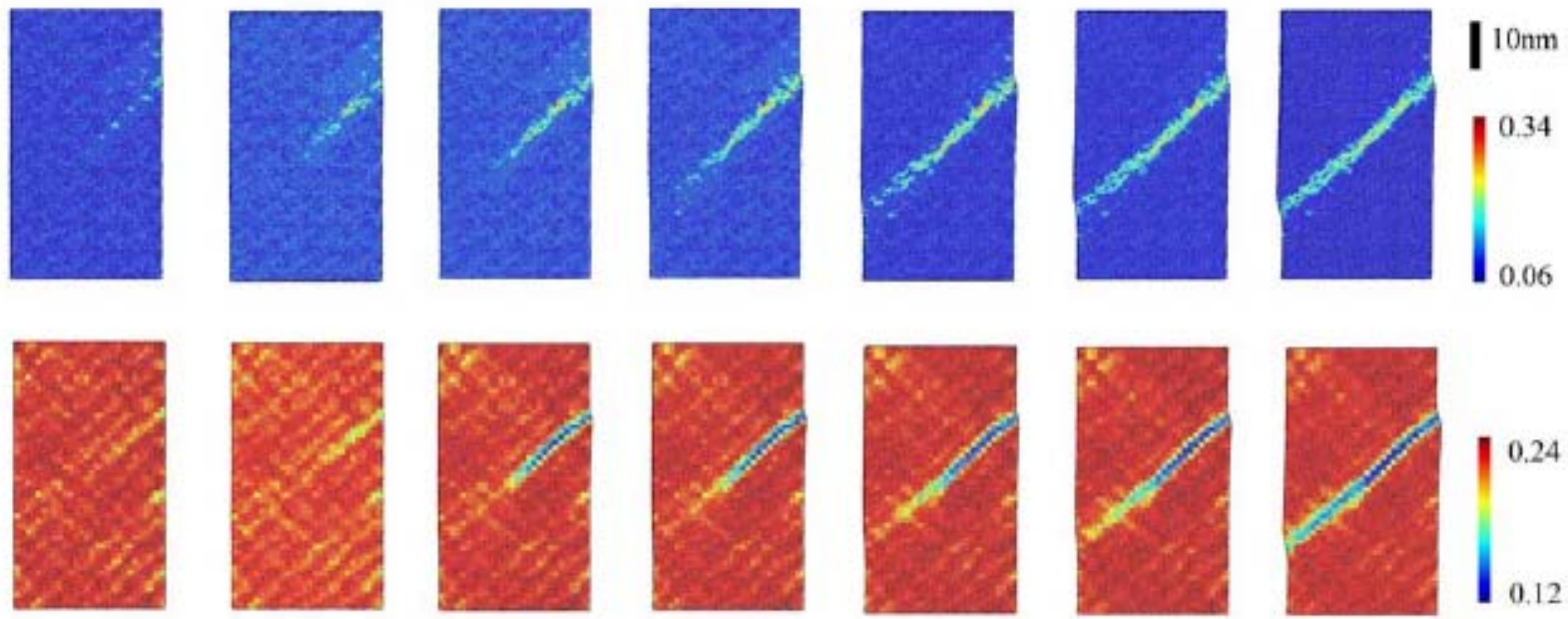

A. J. Cao, Y.Q. Cheng and E. Ma, Acta Mater. 2009

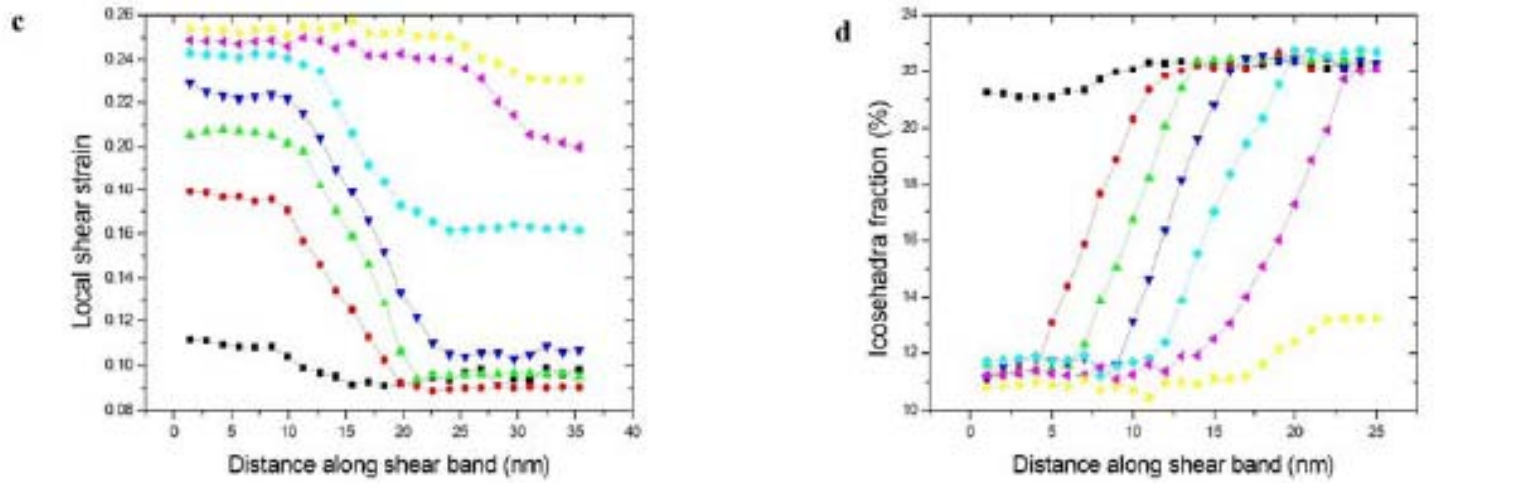

A direct demonstration of structure disordering in a shear band

YQ Cheng, AJ Cao and E Ma, Acta Mater. 57(2009)3253

Different compositions (structures), different tendency for localization

Cu20Zr80

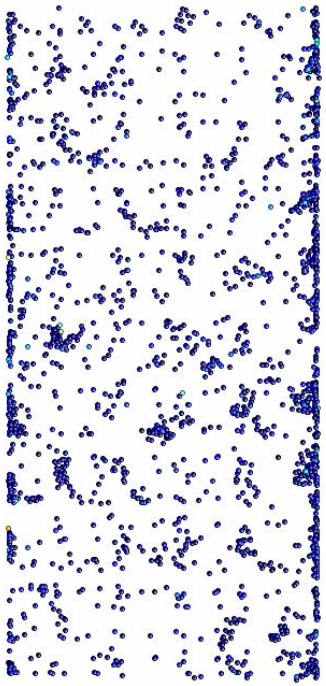

30 nm

Cu64Zr36

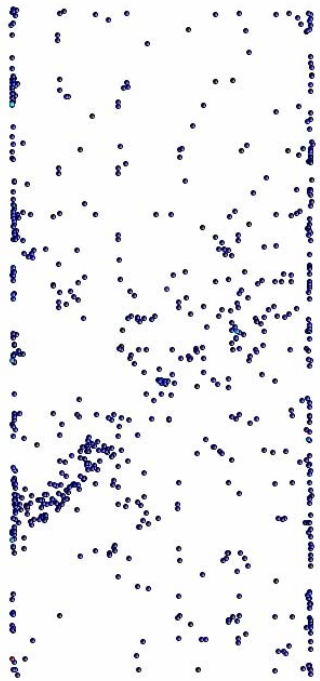

More STs and (wider) SB

More localized strains in narrower SB

Rapidly quenched MG =>

ductility and gradual necking

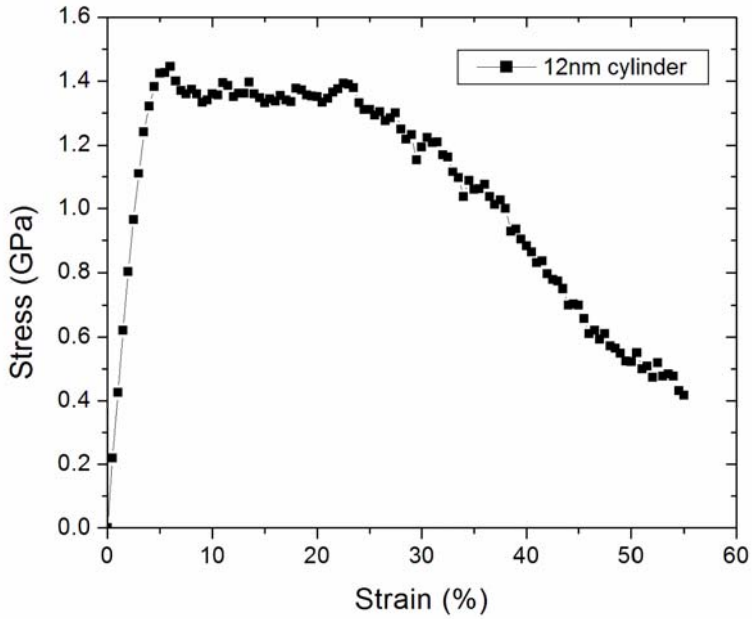

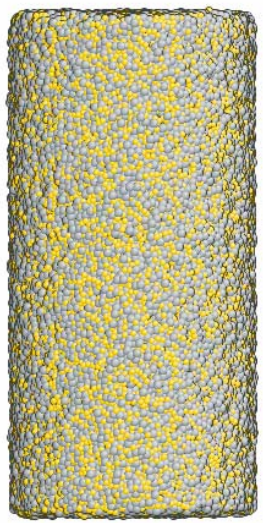

12 nm diameter

MD-generated $Cu_{50}Zr_{50}$ MG

Q#8: What are the structural features in covalently bonded GST glass?

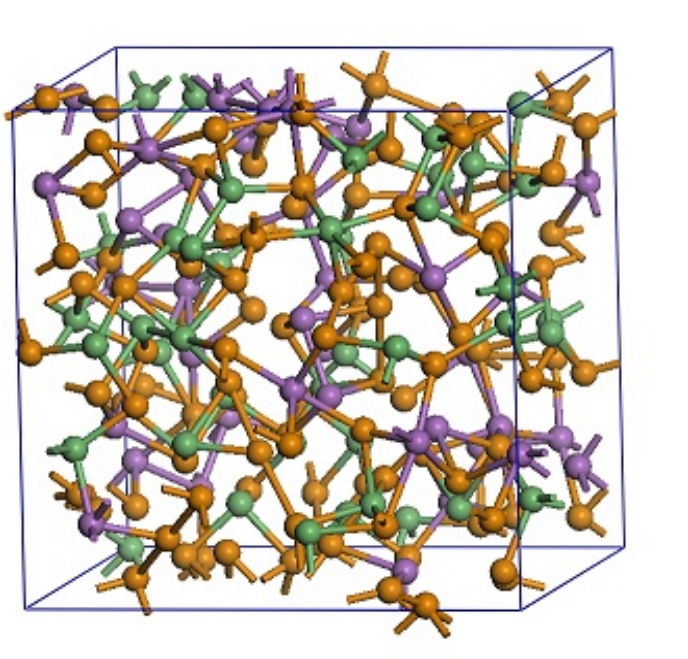

Ball-stick model (189 atoms) of *a*-GST, *ab initio MD*-quenched from liquid to 300 K.

Density: 6.11 g/cm^3.

Ge: green, Sb: purple, Te: orange.

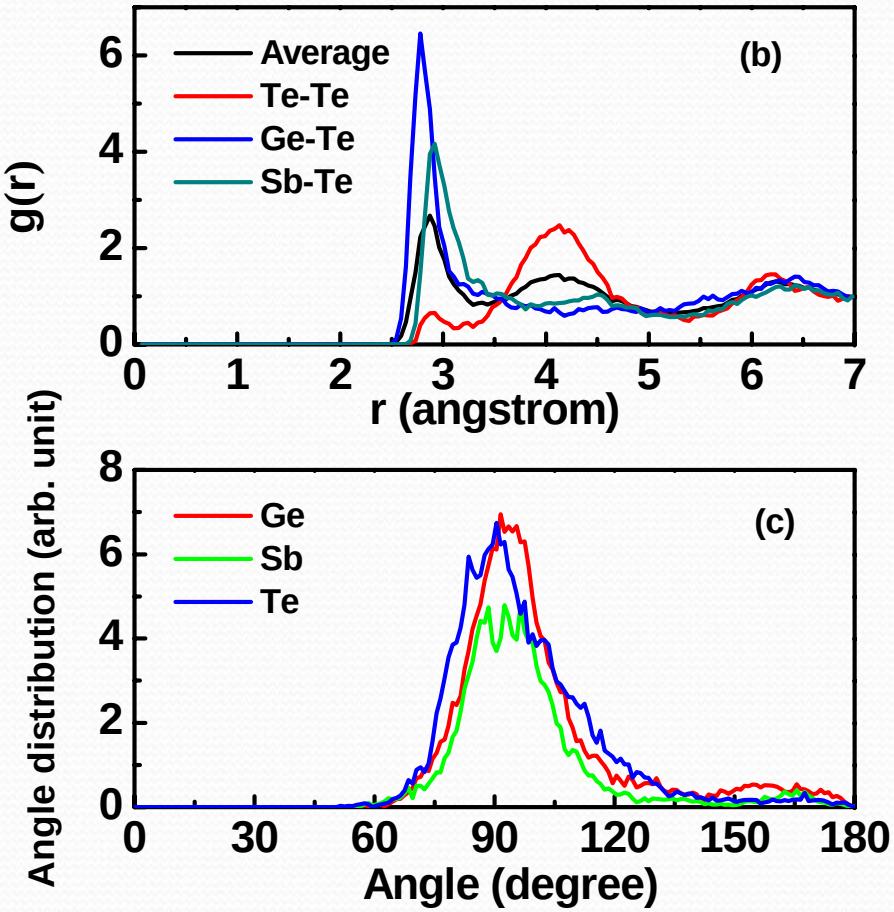

Calculated total and partial pair-correlation functions and bond-angle distributions of *a*-GST, Showing dominant 90^o bonds, even for Ge.

Q#9: Why do we have preferential right-angled environment even for Ge in the GST glass?

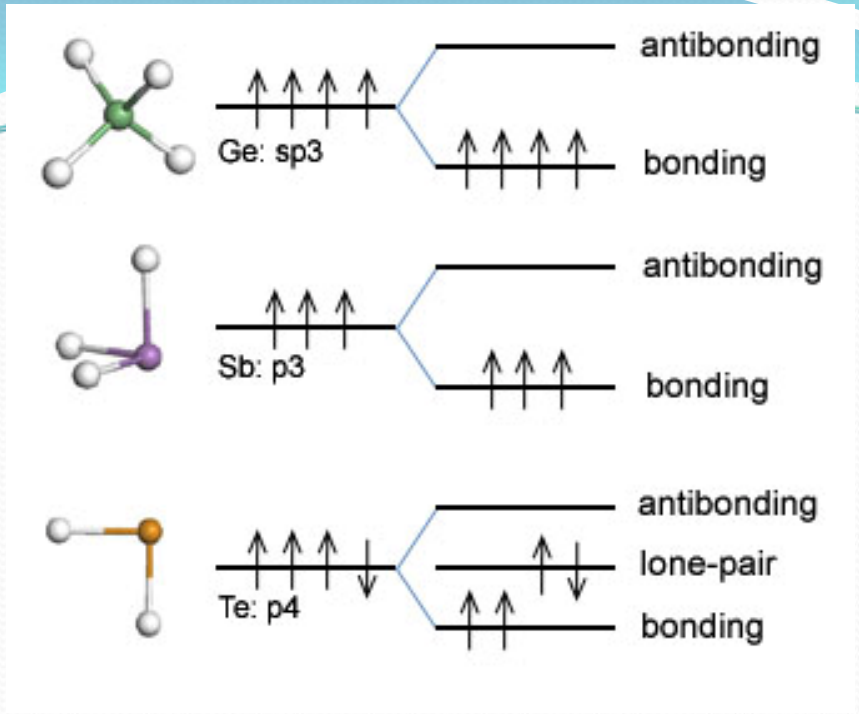

Need to examine valence electrons and their bonding state in a-GST

Schematic of the electronic structure and the bonding geometry of Ge, Sb, and Te in *ideal* glass model

M. Xu *et al*., PRL 103 (2009) 195502

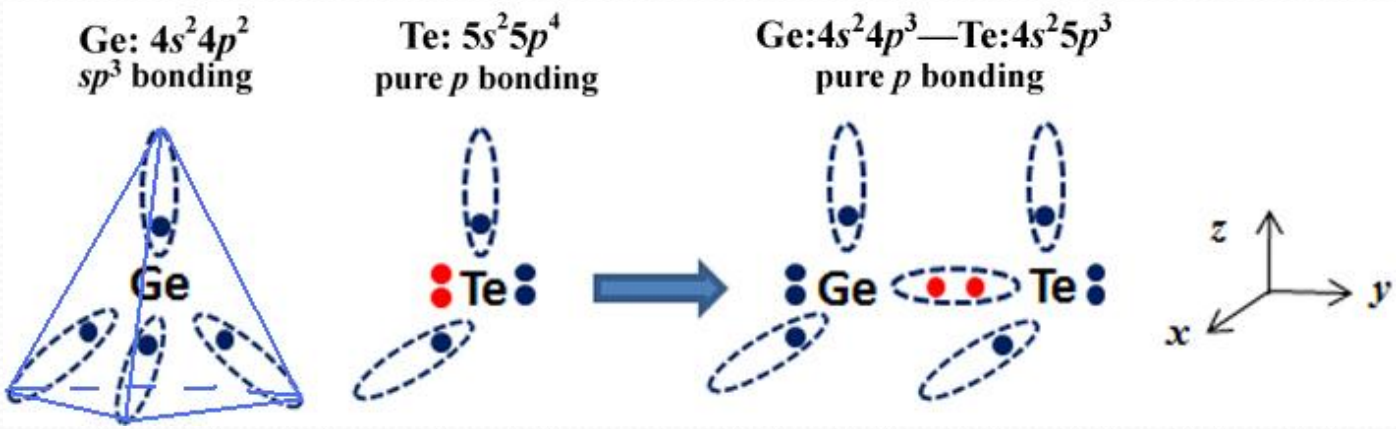

Valence alternation process between Ge and Te. In 3-D, the sp^3 bonds form tetrahedron (hybridization) with bond angles of 109º, while the p bonds are perpendicular to each other. Valence alternation changes the CN of the Ge and Te, as well as the bond angle around Ge.

Are the 90^0-bonded Ge really in 3-fold environment ?

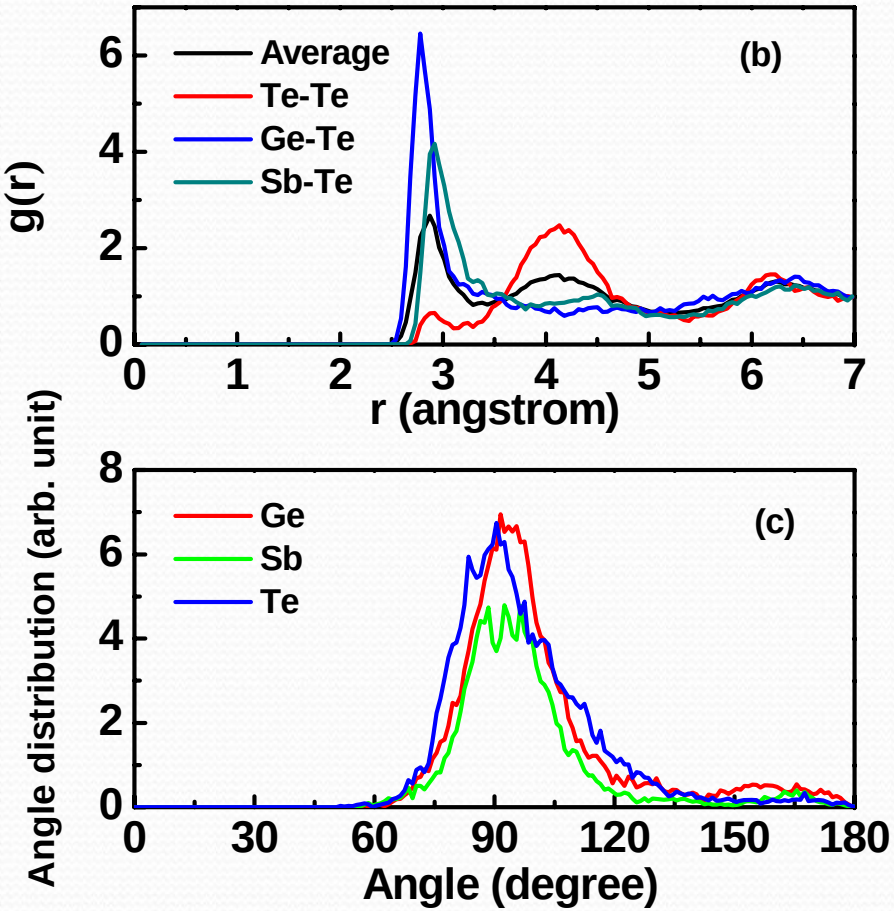

For reliable CN, need to determine who (how many) are really bonded neighbors

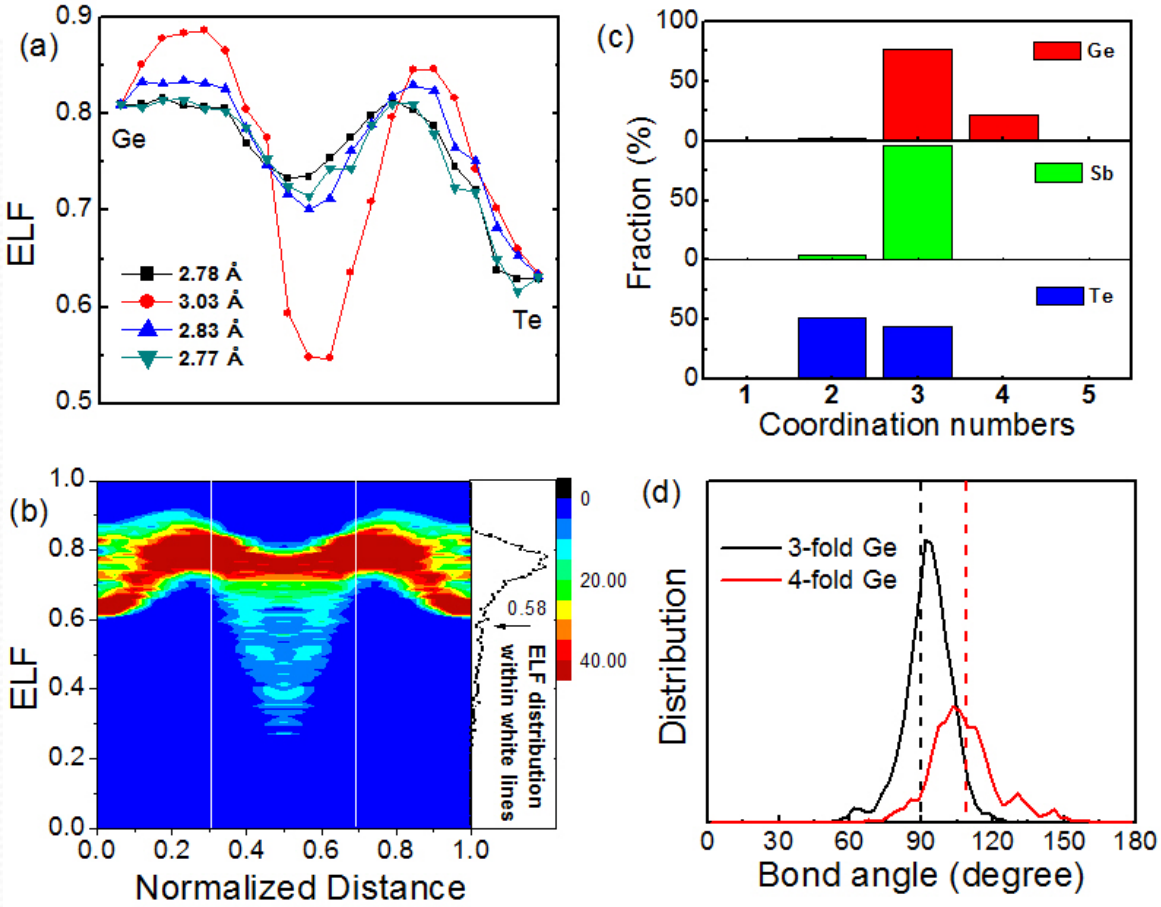

M. Xu *et al.*,
PRL 103 (2009) 195502

(a) Representative ELF profiles for a Ge atom and its neighbors (the neighboring atom at 3.03 Å appears to be not covalently bonded). (b) The ELF distribution between all atom pairs within a distance cutoff of 3.5 Å. The threshold ELF value (0.58 for actual bonding) is labeled by the arrow, which cuts across the valley separating the peak and tail. (c) The **CN** around each element, for chemically bonded neighbors. (d) Bond angle distributions for Ge atoms with CN=3 and CN=4, respectively. The 90º and 109º angles are marked with dashed lines.

Nature of Atomic Bonding and Atomic Structure in the Phase-Change $Ge_2Sb_2Te_5$ Glass

M. Xu,[1,*] Y. Q. Cheng,[1] H. W. Sheng,[2] and E. Ma[1,†]

[1]*Department of Materials Science and Engineering, Johns Hopkins University, Baltimore, Maryland 21218, USA*

[2]*Department of Computational and Data Sciences, George Mason University, Fairfax, Virginia 22030, USA*

(Received 22 August 2009; published 6 November 2009)

Using electronic structure calculations, we demonstrate a global valence alternation in the amorphous $Ge_2Sb_2Te_5$, a prototype phase-change alloy for data storage. The resulting p bonding profoundly influences the local atomic structure, leading to right-angle components similar to those in the crystalline counterpart of this chalcogenide glass. The dominance of p bonding is revealed by (i) distributions of the coordination number (CN) and the bond angle, for truly bonded atoms determined based on the electron localization function, and (ii) a direct evaluation of the p (and s) orbital occupation probability for the CN = 3 Ge atoms that form 90° bonds with neighbors.

For more information,
see details in this paper

rimary signature of a covalent bond is the sharing and localization of valence electrons between the bonding atoms. The degree of localization and hence the relative strength of a covalent bond can be reflected by the electron localization function [24,25],

$$\mathrm{ELF} = \frac{1}{1 + (D_\sigma / D_\sigma^0)^2} \qquad (1)$$

where D_σ is a measure of Pauli repulsion and scales with the probability density of finding another same-spin electron near the reference electron. The smaller this probability, the more localized is the latter electron [25]. D_σ^0, which is used to normalize D_σ, is the D_σ value in a homogeneous electron gas having the same local spin-density. ELF = 0.5 thus represents the same level of Pauli repulsion as in the homogeneous electron gas, and a higher ELF value indicates that the electrons are more localized (ELF = 1 can be interpreted as perfect localization).

Can we confirm the 3-fold Ge are p-bonded

(and sp^3 bonding for 4 fold-Ge) ?

Compare the DOS, and the occupation probability of *s* and *p* electrons

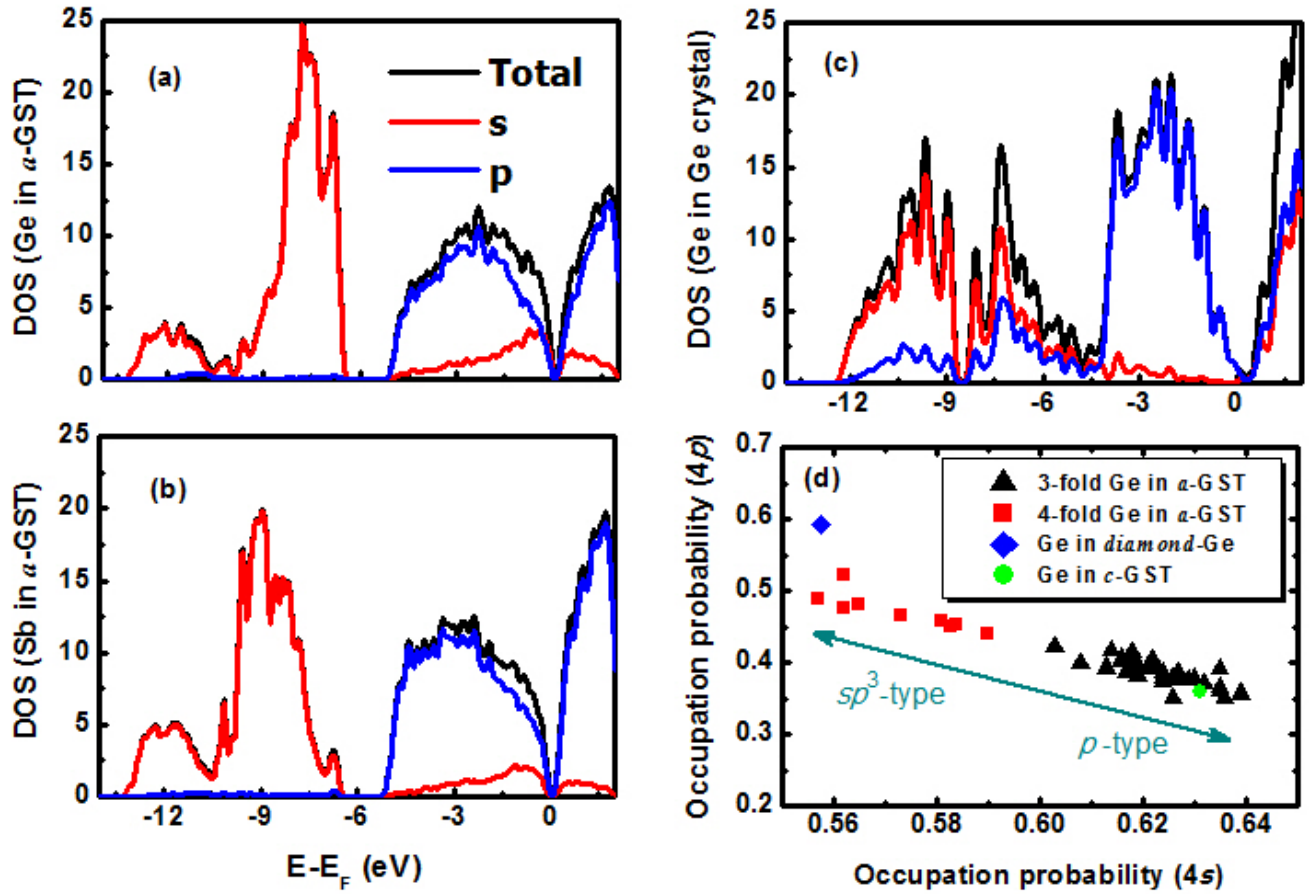

M. Xu *et al.*,
PRL 103 (2009) 195502

The total and projected DOS for (a) Ge in *a*-GST, (b) Sb in *a*-GST, and (c) Ge in diamond Ge. (d) Occupation probability of 4*s* and 4*p* orbitals (within the core region) for Ge atoms in *a*-GST, showing that the CN=3 and CN=4 Ge atoms belong to two bifurcated groups. Average values for Ge in crystalline Ge (sp^3) and Ge in *c*-GST (*p*-type bonding in rocksalt structure) are also given as references.

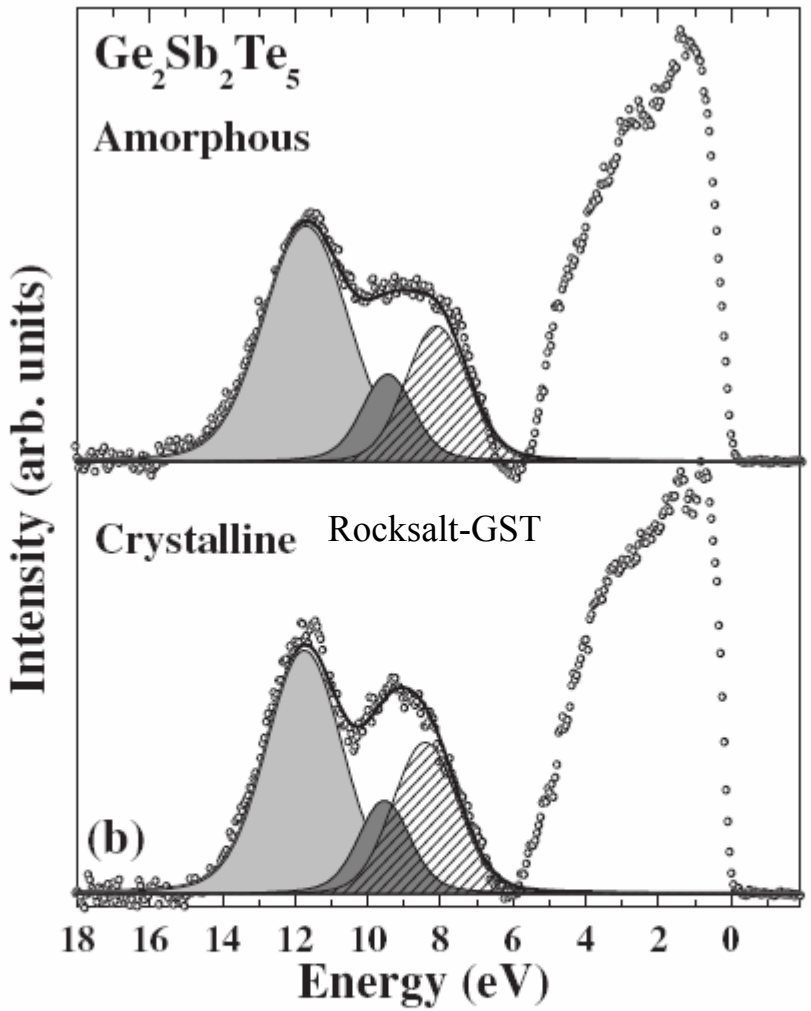

FIG. 4. Valence-band spectra (open circles) and curves fitted (solid lines) over the range from 6 to 18 eV for (a) GeTe and (b) $Ge_2Sb_2Te_5$. The Ge 4*s*, Sb 5*s*, and Te 5*s* orbitals lie within the fitted energy region.

Experimental supporting evidence:

XPS spectra showing similar Ge 4*s* for the glass and the rocksalt GST, little *s-p* hybridization for sp^3

J.-J Kim *et al*., PRB 76 (2007) 115124

Q#10: Implications for the rapid crystallization upon laser or electrical-pulse excitation at elevated T?

The *p*-bonding-controlled glass local structure resembles the
right-angled configuration in rocksalt-like c-GST, the crystallization product

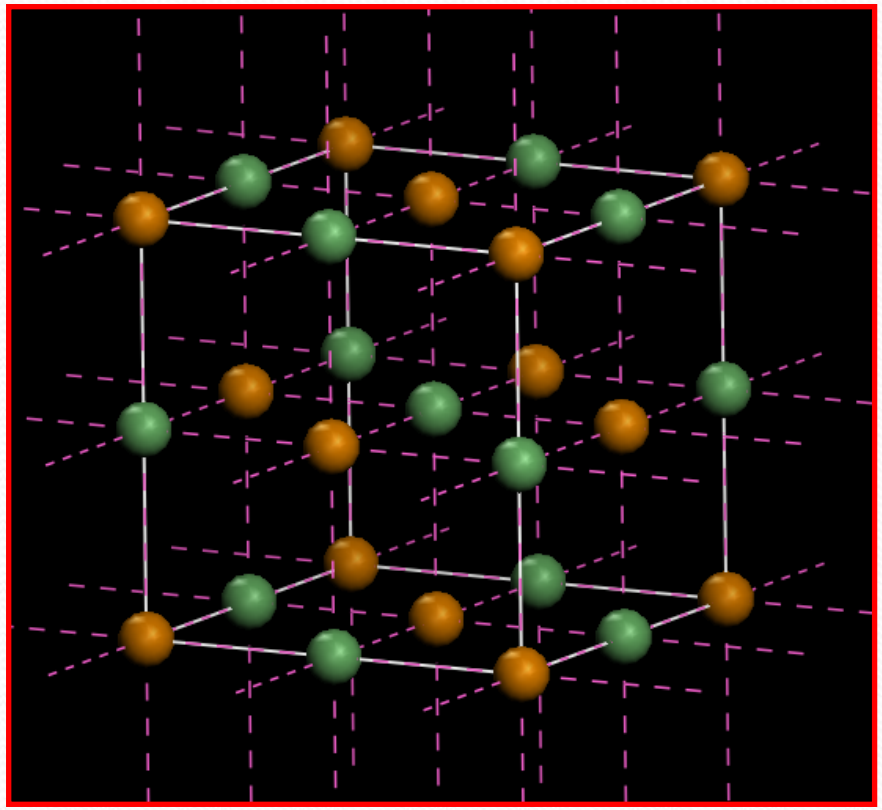

Te atoms occupy one sub-lattice, while Ge/Sb/vacancies occupy the other

Ge-Te and Sb-Te: 0.3 nm
Te-Te: 0.4242 nm

Summary message

- *Zr-Cu based BMGs can be pictured as composed of densely packed (due to metallic bonding) Cu-centered icosahedra as local motifs distinctly different from crystals. Al plays a special role, both in terms of chemistry and topology. Such structural features promote slow dynamics, resistance to shear transformations, and high barrier to crystallization (good bulk glass former).*

- *GST glass is semiconducting and characterized by p bonding, with right-angled local motifs resembling those in c-GST. This may be related to the rapid crystallization & poor GFA.*

End of talk

Nature of fast transition

Hopping between two low-energy states,
A transition of electronic structure with subtle/partial atomic rearrangement, facilitated by intrinsic vacancies.

Low hybridization -> pure p bonding
Low ionicity -> resonance of covalent bond

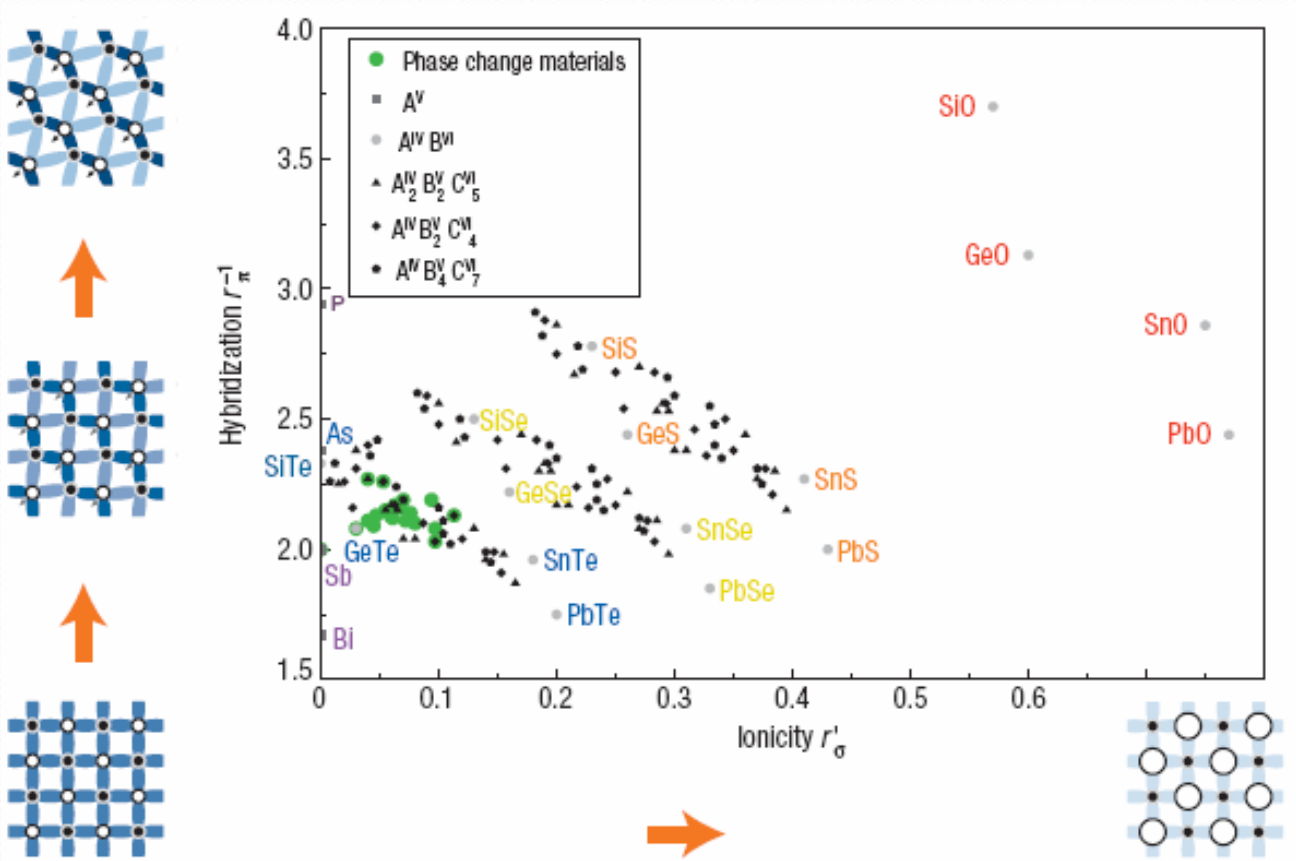

M. Wuttig's map
Nature Mater. 2008

QS Zeng *et al*.,
PRL 104 (2010) 105702

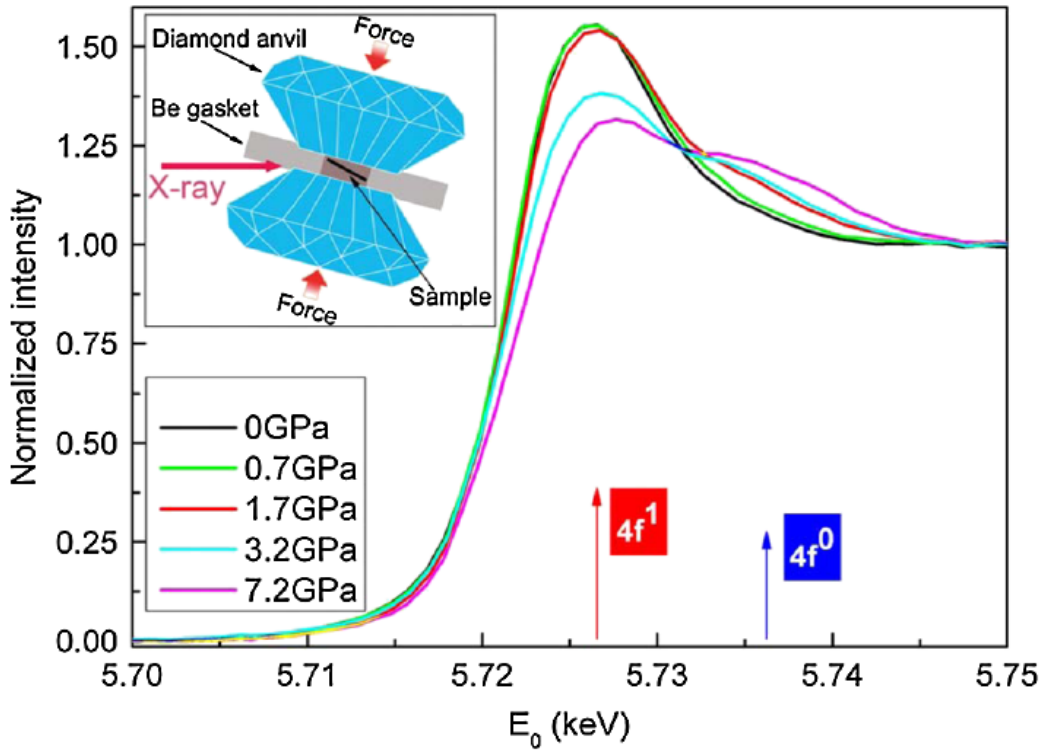

FIG. 4 (color online). *In situ* high-pressure Ce L_3-edge XAS spectra of $Ce_{75}Al_{25}$ metallic glass. The arrows point to the $4f^0$ and $4f^1$ components. The appearance of the $4f^0$ feature indicates the delocalization of $4f$ electron, and coincides with the volume collapse in XRD results. The inset shows a schematic of the *in situ* high-pressure XAS experimental geometry.

QS Zeng *et al*.,
PRL 104 (2010) 105702

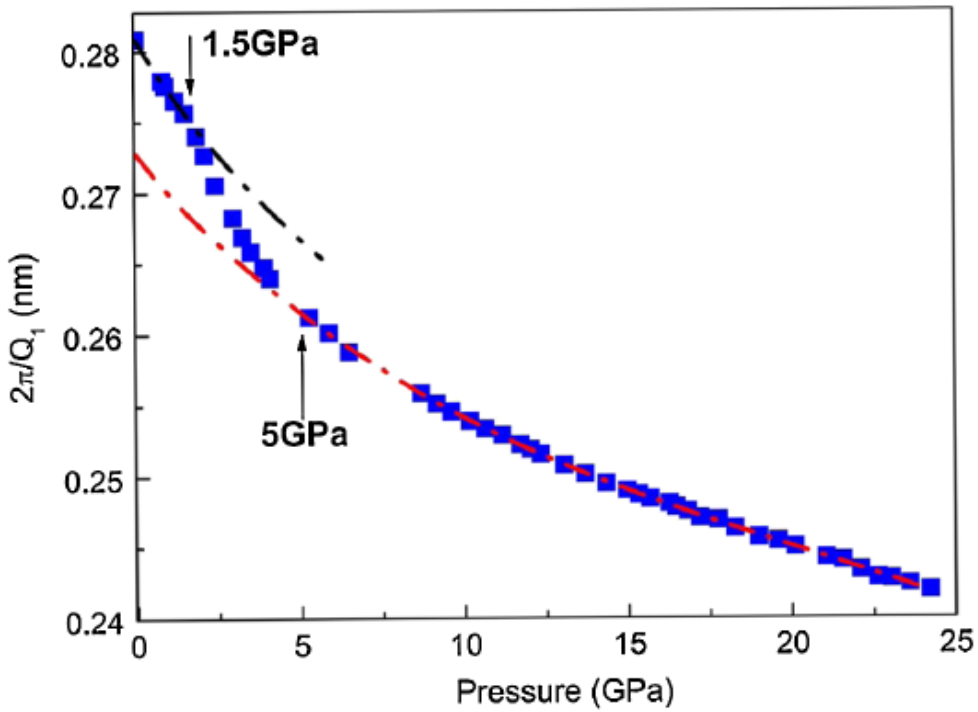

FIG. 3 (color online). Inverse FSDP positions $2\pi/Q_1$ of $Ce_{75}Al_{25}$ metallic glass as a function of pressure. Two distinct states, LDA (dashed black line) and HDA (dashed red line) along with a transition region from about 1.5 to 5 GPa can be identified. The data are smooth owing to the hydrostatic pressure conditions, and the pressure uncertainty is smaller than the symbol size.

Stochastic nucleation in small crystalline marks —

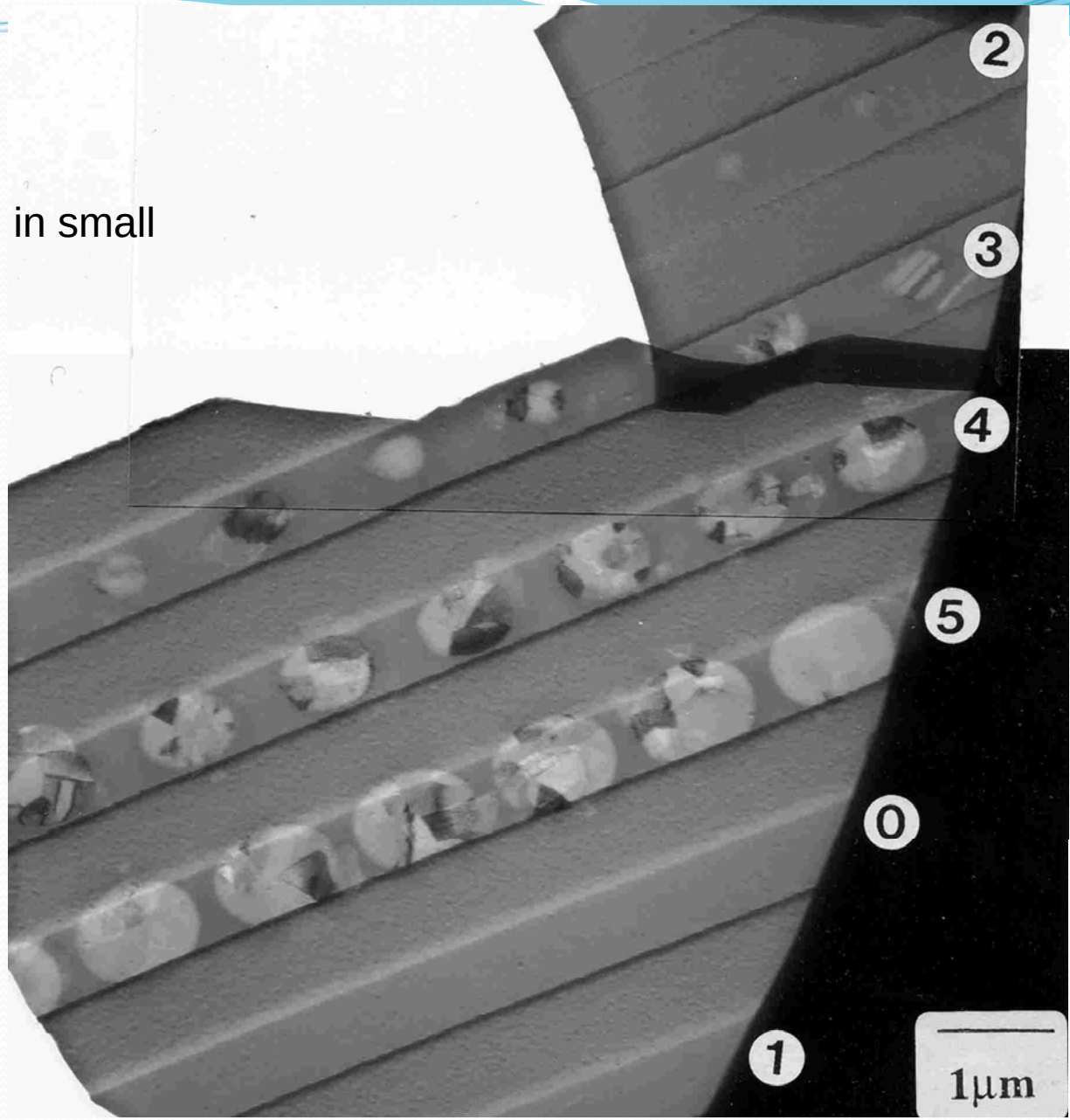

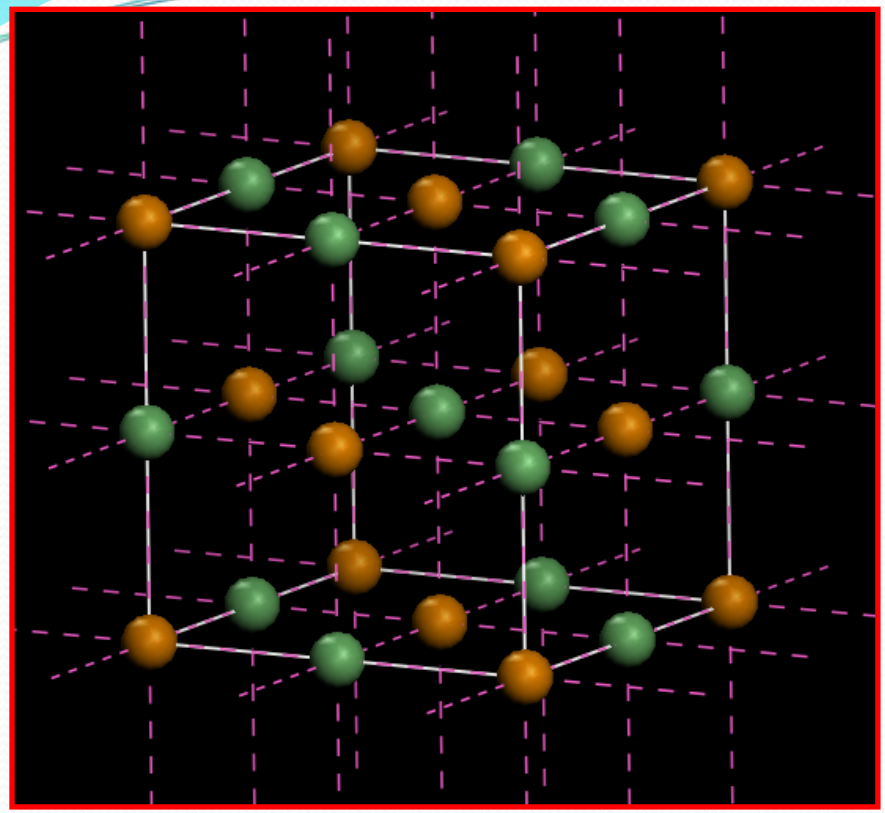

octahedra

Ge-Te and Sb-Te: 0.3 nm
Te-Te: 0.4242 nm

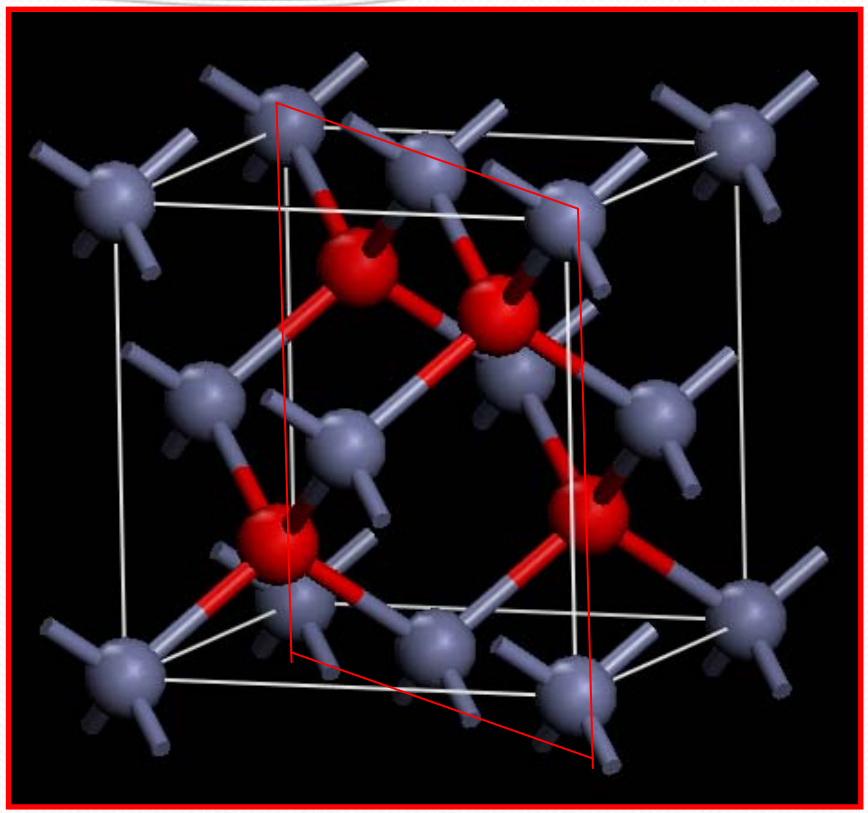

tetrahedra

Ge-Te and Sb-Te: 0.26nm
Te-Te: 0.4242nm

存储技术

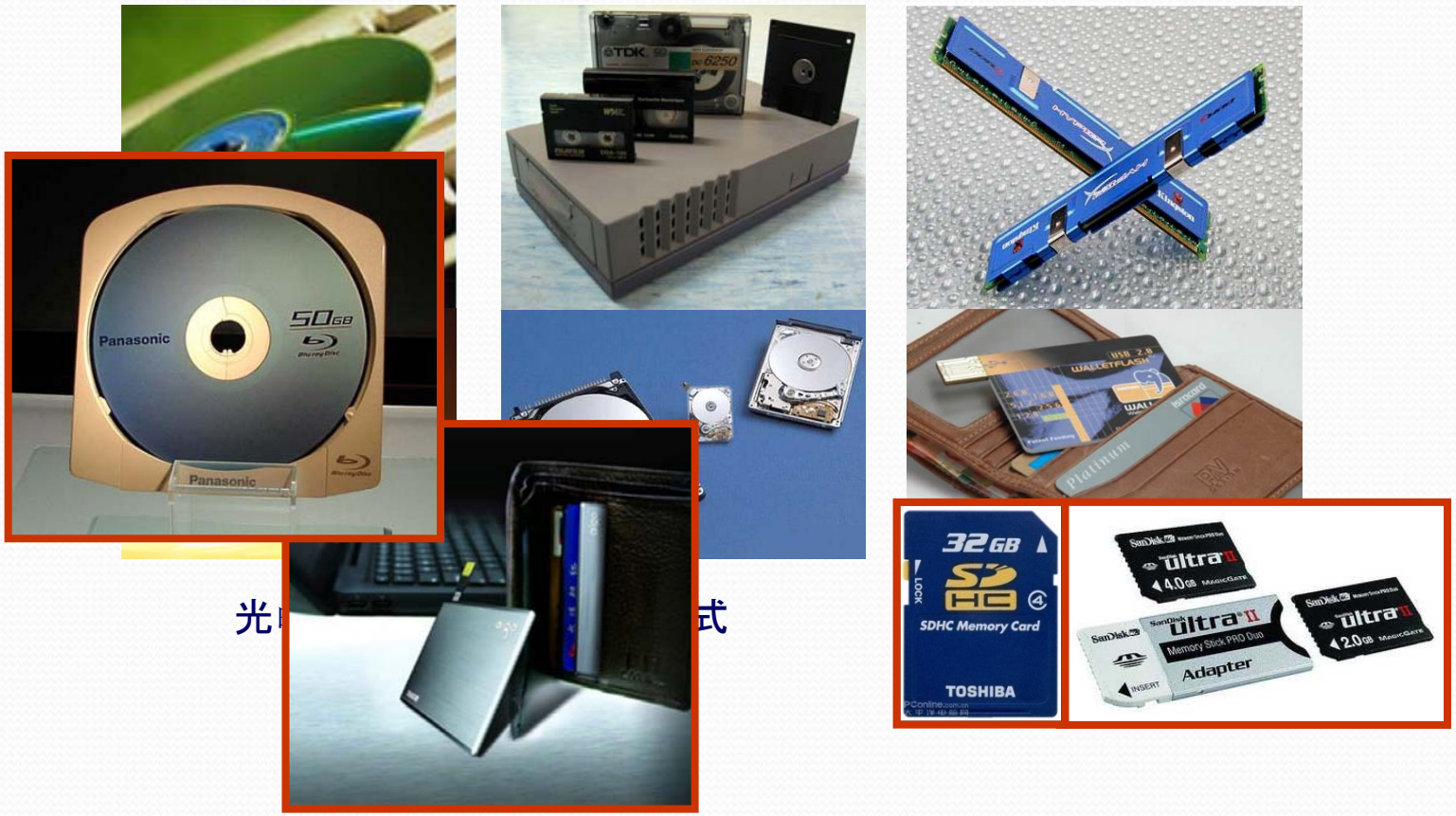
TDK
Panasonic
50GB
Panasonic
32GB
SDHC Memory Card
TOSHIBA
Adapter

光 式

Layer Stack in a CD-RW

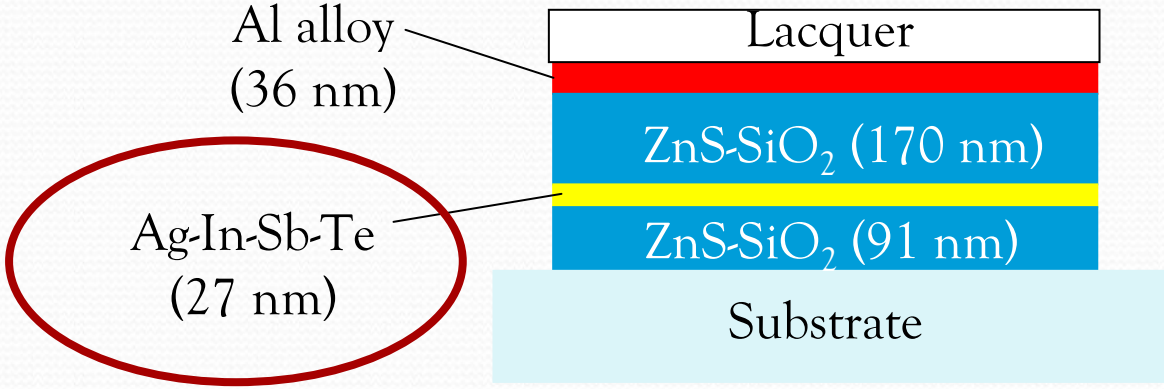

- as-deposited Ag-In-Sb-Te is amorphous

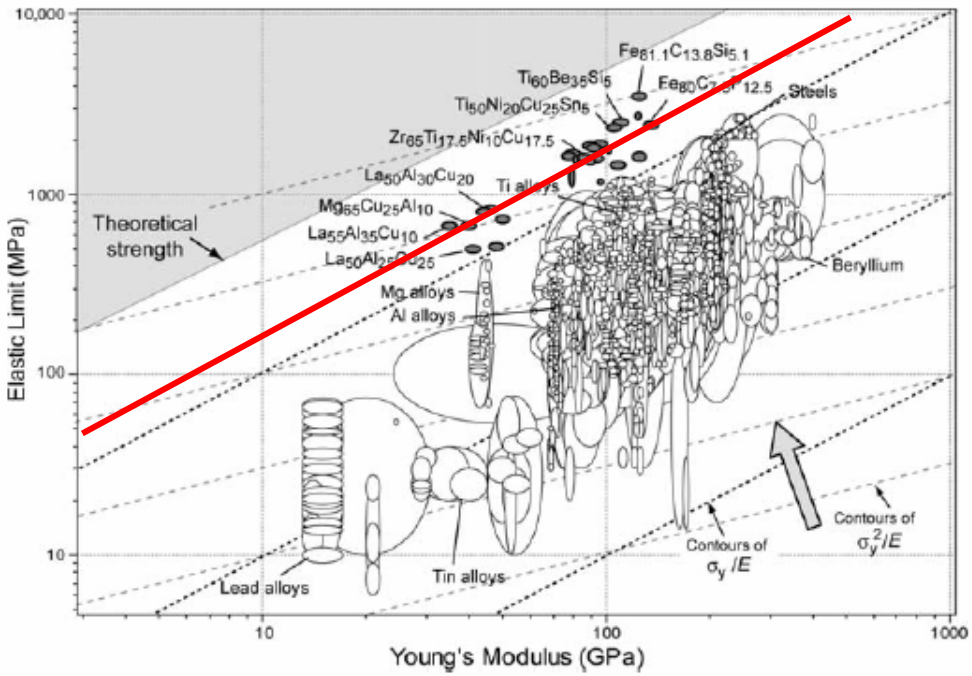

AL Greer and E Ma, MRS Bulletin 2007

Adapted from M Ashby and AL Greer, Scripta Mater. 2005

Perfume bottles by J. Schroers et al., 2008

Blow molding to 1000% strain, 0.1 MPa

J. Schroers et al., Scripta Mater. 2007

Calculations and experimental studies suggest that the smallest stable mark at RT is ~ 6 nm dia. in $Ge_2Sb_2Te_5$ (GST)

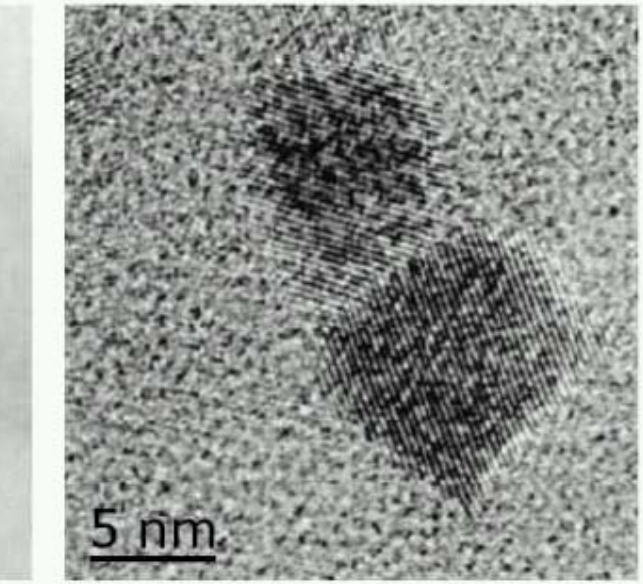

b)

Ge-Sb-Te	Si-Sb-Te
GeTe	Si-Sb
GeTeBi	InTe
GeTeAs	AgInTe
GeTeAsSi	AgSbTe
GeSb(CuAg)	AgInSbTe
AuSbTe	AsSbTe
AuInTe	AsTeAg
SeSbTe	PbGeSb
$(Ge_1Sb_2Te_4)_{1-x}(Sn_1Bi_2Te_4)_x$	

Scanning-probe memories

T. Gotoh, K. Sugawara & K. Tanaka: "Minimal phase-change marks produced in amorphous $Ge_2Sb_2Te_5$ films", *Jap. J. Appl. Phys*. **43** (6B) (2004) L818.